THE UNIVERSITY OF QUEENSLAND

AUSTRALIA

Liver-glycogen metabolism: A structural perspective.

Mitchell A. Sullivan

A thesis submitted for the degree of Doctor of Philosophy at

The University of Queensland in 2014

Queensland Alliance for Agricultural and Food Innovation

Abstract

Liver glycogen, a highly branched glucose polymer, has a critical role in the maintenance of blood glucose homeostasis. Liver glycogen consists of glucose units that are attached to form linear chains via α-(1→4) linkages. These chains are connected via α-(1→6)-linked branch points to form highly branched glycogen "β" particles (~20 nm in diameter) that can further join to form much larger "α" particles (~100-200 nm). Given the characteristically poor blood-glucose control associated with type 2 diabetes, a link between the structure/function relationships of liver glycogen and type 2 diabetes is probable. It is shown that diabetic (*db/db*) mice have an impaired ability to synthesize the large composite glycogen α particles present in normal, healthy mice and that α particles are held together via a bond more acid-labile than normal glycosidic linkages, with the most likely bond being proteinaceous. The structure of healthy mouse-liver glycogen over the diurnal cycle is characterized using size exclusion chromatography and transmission electron microscopy. Glycogen is observed to be initially formed as smaller β particles, only being assembled into the larger α particles significantly after the time when glycogen content reaches a maximum. This pathway, impaired in diabetic animals, is likely to give optimal blood-glucose control, as explained by the particles' surface area to volume ratio. Lack of this control may result from, or contribute to, the poor glycaemic regulation associated with diabetes. This discovery suggests novel approaches to diabetes management that promote α particle formation. Significant improvements in the extraction and characterization of liver glycogen has also been achieved, paving the way for future experiments exploring glycogen's role in diabetes. Glycogen can now be effectively and rapidly extracted from formalin-fixed tissues using a novel technique, allowing the analysis of human tissue samples from pathology laboratories that routinely employ this method of fixation. The use of aqueous size exclusion chromatography has been shown to dramatically

improve peak resolution when compared to the previously used dimethyl sulfoxide method, achieving separation of α-particle and β-particle peaks. This allows for a more detailed and quantitative analysis and comparison between liver glycogen samples.

Declaration by author

This thesis is composed of my original work, and contains no material previously published or written by another person except where due reference has been made in the text. I have clearly stated the contribution by others to jointly-authored works that I have included in my thesis.

I have clearly stated the contribution of others to my thesis as a whole, including statistical assistance, survey design, data analysis, significant technical procedures, professional editorial advice, and any other original research work used or reported in my thesis. The content of my thesis is the result of work I have carried out since the commencement of my research higher degree candidature and does not include a substantial part of work that has been submitted to qualify for the award of any other degree or diploma in any university or other tertiary institution. I have clearly stated which parts of my thesis, if any, have been submitted to qualify for another award.

I acknowledge that an electronic copy of my thesis must be lodged with the University Library and, subject to the General Award Rules of The University of Queensland, immediately made available for research and study in accordance with the *Copyright Act 1968*.

I acknowledge that copyright of all material contained in my thesis resides with the copyright holder(s) of that material. Where appropriate I have obtained copyright permission from the copyright holder to reproduce material in this thesis.

Publications during candidature

1) M. A. Sullivan et al. A rapid extraction method for glycogen from formalin-fixed liver. *Carbohydrate Polymers* **2014,** *submitted*.
2) M. A. Sullivan et al. Changes in glycogen structure over feeding cycle sheds new light on blood-glucose control. *Biomacromolecules* **2014**, *15*, 660.
3) M. A. Sullivan et al. Improving size-exclusion chromatography for glycogen. *J. Chromatography A* **2014**, *1*, 21.
4) R. G. Gilbert; M. A. Sullivan **(equal first authors).** Structural characterisation of liver glycogen and human health. *Australian Journal of Chemistry* **2014**, *67*, 538.
5) P. O. Powell, M. A. Sullivan et al. Extraction, isolation and characterisation of phytoglycogen from su-1 maize leaves and grain. *Carbohydrate Polymers* **2014**, *101*, 423.
6) R. G. Gilbert; A. C. Wu; M. A. Sullivan et al. Improving human health through understanding the complex structure of glucose polymers. *Analytical & Bioanalytical Chemistry* **2013**, *405*, 8969.
7) M. A. Sullivan et al. Molecular Insights into Glycogen Alpha-Particle Formation. *Biomacromolecules* **2012**, *13*, 3805.
8) Q. A. Besford; M. A. Sullivan et al. The structure of cardiac glycogen in healthy mice. *Int. J. Biol. Macromolecules* **2012**, *51*, 887.
9) M. A. Sullivan, J. Li, C. Li, F. Vilaplana, L. Zheng, D. I. Stapleton, A. A. Gray-Weale, S. Bowen, R. G. Gilbert. Molecular structural differences between type-2-diabetic and healthy glycogen. *Biomacromolecules* **2011**, *12*, 1983.

Publications included in thesis

1) M. A. Sullivan et al. A rapid extraction method for glycogen from formalin-fixed liver. *Carbohydrate Polymers* **2014,** *submitted*.

Contributor	Statement of contribution
M. A. Sullivan	Designed experiments (70%) Wrote the paper (90%) Performed experiments (65%) Collected tissue samples (50%)
S. Li	Designed experiments (10%) Performed experiments (15%)
S. T. N. Aroney	Performed experiments (15%)
B. Deng	Performed experiments (5%)
C. Li	Collected tissue samples (10%)
E. Roura	Designed experiments (5%) Edited Paper (20%)
B. L. Schulz	Designed experiments (5%) Wrote the paper (10%)
B. E. Harcourt	Collected tissue samples (40%)
Josephine M. Forbes	Designed experiments (5%) Edited paper (10%)
Robert G. Gilbert	Designed experiments (5%) Edited Paper (70%)

2) M. A. Sullivan et al. Changes in glycogen structure over feeding cycle sheds new light on blood-glucose control. *Biomacromolecules* **2014**, *15*, 660.

Contributor	Statement of contribution
M. A. Sullivan	Designed experiments (60%) Wrote the paper (100%) Performed experiments (70%)
S. T. N. Aroney	Performed experiments (20%)
S. Li	Performed experiments (10%)
F. J. Warren	Designed experiments (10%)
J. S. Joo	Collected tissue samples (10%)
K. S. Mak	Collected tissue samples (10%)
D. I. Stapleton	Designed experiment (5%) Edited paper (10%)
K. S. Bell-Anderson	Designed experiments (20%) Collected tissue samples (80%) Edited paper (20%)
Robert G. Gilbert	Designed experiments (5%) Edited Paper (70%)

3) M. A. Sullivan et al. Improving size-exclusion chromatography for glycogen. *J. Chromatography A* **2014**, *1*, 21.

Contributor	Statement of contribution
M. A. Sullivan	Designed experiments (80%) Wrote the paper (90%) Performed experiments (90%)
P. O. Powell	Performed experiments (10%)
T. Witt	Designed experiments (10%) Edited paper (20%)
F. Vilaplana	Wrote the paper (10%) Edited paper (20%)
E. Roura	Collected tissue samples (100%) Edited paper (20%)
R. G. Gilbert	Designed experiments (10%) Edited Paper (40%)

4) M. A. Sullivan et al. Molecular Insights into Glycogen Alpha-Particle Formation. *Biomacromolecules* **2012**, *13*, 3805.

Contributor	Statement of contribution
M. A. Sullivan	Designed experiments (80%) Wrote the paper (100%) Performed experiments (90%)
M. J. O'Connor	Performed experiments (10%)
F. Umana	Collected tissues (50%)

E. Roura	Collected tissues (50%) Edited paper (20%)
K. Jack	Designed experiments (10%)
D. I. Stapleton	Edited paper (30%)
R. G. Gilbert	Designed experiments (10%) Edited Paper (50%)

Sections of the following review articles were also used throughout the thesis:

1) R. G. Gilbert; M. A. Sullivan **(equal first authors)** Structural characterisation of liver glycogen and human health *Australian Journal of Chemistry* **2014**, *67*, 538.

Contributor	Statement of contribution
M. A. Sullivan	Wrote paper (50%)
R. G. Gilbert	Wrote paper (50%)

2) R. G. Gilbert; A. C. Wu; M. A. Sullivan et al. Improving human health through understanding the complex structure of glucose polymers. *Analytical & Bioanalytical Chemistry* **2013**, *405*, 8969.

Contributor	Statement of contribution
R. G. Gilbert	Wrote the paper (20%)
A. Wu	Wrote the paper (20%)
M. A. Sullivan	Wrote the paper (20%)

G. E. Sumarriva	Wrote the paper (5%)
N. Ersch	Wrote the paper (5%)
J. Hasjim	Wrote the paper (30%)

Contributions by others to thesis

1) Robert Gilbert (Principal supervisor): Experimental design, interpretation of results and manuscript preparation.
2) Eugeni Roura (Co-supervisor): Experimental design and collection of pig-liver tissues.
3) Kim Bell-Anderson, Brooke Harcourt and Josephine Forbes: Experimental design and collection of mouse-liver tissues.
4) David Stapleton, Benjamin Schulz and Fredrick Warren: Interpretation of results.
5) Samuel Aroney, Mitchell O'Conner: Experimental work.
6) Shihan Li, Prudence Powell and Bin Deng: Experimental work and interpretation of results.
7) Cheng Li, Jin Suk Joo, Ka Sin Mak, Felipe Umana, Ling Zheng, Chuanzhou Li, Jiong Li, Barbarra Williams, Helen Keates and Haichen Shou: Collection of liver tissues.
8) Francisco Vilaplana and Torsten Witt: Interpretation of results and manuscript preparation.
9) Kevin Jack and Richard Webb: Transmission electron microscopy assistance.
10) Sarah Chung, Kai Wang, Enpeng Li and Ming Li: Size exclusion chromatography assistance.
11) Lachlan Kann and Ian Godwin: Phytoglycogen extraction.
12) Thea Darnell: Designing schematics.

Statement of parts of the thesis submitted to qualify for the award of another degree

None.

Acknowledgements

I wholeheartedly thank Professor Robert (Bob) Gilbert for his incredible supervision over the course of my PhD. He has provided endless intellectual and emotional support, making the past few years extremely rewarding. He has generously devoted huge amounts of time and energy into my projects and has truly inspired me to continue to grow as a researcher. The opportunities he has provided me with in terms of performing and presenting my research both domestically and internationally is highly appreciated. He has also been an amazing friend, with many a good beer, single malt or Cab Sav being shared over some great times. Honestly, I can not overstate how much I appreciate Bob's supervision and support and look forward to remaining colleagues and mates for life.

It is also impossible to even begin to put into words how thankful I am for my parents' and sister's love and support. Besides the obvious benefits of having a loving family who have always been there for me, they have also given me invaluable advice and wisdom over the course of my PhD. My Dad has been actively and ethusiastically involved in discussions regarding all of my projects, always giving wonderful advice and insights and my Mum has continued to be the amazing person she so naturally is. Their advice, encouragement, love and support has been crucial to the completion of my PhD.

A huge thankyou goes to my beautiful partner, Thea. The love and support she has given me is enormous. She has always been there to cheer me up when experiments, as they often do, do

not turn out the way I optimistically planned. She also really embraced and celebrated any victory, big or small, I happened to have, ranging from a good day in the lab to a paper being accepted. I have been so lucky to have her so consistently there for me to share in the highs and lows and cannot thank her enough for her love and support. I also greatly appreciate the support from Thea's family who have been so amazingly kind and generous. There is a large and growing list of people I would like to thank for their help and guidence during my PhD. In no particular order this includes: Eugeni Roura, David Stapleton, Mike Gidley, Francisco Vilaplana, Torsten Witt, Prudence Powell, Alex Wu, Jovin Hasjim, Tony Li, Samuel Aroney, Fred Warren, Mitchell O'Connor, Felipe Umana, Kevin Jack, Kim Bell-Anderson, Josephine Forbes, Brooke Harcourt, Bin Deng, Xinle Tan, Enpeng Li, Chuanzhou Li, Cheng Li, Haichen Shou, Benjamin Schulz, Michael Sweedman, Canon Li, Sarah Chung, Kai Wang, Ming Li and all other Gilbert Group members. Emotional support has also come from all of my close friends. These include (but are by no means limited to): Matt Kosack, Claire Tuffield, Mathew Sheehan, Camille Charlotte, Tim Cochrane, Geordie Jay, Mitchell Brown, Steve Mison, Huw Darnell, Rachael Pittard, Banjo James, Abbey Richards, Markus Ravik, Sophie Kosack, Tom Harrison, Luke Chang and Monique Chang. Claire Tuffield generously helped with editing this thesis.

I would also like to thank anyone else who has been in my life during my PhD, I am extremely lucky to be surrounded by such amazing people.

Keywords

Glycogen, Size exclusion chromatography, Glycaemic control, Structural characterization, Diabetes, α particle.

Australian and New Zealand Standard Research Classifications (ANZSRC)

ANZSRC code: 060104 Structural Biology 50%

ANZSRC code: 030304 Physical Chemistry of Materials 50%

Fields of Research (FoR) Classification

FoR code: 0601 Biochemistry and Cell Biology 50%

FoR code: 0306 Physical Chemistry (incl. Structural) 50%

Table of Contents

List of abbreviations used in the thesis

AMPK	AMP-dependent protein kinase
AUC	Area under the curve
DBE	Debranching enzyme
DMSO	Dimethyl sulfoxide
DRI	Differential refractive index
DLS	Dynamic light scattering
EGP	Endogenous glucose production
GPC	Gel permeation chromatography

GLUT-2	Glucose transporter 2
GN	Glycogenin
GS	Glycogen synthase
GSK	Glycogen synthase kinase
IUPAC	International Union of Pure and Applied Chemistry
LF	Laforin
MALLS	Multiple-angle laser light scattering
MS	Mass spectroscopy
NADPH	Nicotinamide adenine dinucleotide phosphate
NBF	Neutral buffered formalin
NMR	Nuclear magnetic resonance
PCS	Photon correlation spectroscopy
PH	Phosphorylase
PP1c	Protein phosphatase 1c
PTG	Protein targeting to glycogen
R_{GL}	Regulatory-targeting subunit
SEC	Size exclusion chromatography
Stbd1	Starch-binding domain-containing protein 1
TCA	Trichloroacetic acid

TEM	Transmission electron microscopy
UDP	Uridine diphosphate
V_{el}	Elution volume
V_h	Hydrodynamic volume
$\overline{X}_n$	number-average degree of polymerization
$\overline{X}_{n,e}$	number-average exterior degree of polymerization
$\overline{X}_{n,i}$	number-average interior degree of polymerization

Chapter 1: Literature Review

Liver glycogen, a highly branched polymer of glucose, acts as a blood-glucose buffer. After a meal, blood glucose concentrations can be rapidly controlled by trapping glucose in glycogen. In animals, the cells with the largest stores of glycogen are in the liver and skeletal muscle. Glycogen is also contained in brain, heart, skin and adipose tissues[1]. Liver glycogen is synthesized when blood-glucose levels are high, removing excess glucose from the blood and storing it for future use. When blood-glucose levels are low, liver glycogen is degraded, releasing glucose into the blood[2].

1.1 Glycogen Structure

1.1.1 The three levels of glycogen structure

Liver glycogen has three levels of structure: 1) glucose units are attached to form linear chains via α-(1→4) linkages with branch points joined together via α-(1→6)-linkages; 2) these chains are able to form highly branched glycogen "β" particles (~20 nm in diameter); and 3) these β particles are joined together to form much larger "α" particles (~100-200 nm).

These three levels of structure are illustrated in Figure 1.

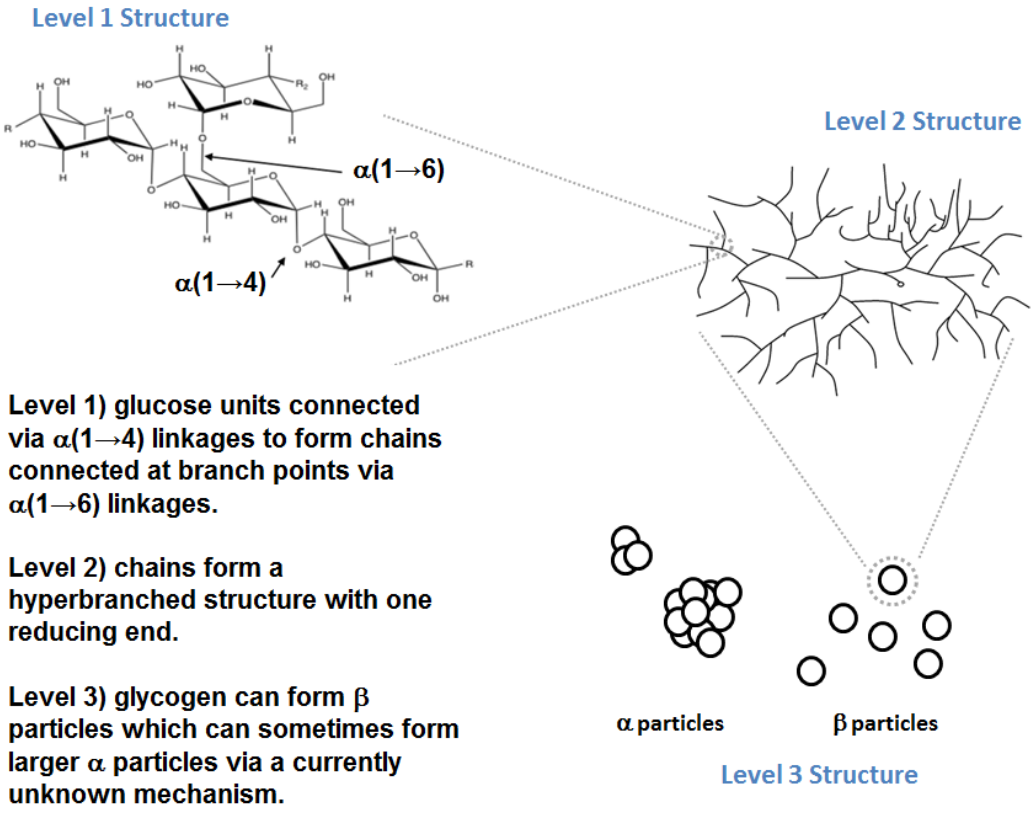

Figure 1: The three levels of glycogen structure.

Glycogen's average chain-length has been reported to be anywhere between 10-18 glucose residues, with the majority of studies finding the average length to be between 10-14 residues[3]. The β particles have diameters varying between 10 nm and 50 nm[4], with average molecular weights of ~10^6-10^7, as measured by mulitple-angle laser light scattering (MALLS)[5]. In liver cells these β particles are joined, forming large super-molecular complexes known as α particles (or α rosettes), which can have diameters as large as 300 nm[6] and molecular weights as high as 10^9.

A transmission electron microscope (TEM) image is given in Figure 2[7].

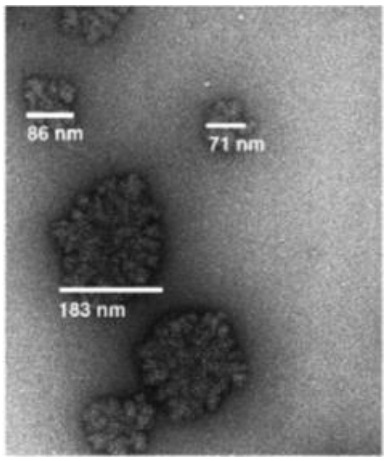

Figure 2[7]: TEM images of rat-liver glycogen samples[7].

The three main parameters associated with glycogen's branching structure that are generally reported include the number-average degree of polymerization ($\overline{X}_n$), number-average exterior degree of polymerization ($\overline{X}_{n,e}$) and number-average interior degree of polymerization ($\overline{X}_{n,i}$). $\overline{X}_n$ is simply the statistical average length of chains in a sample; $\overline{X}_{n,e}$ is the average length of chain between the terminal glucose unit and the outermost branch point; and $\overline{X}_{n,i}$ is defined as the average length of chain between two branch points. $\overline{X}_n$ can be obtained experimentally using isoamylase, an enzyme that breaks α-(1→6) bonds (branch points), and characterizing the molecular weight distribution of the resulting linear molecules by standard methods such as size-exclusion chromatography. Another parameter often tested is the β-amylolysis limit (β-limit), referring to the degree of hydrolysis glycogen undergoes when treated with β-amylase. β-amylase degrades the exterior part of chains down to a few glucose residues from the outermost branch points. The β-limit is then calculated by measuring the amount of maltose released. This parameter allows the calculation of $\overline{X}_{n,e}$, and if $\overline{X}_n$ has been calculated then $\overline{X}_{n,i}$ can be calculated from Equation 1[8]:

$$\overline{X}_{n,i} = \overline{X}_n - \overline{X}_{n,e} - 1 \qquad 1$$

Typical values for glycogen include a β-limit of 45-55%, $\overline{X}_n$ of 10-14, $\overline{X}_{n,e}$ of 6-9 and a $\overline{X}_{n,i}$ of 3-4[9].

Glycogen chains can either be labelled as A-, B- or C-chains, a concept introduced by Peat et al.[10], where A-chains are the chains with no substituents, B-chains have one or more branching points along the chain and C-chains carry the sole reducing group in the molecule and have multiple branching points.

A number of models for glycogen's branching structure were proposed in the 1940s. The Haworth "laminated" form[11] is a proposed structure where each new branch would have another new branch connected via an α-(1→6) linkage, practically making all chains B-chains (see Figure 3a). Staudinger and Husemann's model involves a comb-like structure[12], where chains are connected at C2, C3 and C6 of a central chain, consisting of ~100 α-(1→4)-linked glucose units, practically making all chains A-chains (see Figure 3b). In 1941 Meyer and Fuld proposed a different tree-like structure[13], where there are inner chains that have multiple branching points connected via α-(1→6) linkages (see Figure 3c). This model has both A- and B-chains in approximately equal numbers. Meyer's model was shown to be the most correct out of these early three models, with Larner et al.[14] using stepwise enzyme degradation experiments to determine that glycogen consists of multiple branching.

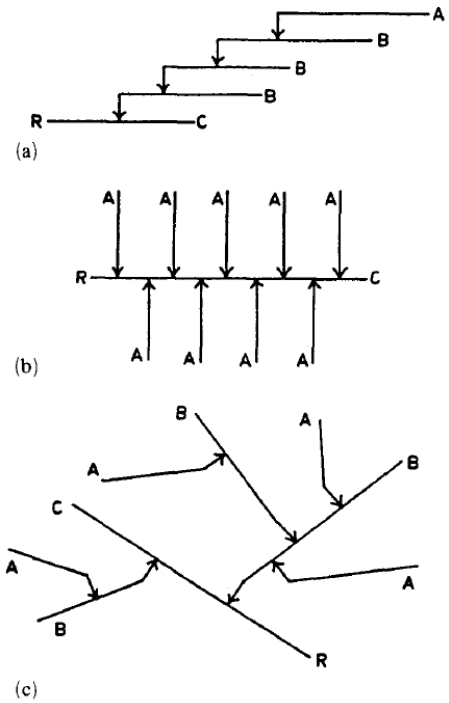

Figure 3[15]: The three early models proposed for the structure of glycogen. (a) represents Haworth's "laminated" form; (b) the comb form proposed by Staudinger et al.; and (c) the Meyer "tree" form.

While the Meyer model was shown to be the most accurate of these early models, this model suggested that every B-chain contains at least one A-chain, a feature that was shown to be inconsistent with debranching (isoamylase) experiments[16]. Enzymatic data from these experiments using isoamylase, phosphorylase and β-amylase led to a new model being proposed, the Whelan model (see Figure 4).

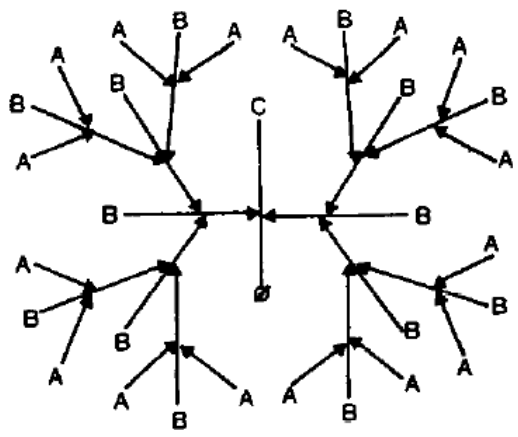

A = chains with no substituents

B = chains with substituents

C = chain with free reducing group

Figure 4[9,17]: The structure of glycogen proposed by Whelan[17].

The structure of glycogen suggested by Whelan[17] consists of an equal number of A (those carrying no substituents) and B (substituent-carrying) chains (see Figure 4). This model was supported by experiments which found that the A:B chain ratio is close to 1:1[14,17]. Other evidence that supported this model was obtained using fractionation of isoamylase-debranched glycogen and by using radioactive labels on the reducing ends[16].

1.1.2 Glycogen-associating proteins

Glycogen forms granules in cells that contain not only glycogen, but also a variety of bound proteins such as glycogen phosphorylase and glycogen synthase, all involved in glycogen metabolism (see section 1.2 for these enzymes' roles)[18]. Many of the proteins involved can be seen in Figure 5 and have been confirmed using proteomics[19].

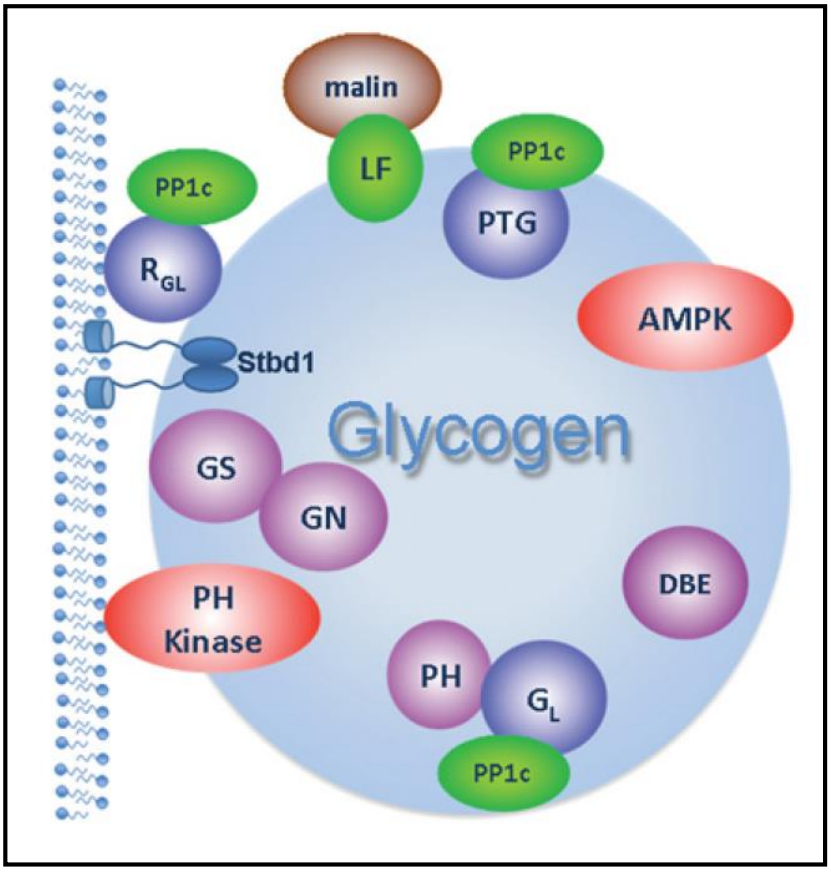

Figure 5[20]: Proteins associated with glycogen: metabolic enzymes shown in mauve include glycogenin (GN), glycogen synthase (GS), phosphorylase (PH) and debranching enzyme (DBE); protein kinases shown in red include phosphorylase kinase (PH kinase) and AMP-dependent protein kinase (AMPK); phosphatases are shown in green and include type 1 catalystic subunit protein phosphatase 1c (PP1c) and laforin (LF); units that target PP1 are shown in blue and include the regulatory-targeting subunit R_{GL}, G_L and protein targeting to glycogen (PTG)[20]. Starch-binding domain-containing protein 1 (Stbd1) has recently been shown to bind to glycogen[19] and is generally regarded as a membrane-anchoring protein. Malin, a protein catalysing the polyubiquitylation (and hence degradation) of laforin is shown in brown.

1.1.3 Phosphorylation of glycogen

Before the 1980s the presence of phosphate in glycogen was considered to be a contaminant, with the purity of samples often being correlated to the phosphate content[20]. After phosphate

was demonstrated to be an integral part of glycogen[21], a number of studies focused on determining the chemical linkage between phosphate and glycogen, as well as the role of phosphate in glycogen structure/metabolism. The concentration of phosphate has been reported to be ~one per 1500 glucose units in mouse skeletal muscle[22] and ~one per 650 units in rabbit muscle[23], with levels of phosphorylation shown to be significantly less in the liver of rabbits[24].

It was initially postulated that phosphate was both: 1) connected to some of the C_6 positions of glycogen, forming monoesters and blocking a potential branchpoint; and 2) forming C_1-C_6 phosphodiesters, essentially being an alternative method for forming a branch point. It was also suggested that perhaps the level of phosphorylation of a glycogen molecule may be related to its age, acting as a molecular marker and potentially signalling the transport of glycogen to the lysosome[21]. A subsequent study using mass spectroscopy and NMR found phosphate to exist as C_2- and C_3-phosphomonoesters, with no evidence for the previously hypothesized C_6-phosphoesters[25]. A more recent study however developed an assay that was able to specifically measure phosphorylation at the C_6 position, finding a significant amount in muscle glycogen (with less occurring in liver glycogen). This study also addressed whether glycogen phosphorylation has a specific role in glycogen structure/metabolism or simply resulted from a catalytic error from glycogen synthase. They found that phosphophorylation is not mediated by glycogen synthase or glycogen phosphorylase, providing evidence that there may be an important function in the phosphorylation of glycogen and raising the question of what enzyme is responsible. Interestingly, they found that the inner part of the molecule had higher levels of phosphorylation, leading them to suggest that perhaps this plays a role in preventing excessive branching (and thus crowding) in the early stages of glycogen synthesis[26].

While some phosphorylation may be physiologically important, overphosphorylation has been shown to be associated with Lafora disease, a form of epilepsy that ultimately leads to neurodegeneration and death[23]. This overphosphorylation results from an inability to remove

phosphate from the glycogen, with half of the cases of Lafora disease resulting from mutations in the gene encoding laforin, a phosphatase able to cleave the phosphate covalently attached to glycogen. This hyper-phosphorylated glycogen forms insoluble polyglucosan bodies (known as Lafora bodies), which accumulate in neurons, causing the pathology of the disease[22].

1.1.4 α-Particle binding

Although a number of studies have provided insight into the formation of α particles, there has been conflicting theories regarding not only how these particles form, but what bonds hold them together.

One possibility that has almost been eliminated is that of non-covalent bonds, with a broad range of disaggregating agents such as urea, guanidine, LiBr and thiocynate having been reported to have no effect on the molecular weight spectrum of the glycogen[27]. These results have been confirmed in a number of subsequent experiments[28].

After the determination that a gluco-protein (glycogenin) is the precursor for glycogen synthesis and the suggestion that this protein may be involved in α-particle binding[29], it was reported[30] that there was an elimination of large glycogen particles upon treatment with 2-mercaptoethanol (which disrupts disulfide bonds) with the reduced sulfhydryl groups being subsequently blocked by adding iodoacetamide. This resulted in the conclusion that α particles are composed of β particles attached via disulfide linkages[31,32]. The properties of this 2-mercapoethanol treated glycogen were further studied, showing that the number-average molecular weight ($\bar{M}_n$) decreased from 6.2 x 10^7 to 2.7 x 10^7, a decrease of ~ 56%[33]. However it was suggested by Manners[3] that a possible by-product in this experiment, hydroiodic acid, could hydrolyze α particles. Another factor noted by Manners was that it has now been determined that glycogenin only contains 2 cysteine residues[34], reducing the ability of this protein to form multiple disulfide bonds, an important factor in Geddes et al.'s model. Matsuda

et al.[35] constructed size frequency histograms from electron micrographs of glycogen treated with 2-mercaptoethanol and iodoacetamide and reported no significant size decrease, suggesting that Nakumara's hypothesis[36] that α particles are created on elongated exterior chains was correct, implying an α-(1→4)-link between β particles[35]. It has been theorized[37] that in β particles, the local molecular density becomes so high after ~12 layers of glucose monomer units that further growth cannot occur (perhaps due to inaccessibility to glycogen synthase). One can combine these ideas into a "crowding/budding" mechanism, where occasional exterior chains in a β particle are less crowded and can form new "buds" of growing branches via glycogen synthase, which grow to become β particles bonded to the original particle. While some time ago we had suggested[38] that this postulate was inconsistent with observed glycogen number distributions[28,30], which does not show the maximum that might be expected at a size corresponding to the onset of crowding, we can now point out that because new β particles can start after molecules reach this size, a shoulder rather than a maximum is more likely, as is indeed observed[28]. Further evidence consistent with such a model, as opposed to one where β particles or β particle units come together to form α particles, is that there is approximately one glycogenin molecule for every α particle in the liver[39]. If β particles, each needing an initiating glycogenin molecule, were synthesized separately and then joined, there should be many more glycogenin molecules than α particles. However a more recent study found that there may actually be much more glycogenin in liver than the previous study reported[19].

1.2 Glycogen Metabolism

1.2.1 Glucose homeostasis

Glucose is an important cellular energy source that must be tightly regulated to maintain blood-glucose homeostasis. A non-diabetic range of blood-glucose levels lies within the narrow range

of 3.9 to 5.6 mM[40]. If blood-glucose levels are too high or too low, the body's functioning is impaired and conditions such as diabetes or hypoglycaemia may result. An equilibrium between endogenous glucose production (EGP) and glucose utilization maintains homeostasis. Insulin, epinephrine and glucagon are the main hormones regulating this process with metabolites (such as glucose) also playing a crucial role[40].

Insulin-producing cells (β-cells) in the pancreas are able to sense glucose concentrations in the blood and adjust the amount of insulin released[41]. Insulin is secreted following food digestion, promoting the uptake of glucose into the liver, skeletal muscle, heart and adipocytes. In the liver this increased concentration of glucose results in the synthesis of glycogen and the inhibition of glycogenolysis and gluconeogenesis. After fasting, the level of glucose in the blood drops, causing the secretion of the hormone glucagon from pancreatic α-cells. The glucagon peptide promotes a rapid increase in gluconeogenesis and glycogenolysis, resulting in the restoration of blood-glucose levels[42]. Epinephrine (adrenaline) stimulates glycogen breakdown in the muscle, and to some extent glycogen breakdown in the liver[43].

To ensure that the net flux is in the appropriate direction, key enzymes in opposing metabolic pathways, glycolysis and glycogenesis, must be regulated[42].

The concentration of human hepatic glycogen varies from approximately 200 to 450 mM, depending on whether the person is in the fed or fasting state. Diabetic sufferers (both type 1 and type 2) synthesize only 25-45% of the hepatic glycogen synthesized by non-diabetic humans[40].

Insulin-independent uptake of glucose in the hepatocytes is achieved via the GLUT-2 glucose transporter. This transporter allows the entry of glucose even when there are high concentrations of glucose in the sinusoids (small blood vessels in the liver). This glucose is then phosphorylated to glucose-6-phosphate where it can either undergo glycolysis (to be used

for energy release) or undergo further reactions to become UDP-glucose, a precursor for glycogen synthesis (see Figure 6)[40].

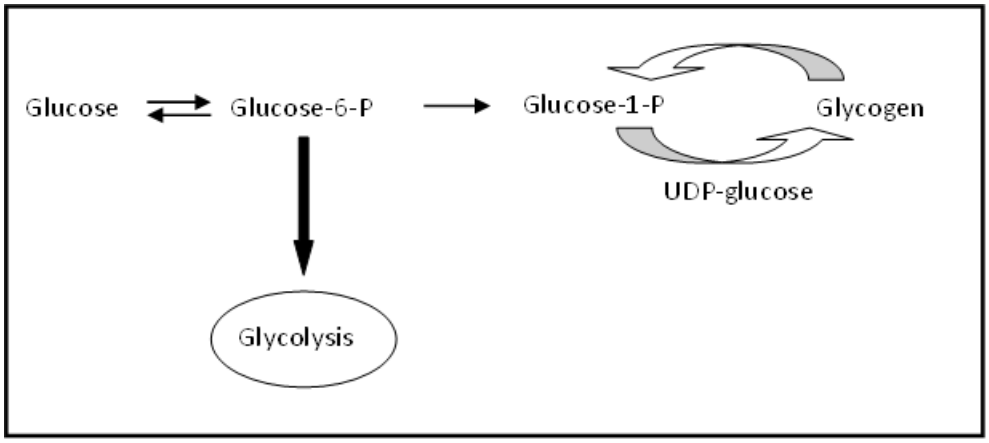

Figure 6[40]: A schematic diagram representing two different fates of glucose after entering hepatic cells.

1.2.2 Glycogen synthesis

Glycogen biosynthesis is initiated by the autocatalytic enzyme glycogenin, which is glycosylated on tyrosine-194 from an active form of glucose, uridine diphosphate glucose (UDP-glucose) (see Figure 7). Glycogenin forms an active dimer with a coordinated Mn^{2+}, which is believed to interact with UDP-glucose (see Figure 7), acting as a Lewis acid to make the UDP leaving group more stable[44]. Approximately 8-12 more glucose residues are subsequently added to the glycosylated tyrosine-194 residue, catalysed by the other glycogenin subunit, allowing the biosynthesis of glycogen to begin[43,45,46].

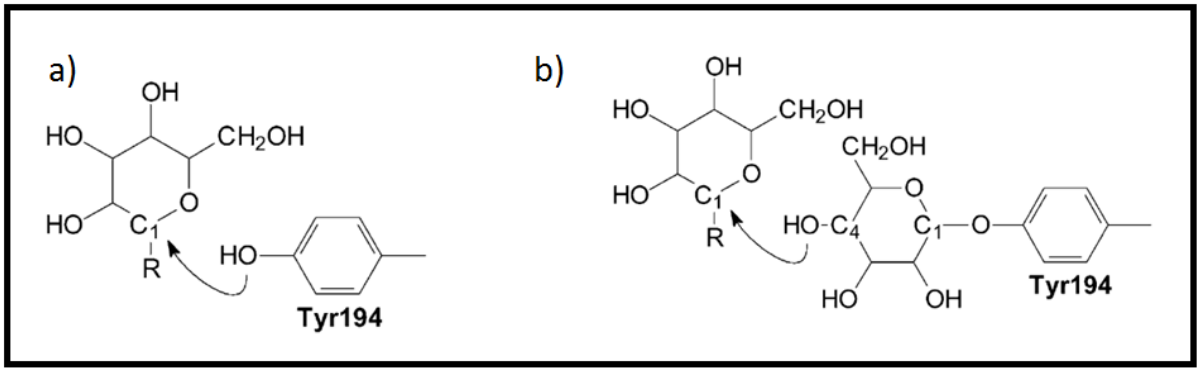

Figure 7: Glycogenin catalyses the above two reactions. Firstly, Tyr194 is glycosylated from UDP-glucose (a), which is followed by the glycosylation of the C4-hydroxyl group of the terminal glucose (b), forming an α-(1→4) glycosidic link[47].

After the initial stages of glycogen production, glycogen branching enzyme is able to cleave the distal end of the growing chain and attach it via an α-(1→6) link to either another chain, or the same chain, creating a new branch[48]. During glycogen synthesis, glycogen branching enzyme continues to create new branching points, resulting in a hyperbranched molecule. Typically, the number of residues transferred is approximately 7 monomer units in length and comes from a chain with a minimum length of 11 units. Another specific requirement is that the new branch point is at least 4 monomer units away from another branch point. The high level of branching increases the solubility of the molecule, both by exposing more terminal hydroxyl groups, as well as preventing chains from undergoing retrogadation, as seen in starch. Also more terminal sites become available for glycogen synthase and glycogen phosphorylase to act, increasing the rate of synthesis and degradation of glycogen[43].

Glycogen synthesis is mainly regulated by the reversible phosphorylation of a number of sites on glycogen synthase. The phosphorylation state of these sites is controlled by several protein kinases such as glycogen synthase kinase (GSK) and protein kinase A. The phosphorylation of glycogen synthase converts it from the active *a* form to the inactive *b* form.

1.2.3 Glycogen degradation

Glycogenolysis is the degradation of glycogen into glucose 6-phosphate, an important metabolite. Four enzymatic activities are required for efficient glycogen breakdown. The first key enzyme involved with this process is glycogen phosphorylase, which cleaves terminal glucose monomers from glycogen using orthophosphate (P_i). The product of this phosphorolysis reaction, glucose-1-phosphate, is converted to glucose-6-phosphate by phosphoglucomutase. Glucose-6-phosphate in the liver can either be converted into free glucose by glucose-6-phosphatase, an enzyme absent from the muscle, to be subsequently released into the bloodstream, or can undergo glycolysis in the liver. The other possible fate of the glucose-6-phosphate (besides simply being incorporated back into glycogen - see Figure 6[40]), is for it to enter the pentose phosphate pathway to create ribose derivatives and NADPH[43]. Glycogen phosphorylase can only remove glucose monomers down to a branch length of 4 glucose units. Two more enzymes are needed to remove these units, making the molecule suitable for further phosphorylase degradation, a transferase and an α-1,6-glucosidase. In mammals glycosyltransferase and glucosidase activity is performed by a single bifunctional enzyme (glycogen debranching enzyme). Once a branch is 4 glucose units long and cannot undergo further degradation by glycogen phosphorylase, the glucosyltransferase catalytic site on glycogen debranching enzyme moves three glucose units to another branch. The glucosidase site then cleaves the remaining α-(1⟶6) bond, allowing further phosphorolysis degradation[43].

The regulation of glycogen degradation depends largely on controlling the activity of glycogen phosphorylase. This regulation is sensitive to a number of allosteric effectors that reflect the energy requirements of the cell, as well as reversible phosphorylation, which is controlled by hormones such as insulin, epinephrine and glucagon. Unlike glycogen synthase, the phosphorylated form of glycogen phosphorylase, phosphorylase a, is the active form[43]. It has

been determined that the elevated glucose output from hepatocytes in type 2 diabetes is partly due to increased glycogenolysis[49].

1.2.4 Diurnal cycle of glycogen metabolism

Liver-glycogen metabolism in mice, like many animal species[50-53], follows a daily rhythm. This rhythm in rodents has been studied during a 12 hour light/12 hour dark cycle, with hepatic glycogen contents peaking during the dark period and decreasing during the light period, as seen in Figure 8[54-58].

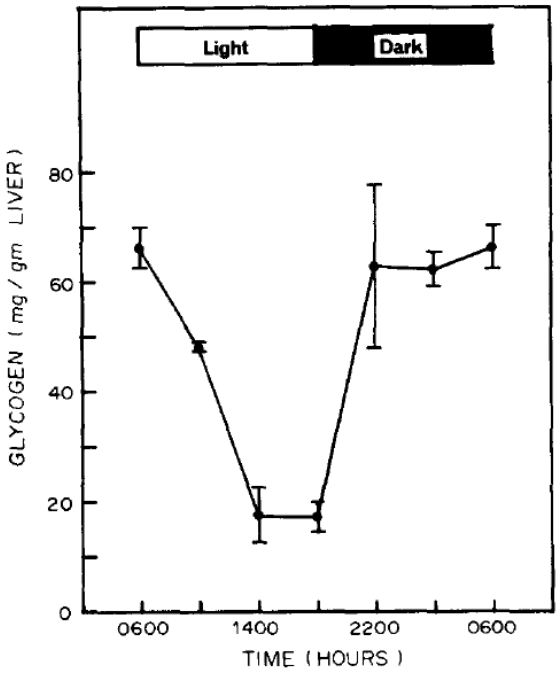

Figure 8[54]: Hepatic glycogen content as a function of time of day.

Previous results and conclusions for glycogen structural changes during synthesis and degradation have been conflicting. In 1967, Parodi reported[59] that, while glycogen content increased significantly after administering glucose to overnight-fasted mice, the glycogen size distributions (using sucrose gradient centrifugation) remained almost unchanged. However, Geddes in 1971[32], found that sucrose-density-centrifugation size distributions varied

significantly with glycogen content in refed rabbits after 4 days of starvation. Further studies into the structural changes of glycogen during the diurnal cycle are needed in order to obtain a better understanding of the role glycogen structure plays in its metabolism.

1.3 Characterizing Glycogen Structure

1.3.1 Size-exclusion chromatography

Glycogen molecules have a wide distribution of sizes, and due to differences in branching structure, for each size there is a range of molecular weights[60]. The shape and breadth of these distributions will depend on the polymerization mechanism, as well as the kinetics and conditions of biosynthesis[60].

Size-exclusion chromatography (SEC), also known as gel permeation chromatography (GPC), is a method which separates polymer molecules, including glycogen, based on their hydrodynamic volume (V_h); it is a common misapprehension that SEC separates by molecular weight[60]. V_h is defined by the International Union of Pure and Applied Chemistry (IUPAC) as 'the volume of a hydrodynamically equivalent sphere'[61], as applicable to the particular technique being used. In this thesis, results are usually reported in terms of the corresponding hydrodynamic radius R_h with $V_h = {}^4/_3 \ \pi R_h^3$. Some examples of detectors that allow the conversion of hydrodynamic volume data into structurally relevant and meaningful information include differential refractive index (DRI), viscometry and multiple-angle laser light scattering (MALLS).

One useful distribution that can be obtained is the SEC weight distribution, which gives the total weight of molecules that have a size between $\log_{10}V_h$ and $\log_{10}V_h + d\log_{10}V_h$. Obtaining this distribution requires a DRI detector, which measures the refractive index of the solution passing through the SEC column in reference to a cell that contains pure solvent. The instrument factor f_{DRI}, the concentration of molecules at each elution volume $c(V_{el})$, and the

refractive index increment dn/dc (where n is the refractive index) all determine the DRI signal intensity (Equation 2).

$$S_{DRI}(V_{el}) = f_{DRI}\, dn/dc\, c(V_{el}) \qquad 2$$

The SEC weight distribution is given by the DRI detector in conjunction with the universal calibration curve (Equation 3)[31].

$$w(\log V_h) = -S_{DRI}(V_{el}) \frac{d\, \tilde{V}_{el}(V_h)}{d \log V_h} \qquad 3$$

1.3.2 Dynamic light scattering

Dynamic light scattering (DLS), also known as photon correlation spectroscopy (PCS), is a technique that relates a particle's Brownian motion, that is the movement of particles due to random collision with solvent molecules, to its size. This is done by exposing the particles to a laser and analysing the intensity of scattered light at a fixed angle. The relationship between the diffusion coefficient corresponding to Brownian motion and the size of a spherical impenetrable particle is given in the Stokes-Einstein Equation (Equation 4).

$$D = \frac{RT}{N} . \frac{1}{6\pi Zr} \qquad 4$$

Here, R is the gas constant, N is Avogadro's number, T is the temperature, Z is the viscosity of the solvent and r is the radius of the diffusing particle. There are a number of assumptions in this relationship, with the most relevant being that the particles are hard spheres. Because glycogen is not a hard sphere, DLS is only able to measure an apparent molecular size as opposed to an absolute size.

1.3.3 Transmission electron microscopy

Transmission electron microscopy (TEM) uses electrons instead of light to obtain images with significantly higher resolution than light microscopes. This higher resolution results from the considerably shorter wavelength of electrons compared to visible light. Because electrons are used instead of light, a viewing screen that translates electron intensity to light intensity is required[62].

The image resolution of TEM can be expressed in terms of the Rayleigh equation for light microscopy (Equation 5), which gives the smallest distance able to be resolved, δ.

$$\delta = \frac{0.61}{\mu \sin \beta}\lambda \qquad 5$$

Here, μ is the refractive index of the viewing medium, λ is the wavelength of the electrons and β is the semi-angle of the magnifying lens. The constant (0.61) comes from the Rayleigh criterion that estimates angular resolution based on diffraction patterns. This usually results in the resolution being approximately half of the wavelength[62].

1.4 Type 2 Diabetes

Type 2 diabetes, a disease associated with poorly controlled blood-glucose levels, is one of the Australian Government's National Health Priority Areas, with the prevalence of this disease in Australia expecting to increase from ~7.6 % in 2000 to ~11.4 % in 2025[63]. Developing countries are also undergoing rapid increases in the incidence of type 2 diabetes[64], with a recent survey showing that the prevalence and rate of increase in China is even greater than those in countries such as Australia and the United States[65]. Prevention, mitigation, and treatment are critical problems, which have attracted considerable research resources worldwide; despite this effort, problems associated with type 2 diabetes are increasing because of lifestyle changes.

Knowledge of the components that control the initiation and progression of type 2 diabetes is still limited and the elucidation of these factors is an active part of current global research.

Reasons for the poor control of blood-glucose levels in type 2 diabetics are associated with the body's production and response to insulin, a hormone important for lowering blood-glucose levels and stimulating glycogen production. It has been shown that there is an increase in β-cell apoptosis in type 2 diabetic sufferers, resulting in a reduction of β cell mass of ~20-40%[66-68]. β cell dysfunction generally occurs in early stages of type 2 diabetes resulting in an impaired insulin release. This prevents the transitioning of the body into the fed state where hepatic glucose production is suppressed[69]. Not only is insulin secretion impaired in type 2 diabetic patients, but there is some evidence that glucagon secretion increases (see Figure 9)[70]. Because glucagon works in the opposite direction to insulin, this results in an even further increase in blood-glucose levels, as glycogenolysis is stimulated.

One of the main differences between type 2 and type 1 diabetes is that type 2 diabetic sufferers not only have an impaired insulin release, but they are also resistant or less responsive to insulin. This effect is seen mainly in the muscle (see Figure 9), which relies significantly more on insulin to transport glucose than the liver, as muscle is unable to passively acquire glucose[71,72]. Initially insulin secretion is increased to respond to the lack of insulin sensitivity[73-75], but due to the damaged β cells associated with diabetes, this compensatory effect eventually decreases, leading to hyperglycemia.

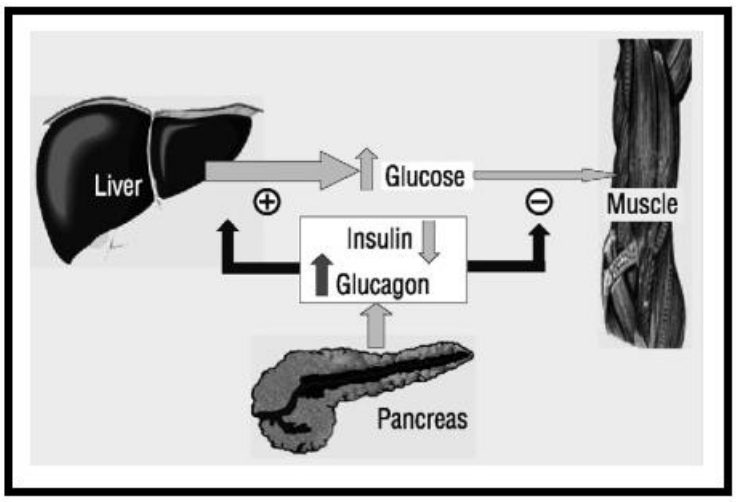

Figure 9[70]: A schematic diagram of how hyperglycemia is caused by type 2 diabetes. Decreased insulin and increased glucagon secretion from the pancreas result in an increased release of hepatic glucose and a decrease in glucose uptake from the muscle; this results in high blood glucose levels.

There is extremely strong epidemiological evidence that obesity is linked to type 2 diabetes, with 80% of people with the disease being obese[70]. Specifically it has been statistically concluded that there is a very strong correlation between abdominal obesity and the onset of type 2 diabetes[76]. Obesity in both children and adults is a pandemic that is resulting partly due to our genetic ability to store energy efficiently[77] (evolving over millions of years during times of less accessibility to large amounts of food) in combination with today's access to large amounts of high-calorie food[78,79].

Through a series of experiments it was shown that increased levels of diacylglycerol (resulting from high levels of free fatty acid concentrations) may activate specific protein kinases that lead to insulin resistance. This provides an explanation for the link between obesity and insulin resistance, since the adipose tissues in obese people have been shown to be dysfunctional, resulting in increased levels of free fatty acids[19,20].

1.4.1 The discovery of the type 2 diabetic db/db mouse and leptin

The diabetes (*db*) mutation in mice, occurring in an inbred mouse strain (C57BL/Ks) from the Jackson Laboratory, was first reported in 1966. This mutation is inherited as an autosomal recessive unit with complete penetrance, with homozygote (*db/db*) mice being infertile, having an increased fat accumulation, hyperglycemia and a shortened life span. Heterozygote (*+/db*) female mice however, cannot be distinguished physiologically from the wild type (+/+) mice[80].

This mutation exhibits a similar phenotype to the autosomal recessive obese gene (*ob*), reported approximately 17 years earlier (from the inbred C57BL/6 strain at the Jackson Laboratory),[81] which also results in infertility, increased fat accumulation and hyperglycemia; however the lifespan of *ob/ob* mice is longer than that of *db/db* mice. While causing similar phenotypes, the *ob* mutation is on chromosome 6 and results in the inability to produce the satiety factor, now called leptin[82,83]; the *db* gene however, is located on chromosome 4 and results in a dysfunctional leptin receptor[84,85]. The elegant experiments that led to the elucidation of the mechanism behind these phenotypes has been outlined in a review by Coleman[86]. In summary, the determination that *ob/ob* mice lacked a certain blood-borne satiety factor and that *db/db* mice, while producing an excessive amount of this factor were unable to effectively respond to it, was determined using a number of parabiosis experiments. This involved the surgical combining of pairs of mice, which upon healing established cross circulation, allowing any potential blood-borne factors to be exchanged. A summary of the parabiosis experiments performed is given in Figure 10. One of the key insights, that *db/db* mice contain an excessive amount of a satiety factor in the blood, but are resistant to it, was deduced from the parabosis of *db/db* mice with wild type (+/+) mice[87]. As seen in Figure 10A, when joined with *db/db* mice, wild type mice drastically reduced their food intake to such an extent that they died of starvation. After it was subsequently shown that *ob/ob* mice, when parabiotically combined with *db/db* mice (Figure 10B) also died of starvation[88], it was clear that *ob/ob* mice were able

to respond to this satiety factor. When surgically joined with wild type mice (Figure 9C), *ob/ob* mice began to consume approximately the same amount of food as wild type mice, leading to a reduction in obesity, insulinemia and blood-glucose levels. This indicated that *ob/ob* mice did not produce the satiety factor observed both in wild type, and in elevated levels in *db/db* mice[88].

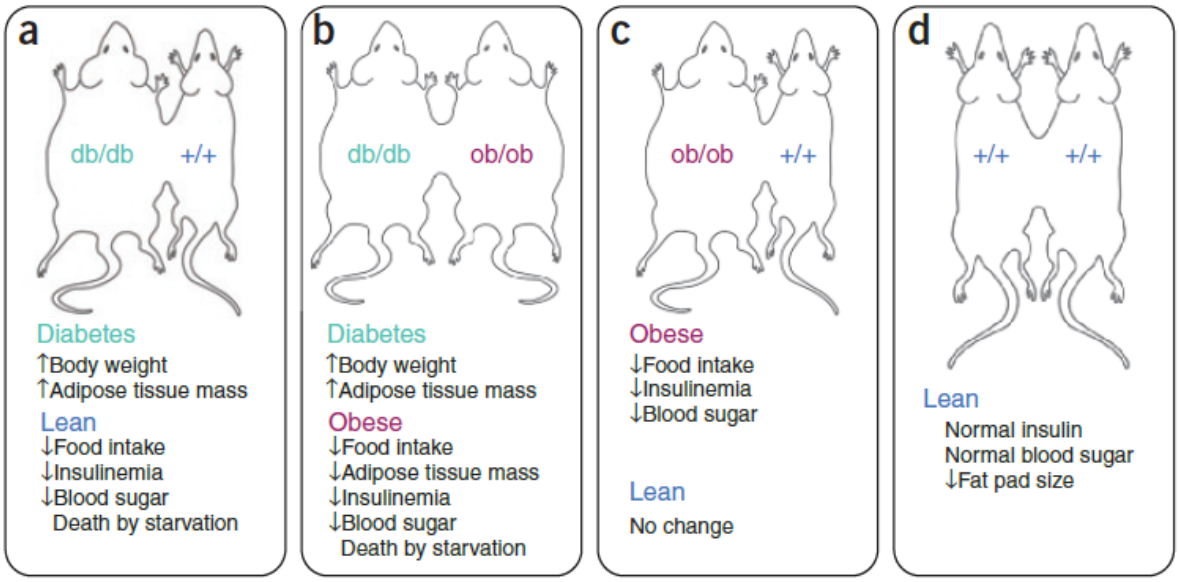

Figure 10:[86] A summary of the key parabiotic experiments performed to elucidate the mechanism behind the phenotypes of *ob/ob* and *db/db* mice.

1.5 Glycogen and Diabetes

Comparisons of the liver-glycogen content of non-diabetic and *db/db* mice has been inconsistent in the past, with some studies reporting similar levels[89], while others have reported diabetic mice having a 2-3 fold increase in hepatic glycogen levels[90,91]. It was suggested that perhaps the discrepancies arose due to an inconsistency in the time of which tissue samples were collected[92]. Given the diurnal nature of glycogen metabolism in many animals such as mice[55,93-95], it is possible that at some stages of this cycle the liver-glycogen content is similar between diabetic and non-diabetic mice, whereas at other stages the diabetic mice have significantly more liver glycogen. This was shown to be the case, as shown in Figure 11, with the liver-glycogen content between *db/db* and non-diabetic mice being similar sometimes during the diurnal cycle, while being much higher in the *db/db* mice at other time points[92]. While non-diabetic mice have a steady decrease in liver-glycogen levels during the light period of a light/dark (day/night) cycle, *db/db* mice consistently have high levels. One suggested reason for this maintained level of hepatic glycogen is that *db/db* mice continue to eat during the light hours[92].

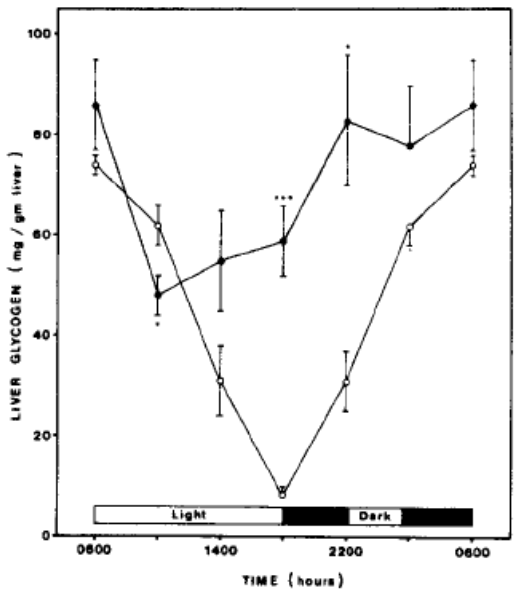

Figure 11[92]. The hepatic glycogen content of control (white circles) and *db/db* (black circles) mice over the course of one diurnal light/dark cycle.

The first indication that *db/db* (on the C57BL/KsJ background) mice may have a different glycogen structure to that of control mice, was the observation that the activity of glycogen synthase was higher in the supernatants after sucrose density centrifugation (used to fractionate glycogen into different sizes) of *db/db* mouse glycogen compared to the controls. As the majority of glycogen synthase is bound to glycogen (diabetic and healthy glycogen having the same affinity for glycogen synthase[20]), this indicated that there were a higher proportion of glycogen molecules that did not sediment; as these are likely to be smaller molecules, this suggested *db/db* samples had a higher proportion of small molecules compared to non-diabetic (*db*/+) glycogen[96,97]. This was then supported by further sucrose density centrifugation experiments, where it was observed that the glycogen from *db/db* mice was missing the "heavier" fraction that was present in the control mice[96]. However, one limitation with this observation was that only a small number of mice were compared (3 separate experiments of just one non-diabetic and one diabetic mouse each time). Also while qualitatively useful, as sucrose density centrifugation separates based on the size, density and the shape of particles, it

is unable to produce quantitative distributions. Size exclusion chromatography however, separates based on size (hydrodynamic volume) and thus, with careful calibration, is able to produce semi-quantitative distributions of glycogen[7]. Recently we compared the SEC distributions of *db/db* mice (females on the C57BL/6J background) to that of controls (*db/+*, +/+), showing that the diabetic glycogen consists of predominantly β particles, while non-diabetic glycogen varied greatly between mouse samples. Some control mouse samples had similar distributions to the *db/db* mice (with few α particles), while others consisted of a large proportion of α particles[38]. This indicates that glycogen is not just simply larger in non-diabetic mice, compared to these diabetic mice, but that non-diabetic mice have a more flexible glycogen metabolism, in which the size distribution of glycogen molecules is dynamic. Diabetic mice however, appear to be locked into having a distribution of small glycogen molecules. It is possible that the small variation in the liver-glycogen content of *db/db* mice (see Figure 11) partially explains the similar lack of variation in glycogen size distributions.

Figure 12(A-C) shows the SEC weight distributions of healthy (*db/+*, blue, A; +/+, green, B) liver glycogen, compared to type 2 diabetic liver glycogen (*db/db*, red, C). Figure 12D shows the weight distribution of liver glycogen from young *db/+* (blue) and young *db/db* (red) mice. The young *db/db* mice were not yet obese or diabetic and were still able to make larger α particles. This provides some evidence that the lack of α-particle formation seen in adult *db/db* mice is not simply a result of having a dysfunctional leptin receptor (the genotypic characteristic of the *db/db* mouse), but is a result of the obesity/diabetes caused by this mutation[98].

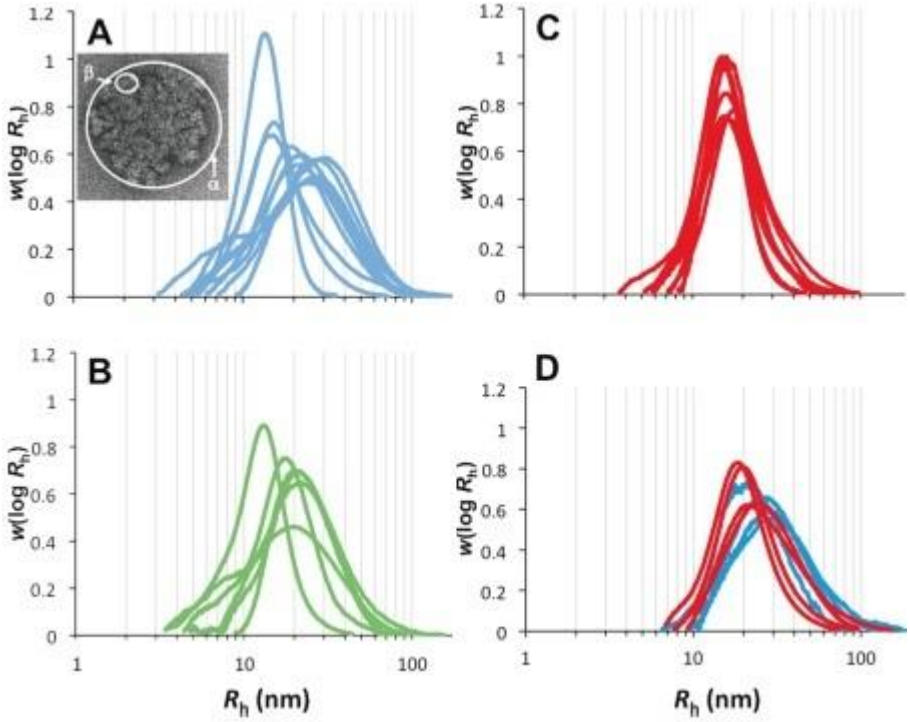

Figure 12[98]: SEC weight distributions of liver glycogen from adult non-diabetic mice (*db/+*, blue, A; +/+, green, B), adult diabetic mice (*db/db*, red, C) and young non-diabetic (*db/+*, blue, D) and diabetic (*db/db*, red, D) mice. Inserted in A is a TEM image of healthy mouse liver glycogen (showing a large α particle ~ 150 nm in diameter that is an assembly of smaller β particles).

Figure 13 shows the weight-average molecular weight of non-diabetic and diabetic mouse-liver glycogen. This also shows how diabetic mice seem unable to produce large α particles (with weight-average molecular weights ~10^7, typical of β particles). Again, non-diabetic glycogen shows a much higher variability indicating more flexibility.

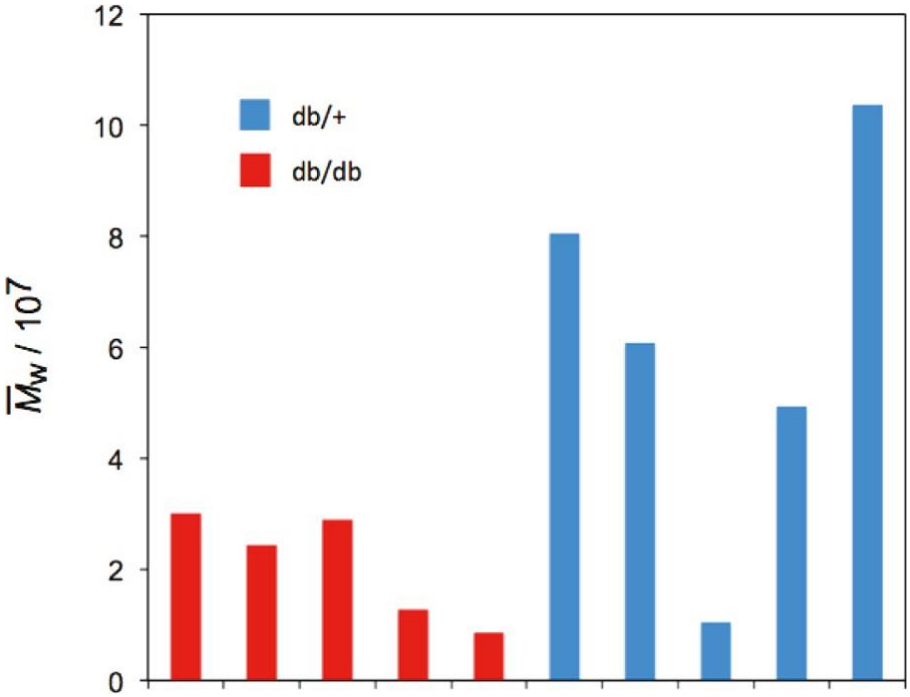

Figure 13[98]**:** The weight-average molecular weight of glycogen from non-diabetic (*db/+*, blue) and diabetic (*db/db*, red) mouse liver.

We suggested[38] that a population of small β particles would be more susceptible to enzymatic degradation, due to the increased surface area to volume ratio and thus exposed chain ends available to be hydrolyzed. This hypothesis is supported by a study that showed that glycogen phosphorylase did indeed have a higher activity for smaller glycogen particles. While this was in the direction of synthesis, it still supports the idea of surface area to volume ratio being important for glycogen phosphorylase action, with a similar trend expected to be seen in the direction of degradation[99]. Glycogen phosphorylase has also been shown to be more associated with[100], and have a higher *in vitro* activity for[31], smaller glycogen particles.

Chapter 2: Molecular Insights into Glycogen α-Particle Formation

2.1 Introduction

This section focuses on obtaining a better understanding of the fundamental characteristics of glycogen structure, with a particular emphasis on determining how α particles are held together. By increasing our understanding of glycogen's structure, we can gain insight into its biosynthesis and degradation. Past discrepancies in the literature regarding the bonding in α particles, explained in section 1.1.4, are resolved here using dynamic light scattering (DLS) and SEC to examine the effects of various reagents designed to test a number of postulated links between β particles. The Supporting Information is given in Appendix 1.

Article

pubs.acs.org/Biomac

Molecular Insights into Glycogen α-Particle Formation

Mitchell A. Sullivan,[†] Mitchell J. O'Connor,[†] Felipe Umana,[†] Eugeni Roura,[†] Kevin Jack,[‡] David I. Stapleton,[§] and Robert G. Gilbert*[,†]

[†]Centre for Nutrition & Food Sciences (Building 83/S434), Queensland Alliance for Agriculture and Food Innovation, The University of Queensland, Brisbane, Qld 4072, Australia

[‡]Centre for Microscopy and Microanalysis, The University of Queensland, Brisbane, Qld 4072, Australia

[§]Department of Physiology, The University of Melbourne, Parkville, Victoria 3052, Australia

Supporting Information

ABSTRACT: Glycogen, a hyperbranched complex glucose polymer, is an intracellular glucose store that provides energy for cellular functions, with liver glycogen involved in blood-glucose regulation. Liver glycogen comprises complex α particles made up of smaller β particles. The recent discovery that these α particles are smaller and fewer in diabetic, compared with healthy, mice highlights the need to elucidate the nature of α-particle formation; this paper tests various possibilities for binding within α particles. Acid hydrolysis effects, examined using dynamic light scattering and size exclusion chromatography, showed that the binding is not simple α-(1→4) or α-(1→6) glycosidic linkages. There was no significant change in α particle size after the addition of various reagents, which disrupt disulfide, protein, and hydrogen bonds and hydrophobic interactions. The results are consistent with proteinaceous binding between β particles in α particles, with the inability of protease to break apart particles being attributed to steric hindrance.

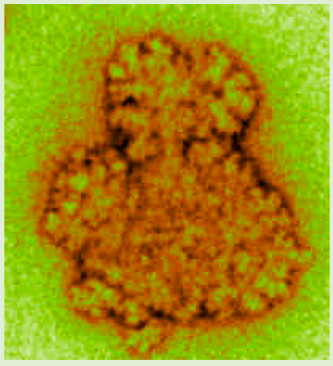

INTRODUCTION

Glycogen is a hyperbranched glucose polymer with an assembly of linear chains of α-(1→4)-linked D-glucose residues connected via α-(1→6) branching linkages. Glycogen comprises smaller glycogen β particles (~10^6−10^7 Da), which can also form much larger rosettes denoted as α particles.[1,2] Whereas α particles are often regarded as a special feature of liver glycogen structure, they have been reported to exist in insect flight muscle,[3] rat muscle,[4] mouse cardiac tissue[5] and even the brain tissue of an infant suffering from glycogenosis.[6]

Although several studies have provided clues into the formation of and binding in α particles, there are conflicting data and theories regarding both how these particles form and what bonds hold them together. It has been acknowledged in a recent review that the chemical basis for the holding together of α particles is not well understood.[2] Possibilities include disulfide linkages and other binding arising from the protein scaffold present in glycogen,[7,8] hydrogen bonding and hydrophobic interactions (addressed by Orrell and Bueding[9]), glycosidic linkages,[10] and chain entanglement.

Liver glycogen, with a molecular size distribution ranging from small β to large α particles,[11−13] acts as a blood glucose buffer, playing a significant role in maintaining blood glucose homeostasis.[14,15] After the recent discovery[12] that db/db mice, a mouse model for type 2 diabetes, are unable to form many large α particles, the question of how these particles form and what holds them together has become of particular interest because it is likely that degradation of α particles into glucose would be slower (and hence more controlled) than in the same mass of β particles due to a lower amount of exposed chains. There are a number of possibilities for this binding, given in the following short overview.

Hydrogen Bonding and Hydrophobic Effects. Past studies have tested a range of disaggregating (hydrogen-bond and hydrophobic disrupting) agents on α particles and have found no effect on overall molecular weight.[9] The number size distributions of liver glycogen[16] are found to be monotonically decreasing in size. This suggests that the process resulting in combined β particles is not aggregation, which would instead give a number distribution with a maximum occurring at some optimal aggregation size. Furthermore, if glycogen was aggregated due to hydrogen-bonding or hydrophobic effects then this would also be expected to occur in the muscle, but muscle glycogen generally comprises few, if any, α particles. If α particles were, however, covalently connected, then there could be a difference in the regulation of the glycogen-producing enzymes causing the differences in glycogen molecular size distributions observed in different tissues such as liver and muscle.

Protein and Disulfide Bonding. After the determination that a gluco-protein (glycogenin) is the precursor for glycogen synthesis and the suggestion[7] that this protein may be involved in the binding in α particles, it was reported[8] that there was an elimination of large glycogen particles upon treatment with 2-mercaptoethanol. This reagent disrupts disulfide bonds, with the reduced sulfhydryl groups being subsequently blocked by

Received: August 12, 2012
Revised: September 21, 2012
Published: September 24, 2012

the addition of iodoacetamide. This resulted in the conclusion that α particles are composed of β particle units attached by disulfide linkages.[8,17] It was, however, suggested[18] that the reported reduction in α particles could be caused by a byproduct of the reaction, hydroiodic acid, which may have hydrolyzed the α particles.

Glycosidic Linkages. Another study[10] constructed size frequency histograms from transmission electron micrographs (TEMs) of glycogen treated with 2-mercaptoethanol and iodoacetamide and reported no significant size decrease; these authors suggested that α particles are created on elongated exterior chains, implying an α-(1→4) link between β particles. It has been suggested[19] that in β particles the local molecular density becomes so high after ∼12 layers of glucose monomer units that further growth cannot occur (perhaps due to inaccessibility to glycogen synthase). It is also noted that it is extremely difficult[20] to obtain, even semiquantitatively, reliable size distributions by TEM in a system as heterogeneous as extracted glycogen.

Crowding/Budding Mechanism. One can combine these ideas into a "crowding/budding" mechanism, where occasional exterior chains in a β particle are less crowded and can form new "buds" of growing branches via glycogen synthase; these branches themselves propagate, branch, and thus grow to β particles bonded to the original one. We had suggested[12] that this "crowding/budding" postulate was inconsistent with the observed glycogen number size distribution,[13] which does not show the maximum that might be expected at a size corresponding to the onset of crowding. However, we now point out that because new β particles can start after molecules reach this size, a shoulder rather than a maximum is more likely, as was observed.[13] Possible support for such a model, as opposed to one where β particles or β particle units come together to form α particles, is that it has been suggested that there is approximately one glycogenin molecule for every α particle in the liver.[21] If free β particles, each needing an initiating glycogenin molecule, were synthesized separately and then joined then there should be many more glycogenin molecules than α particles.

Crowding/Budding Model with Protein "Glue". A new "crowding/budding" model is presented here that maintains the idea that α particles are synthesized as one molecule (as opposed to being an aggregation of previously formed β particles). Our model, however, requires the link between β particles to be less stable to acid hydrolysis than the inherent α-(1→4) glycosidic linkages, with protein being the most likely candidate. Another model that consists of proteins on the outside of already formed β particles, joining them together to form α particles, is also supported by the acid hydrolysis results presented here; this model still needs to explain how β particles are initially formed given the low glycogenin levels that have been reported in liver glycogen.[21] A recent review of glycogen metabolism[2] reports a large number of proteins found to be associated with glycogen, making the idea of a protein "glue" reasonable. Interestingly, a recent study[22] found that there is a significant amount of glycogenin-1 associated with the surface of liver glycogen. The name glycogenin-1 is now used to differentiate this protein, which represents the glycogenin protein generally referred to in the literature (for which a crystal structure is available),[23] from the more recently discovered glycogenin-2. Given that the past studies that have observed approximately one glycogenin per glycogen molecule[21,24] used 10% trichloroacetic acid (TCA) in their glycogen extraction, which is shown to degrade glycogen[9,25,26] and precipitate protein,[27] it is likely that any glycogenin outside (or between) β particles was removed.

The present article systematically tests each of these possibilities by obtaining data on the size of particles resulting from treatment with reagents that would be expected to disrupt each suggested type of bonding. Glycogen was obtained from two sources: extracted from pig liver (performed at the University of Queensland Centre for Advanced Animal Science), which is expected to contain a large amount of α particles, and commercial oyster glycogen, which is expected to contain largely β particles.

MATERIALS AND METHODS

Extraction and Purification of Liver Glycogen. Glycogen was extracted from pig liver as follows: the procedures were approved through the University of Queensland animal ethics procedures. A liver sample (∼25 g) was extracted from a 106 day old male pig (Large White breed) reared at the University of Queensland Centre for Advanced Animal Science. The pig had been fed a diet composed of wheat flour (59%), egg powder (15%), casein and sucrose (5% each), and palm (6%) and sunflower (4%) oils. The pig was sedated and humanely euthanized prior to sample extraction. The liver sample was cut from the central lobe of the liver and immediately frozen in dry ice and kept at −80 °C for 6 weeks before glycogen analysis. The procedure for liver-glycogen extraction and purification with minimal degradation was similar to that described previously.[28] Liver (4 g) was homogenized in five volumes of glycogen isolation buffer, an inhibitor of glucosidase activity (50 mM Tris, pH 8, 150 mM NaCl, 2 mM EDTA, 50 mM NaF, 5 mM sodium pyrophosphate, and protease-inhibiting phenylmethanesulfonylfluoride (PMSF)). The sample was centrifuged at 6000*g* for 10 min at 4 °C with the resulting supernatant centrifuged further at 50 000*g* for 30 min at 4 °C. The pellet was resuspended in 3 mL of glycogen isolation buffer and layered over an 18 mL, stepwise sucrose gradient (25, 50, and 75% in glycogen isolation buffer). The sample was centrifuged at 300 00*g* for 2 h at 4 °C. The glycogen fraction pelleted through all three sucrose layers, whereas the microsomal layer penetrated only to the 25−50% sucrose fraction. The supernatant was discarded, and the pellet was resuspended in 1 mL of 80% ethanol. The sample was then centrifuged at 4000*g* for 10 min at 4 °C, and the supernatant was discarded. This ethanol precipitation step was repeated once more; the pellet was resuspended in 1 mL of deionized water and then lyophilized (freeze-dried; VirTis, Benchtop K).

Characterization of Glycogen. It is essential for these experiments that the oyster glycogen particles comprise largely β particles and that the pig-liver glycogen contains a significant number of α particles. The characterization of these was performed using transmission electron microscopy (TEM), size-exclusion chromatography (SEC) with differential refractive index (DRI) detection, and multiple-angle laser light scattering without size separation ("batch MALLS"). Batch MALLS is necessary because some shear scission of larger molecules will occur in SEC.[29]

TEM images of glycogen were obtained by a method similar to that used elsewhere.[28] Oyster type III glycogen (from Sigma) and pig-liver glycogen were resuspended in 50 mM Tris buffer (pH 7.4) at ∼1 mg mL^{-1}. This suspension was then diluted 10-fold and applied onto a glow discharged copper grid (400 mesh). After 2 min, excess sample was drawn off with filter paper, and two to three drops of 1% uranyl acetate was used to stain the sample. The preparations were examined using a JEOL 1010 transmission electron microscope operating at 100 kV. Micrographs were recorded digitally using a SIS Veleta CCD camera and reports and measurements were prepared using the AnalySiS image management software.

SEC requires a molecularly dispersed solution of the analyte prepared without degradation, which was implemented following a previous procedure.[30,31] Glycogen was dissolved in the desired SEC eluent of dimethyl sulfoxide (DMSO; HPLC grade, Sigma-Aldrich)

with 0.5 wt % LiBr (ReagentPlus) on a thermomixer at 80 °C for 6 h; this gives complete molecular dissolution. The glycogen concentrations were ~1.5 g L^{-1}. SEC separates by hydrodynamic volume or the corresponding hydrodynamic radius R_h; SEC data are reported here as the SEC weight distribution $w(\log R_h)$.

Utilizing a procedure described in the literature,[13] samples were injected into an Agilent 1100 Series SEC system (PSS, Mainz, Germany) using a GRAM preColumn, 30 and 3000 columns (PSS) in series, in a column oven at 80 °C. The chromatography was carried out at a flow rate of 0.3 mL min^{-1} to minimize shear scission of the glycogen.[29] The system used a refractive index detector (RID) (Shimadzu RID-10A, Shimadzu, Japan) to allow the determination of SEC weight distributions.

Pullulan standards (PSS), with an MW range of 342 Da to 2.35 × 10^6 Da, were directly dissolved into eluent and run through the system to generate a universal calibration curve, allowing the determination of the hydrodynamic volume from the elution volume. The Mark–Houwink parameters for pullulan in DMSO/LiBr (0.5 wt %) at 80 °C are $K = 2.427 \times 10^{-4}$ dL g^{-1} and $\alpha = 0.6804$ (Kramer and Kilz, PSS, private communication). Whereas this means that all samples with a hydrodynamic radius above 55 nm were outside of the calibration limit, we are still able to compare relative differences in the total weight of molecules because any inaccuracies will be consistent for all samples.

Oyster glycogen was dissolved for batch MALLS in 0.5 wt % LiBr/DMSO at concentrations ranging from 0.1 to 0.3 g L^{-1}. Pig-liver glycogen was dissolved in 0.5 wt % LiBr/DMSO at concentrations ranging from 0.02 to 0.05 g L^{-1}. These concentrations gave the best signal without overloading the MALLS. The MALLS (BIC-M_wA7000, Brookhaven Instrument, New York,) was then run in batch mode, with detectors at angles 35, 50, 75, 90, and 130°. Each sample was repeated on a different day to determine a more accurate weight-average molecular weight ($\bar{M}_w$). Data were analyzed with Berry plots (see the Supporting Information).

Effects of Low pH on α Particles. To see the effects of acid on glycogen size, we dissolved pig-liver and oyster glycogen in aqueous solvent with a range of pH values and heated them in a thermomixer at 80 °C for 26 h. The apparent z-average diameter of molecules was determined at different times by dynamic light scattering (DLS) with a Zetasizer Nano (Malvern Instruments, Malvern, U.K.) after allowing the samples to equilibrate to room temperature. The different solvents used were distilled water (pH ~7), 0.1 M sodium acetate buffer (pH ~3.5), and HCl solution (pH 0.25 to 0.5).

For acid hydrolysis with SEC characterization, pig-liver and oyster glycogen were dissolved in 0.1 M sodium acetate buffer (2 mg mL^{-1}; pH ~3.5) and heated to 80 °C in a thermomixer for 10 min, 30 min, 2 h, 1 day, 2 days, 3 days, and 1 week. Pig-liver and oyster glycogen were also dissolved in deionized water (2 mg mL^{-1}) and heated in a thermomixer at 80 °C for 1 week. All samples were run in duplicate. After samples were removed from the thermomixer, four volumes of ethanol were added to each to precipitate the glycogen. Samples were centrifuged at 4000*g* for 10 min, and the supernatants were discarded. The centrifugates were dissolved in 1 mL of deionized water and lyophilized (VirTis, Benchtop K). Samples were then dissolved in the SEC eluent and characterized with the same SEC procedure as the starting materials. Pig-liver and oyster glycogen was also directly dissolved in the SEC eluent to act as an initial time point (with no acid hydrolysis). SEC results are presented as the SEC weight distribution $w(\log V_h)$, which is the weight of particles of hydrodynamic volume V_h (the SEC size separation parameter). Data are presented in terms of the corresponding hydrodynamic radius R_h ($V_h = {}^4/_3\pi R_h{}^3$).

Using a similar preparative SEC setup to that used in the literature,[32] samples at the initial time point, 2 h acid hydrolyzed, and 1 day acid hydrolyzed were run through PREP GRAM 30 and PREP GRAM 3000 columns from PSS (Mainz, Germany) in an AF2000 setup (Postnova Analytics, Landsberg-Lech, Germany) at 80 °C with a flow rate of 1.5 mL min^{-1} in the SEC eluent. Samples were manually injected using a Rheodyne 7000 high-pressure switching valve (IDEX Health & Science, Rohnert Park, CA). A DRI detector (RI 3140, Postnova) was used to obtain the weight distribution of molecules at each elution time. This preparative column setup, giving slightly better separation than the other SEC column, was employed to confirm further SEC results. Whereas it is generally necessary to calibrate SEC data to make it reproducible, because we were just interested in the shape of the elugram and all three samples were run in succession, we are able to present the data as raw signal in relation to elution time.

DLS of Glycogen Exposed to a Range of Conditions. Effects of disrupting disulfide linkages were examined as follows. As previously,[8] liver glycogen was dissolved to a concentration of 2 g L^{-1} in 0.1 M Tris buffer (pH 8.5) containing 8 M urea. Nitrogen was then bubbled through the solution for 30 min. The sample was then divided into three parts: one without further treatment (the control); one treated with 2-mercaptoethanol (0.1 mL per mL of Tris buffer, Sigma) for 30 min; and the last treated with 2-mercaptoethanol and subsequently with iodoacetamide (0.3 g mL^{-1}, Sigma). To determine whether hydrophobic interactions were important, glycogen was also dissolved in 2 wt % sodium dodecyl sulfate (SDS) in 8 M urea.

Effects of disrupting a protein scaffold were examined as follows. Glycogen (4 mg mL^{-1}) in 250 mM tricine buffer (pH 7.5) was incubated at 37 °C with 0.9 units mL^{-1} protease (bacterial type XIV, Sigma) for 30 min. Samples were then centrifuged (4000*g*, 10 min), and the supernatant was discarded. Half of the samples were subsequently treated with 0.45% bisulfite solution and incubated at 37 °C for 30 min. These samples were centrifuged again (4000*g*, 10 min), and the supernatant was discarded. All samples were then dissolved in DMSO with 0.5 wt % LiBr,[30] which disrupts hydrogen bonding.

To test whether α particles were held together by hydrogen bonding, glycogen dissolved in DMSO and in DMSO + 5 wt % LiBr (which disrupts very strong H-bonding) were examined.

All samples were measured in quadruplicate.

The apparent z-average diameter of molecules was determined by DLS with a Zetasizer Nano (Malvern Instruments). This DLS instrument uses back scattering (173°) to infer an apparent molecular size. A major problem with applying this to a dissolved complex branched molecule such as glycogen is that DLS probes not only overall center-of-mass motion (whence a z-average size is inferred) but also all types of local motions and sensitivity to the latter (which are, in general, unrelated to overall size) increase with increasing scattering angle, which should be <35° to minimize this artifact.[33−35] It has also been shown that α particles and β particles exhibit different internal dynamical properties, which would affect the DLS data interpretation due to the local mode artifact.[36]

RESULTS AND DISCUSSION

Characterizing Starting Materials. Figure 1A shows a TEM image of oyster glycogen, with particle sizes corresponding to that of β particles at ~20−30 nm in diameter. Figure 1B shows a TEM image of pig-liver glycogen, showing that this contains glycogen particles ranging from β particles up to large α particles ~200 nm in diameter. The SEC distribution given in Figure 1C and the batch MALLS $\bar{M}_w$ data in Table 1 confirm the TEM results.

Effects of Low pH on α Particles. Figure 2 shows the change of the apparent z-average size of both pig and oyster glycogen exposed to a range of pH values.

Figure 3 shows SEC elugrams of pig-liver glycogen initially (A), after 2 h (B), and after 1 day (C) of being exposed to pH ~3.5 at 80 °C. Because larger particles elute first in SEC, the α-particle peak comes before the smaller (largely β-particle) peak.

Calibrated SEC was used to characterize both pig-liver and oyster glycogen before acid hydrolysis and at 10 min, 30 min, 2 h, 1 day, 2 days, 3 days, and 1 week after being exposed to pH ~3.5 at 80 °C. Data for the first 2 h of digestion are given in Figure 4, with the final time points between 1 day and 1 week being presented in Figure 5.

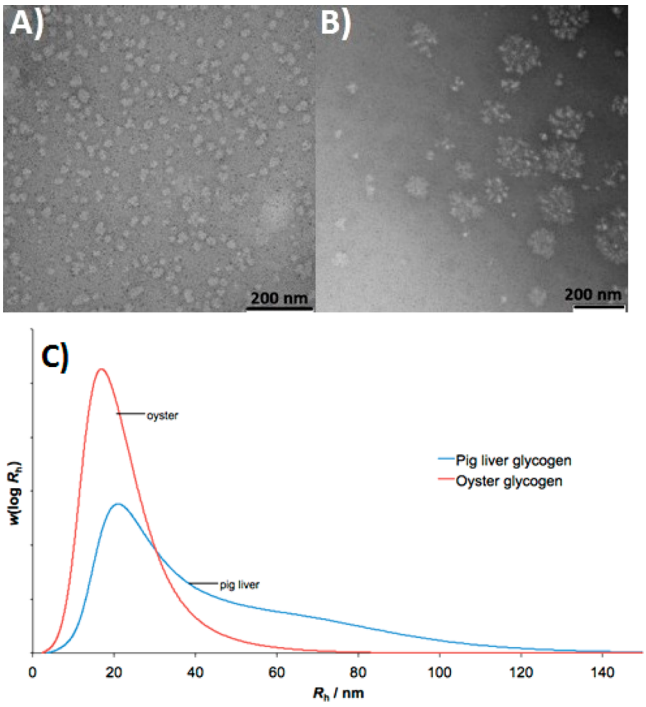

Figure 1. TEM of oyster glycogen (A) and of pig-liver glycogen (B). SEC weight distribution (C) of oyster glycogen (red) and pig-liver glycogen (blue). Both SEC distributions are normalized to equal area.

Table 1. Batch MALLS Results Giving Weight-Average Molecular Weights for Pig-Liver and Oyster Glycogen

sample	$\bar{M}_w/10^6$ Da
pig-liver glycogen	28.7 ± 0.26
oyster glycogen	7.1 ± 0.74

Figure 2 shows pig-liver glycogen under acidic conditions (at 80 °C) degrading over time, with the apparent z-average size of particles approaching that of the oyster β particles after ~26 h. The fact that these molecules appear to be degraded much more than the oyster glycogen suggests that the links between β particles are more susceptible to acid hydrolysis than glycogen α-(1→4) linkages. This is in agreement with early centrifugation experiments[9] and TEM images that found no α particles at pH < 4.[16]

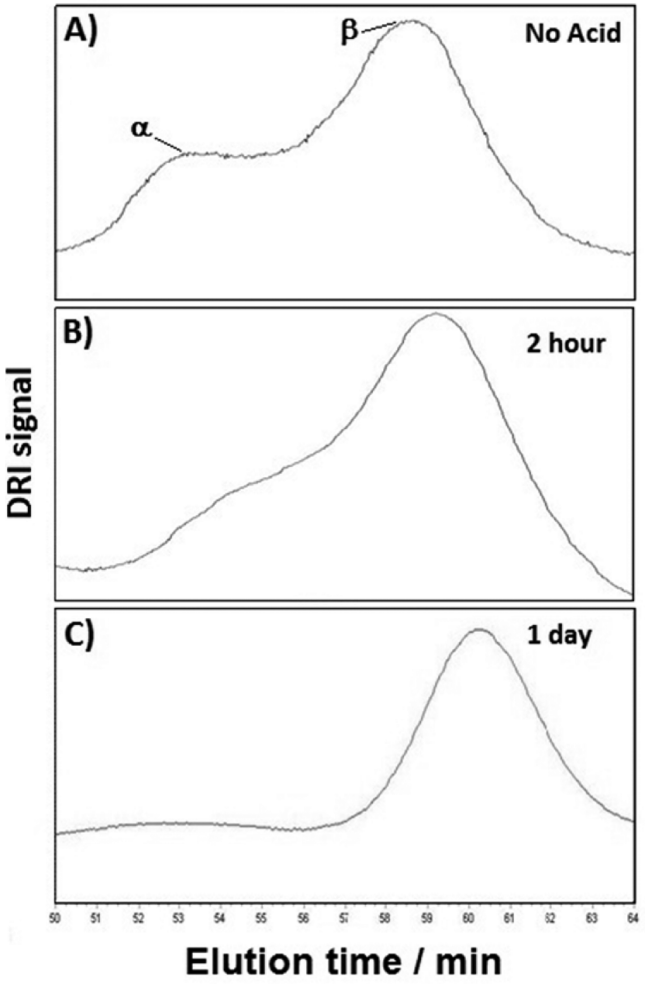

Figure 3. Raw SEC DRI signal of samples separated using preparative SEC separation, with all data obtained in the same run; samples are pig-liver glycogen with no acid hydrolysis (A) after 2 h of acid hydrolysis (B) and after 1 day of acid hydrolysis (C).

To confirm this finding, SEC distributions of both pig-liver and oyster glycogen exposed to pH ~3.5 (at 80 °C) for different times between 10 min and 1 week were obtained (Figures 3–5). The advantages of using SEC are that DLS artifacts[33–35] are avoided and also that each sample is dissolved

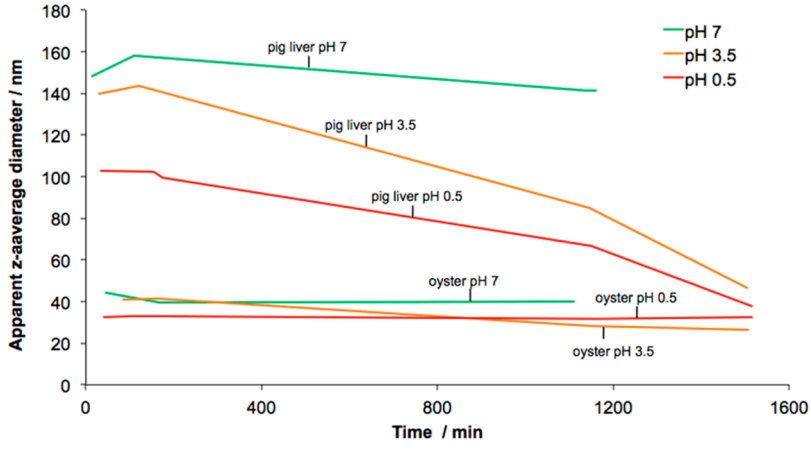

Figure 2. Apparent z-average of pig-liver and oyster (green, pH ~7; orange, pH ~3.5; red, pH 0.25 to 0.5).

dx.doi.org/10.1021/bm3012727 | *Biomacromolecules* 2012, 13, 3805–3813

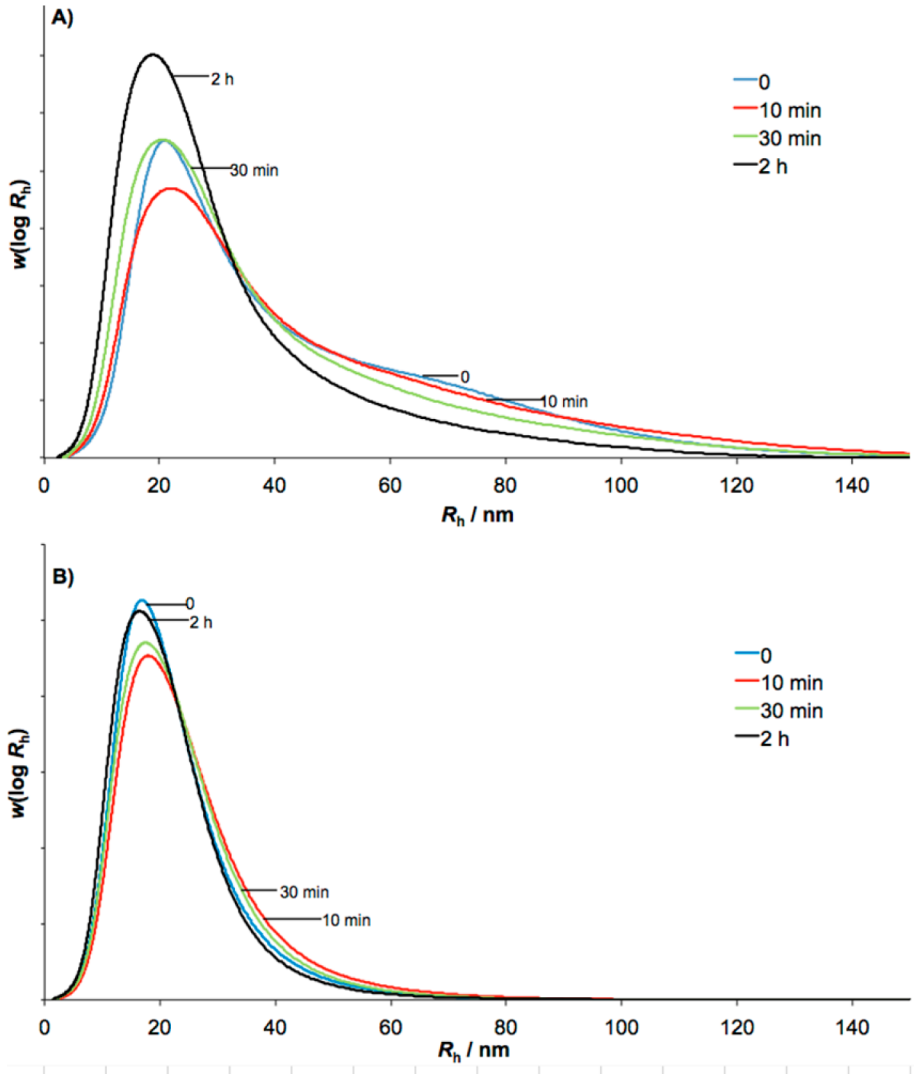

Figure 4. SEC weight distributions for first the 2 h of acid hydrolysis; pig liver (A) and oyster (B) glycogen before acid hydrolysis and after 10 min, 30 min, and 2 h of acid hydrolysis. Curves are normalized to equal areas. Replicate experiments show the same trend. (See the Supporting Information.)

in the same solvent. Whereas the DLS results show what appears to be degradation at low pH, it may be that the negative charge acquired by glycogen following incubation in low pH buffers[37] may be disrupting any noncovalent interaction such as hydrogen bonding.

It can be seen clearly from the elugram in Figure 3 that α particles are degrading preferentially, although smaller (largely β) particles still experience some hydrolysis. Calibrated SEC was also used to obtain confirm that α particles are preferentially degraded by acid hydrolysis.

Confirming DLS and preparative SEC results, the pig-liver glycogen (Figure 4A) shows a significant decrease in α particles after being exposed to low pH for 2 h, with smaller (largely β) particles, both pig-liver (A) and oyster (B), remaining relatively undegraded. If α particles were connected via α-(1→4) linkages, then the distributions would be expected to maintain the same shape as the particles degrade, as all molecules should decrease in size (as a proportion of the whole molecule) at the same rate. This, however, is not seen, with the shape of the distributions being altered as α particles degrade at a faster rate than that of β particles.

For the final stages of acid hydrolysis (1 day to 1 week) both pig-liver (Figure 5A) and oyster glycogen (B) show very similar degradation behavior, which is to be expected, because after 1 day pig-liver glycogen appears to comprise smaller (largely β) particles exclusively and is then thus similar to oyster glycogen.

Figure 6 shows the effect of heating pig-liver (6A) and oyster (6B) glycogen in deionized water at 80 °C for 1 week. These results show that α particles are also hydrolyzed by water at this temperature and that this neutral water hydrolysis at elevated temperatures, as with the acid hydrolysis, preferentially degrades the link between α particles.

Because a protein backbone is covalently linear and glycogen after acid hydrolysis is dissolved in DMSO/LiBr, a potent disrupter of hydrogen bonds, hydrolysis of just one peptide bond would be sufficient to sever completely any link potentially provided by this protein "glue". Glycogen, however, is a highly branched molecule, so any single breakage of an α-(1→4) or α-(1→6) bond will remove only a part of the molecule, and with ∼50% of the molecule being present in outer chains,[38,39] the amount of molecule to be separated from one bond breakage is likely to be relatively small. This means that ∼50% of bonds being hydrolyzed will result in the

dx.doi.org/10.1021/bm3012727 | *Biomacromolecules* 2012, 13, 3805−3813

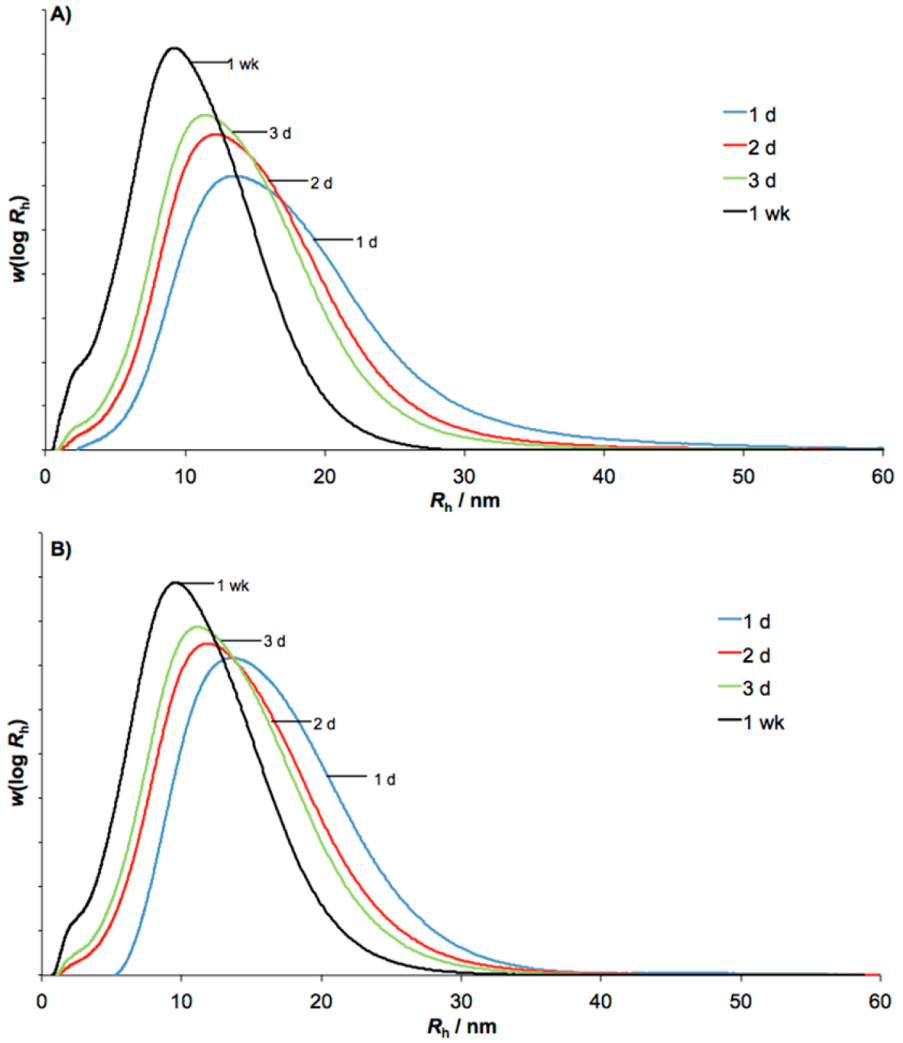

Figure 5. SEC weight distributions for final stages of acid hydrolysis; pig liver (A) and oyster (B) glycogen after 1 day, 2 days, 3 days, and 1 week of acid hydrolysis. Curves are normalized to equal areas. Replicate experiments show the same trend. (See the Supporting Information.)

production of a small chain and a molecule that is of approximately the same size as the molecule before this hydrolysis. As this continues, the SEC-distribution maximum would decrease with the formation of more and more smaller molecules. The hydrolysis of inner glycogen chains will also occur, causing an even greater decrease in the SEC-distribution maximum. This predicted trend is consistent with Figure 5, with the maximum steadily decreasing and the gradual formation of a small shoulder of molecules. It should be noted that many of the small molecules will have been removed in the ethanol precipitation step[40−42] during sample preparation and thus are not seen in the SEC distribution. The minimal degradation of β particles in the first 2 h of exposure to an acidic environment (Figure 4B) indicates that this hydrolysis is relatively slow compared with the degradation of α particles.

It should also be noted that α-(1→6) bonds are much more resistant to acid hydrolysis than α-(1→4),[43,44] making it less likely for whole branches to be removed. This may seem contradictory to the observation that high amylose starches, which contain fewer α-(1→6) linkages, are more acid-resistant than starches with lower amylose contents. However, the analysis of the chain length distributions of different acid-hydrolyzed starches has shown that amylose chains are more susceptible to acid hydrolysis than the shorter amylopectin chains and that a possible reason for the increased acid resistance of high amylose starches is that their hydrolysis results in the production of larger nanoparticles.[45]

It is also unlikely that α particles are held together by other glycosidic linkages because the kinetics for the acid hydrolysis of α-(1→2) and α-(1→3) are very similar to that of α-(1→4), and the acid hydrolysis of the anomeric β glycosidic linkages, while more thermodynamically favorable, occurs at slower rates than glycosidic linkages.[43,46]

It is well-established that peptide hydrolysis is catalyzed by acid,[47] and whereas complete hydrolysis of proteins into single amino acids requires very low pH values at high temperatures, partial hydrolysis occurs under much milder conditions[48] and even occurs spontaneously in water at neutral pH.[49] The first-order rate coefficient for the hydrolysis of internal peptide bonds (exemplified using acetylglycylglycine *N*-methylamide) under neutral conditions has been studied over a range of temperatures.[49] By assuming an Arrhenius form and extrapolating their results to 80 °C (see the Supporting Information), the rate coefficient is estimated to be ∼2.0 × 10^{-8} s^{-1}, corresponding to a half-life of ∼401 days. This is approximately four orders of magnitude faster than hydrolysis at this temperature of the glycosidic bonds that join polysaccharides.[35,36] Using the same first-order kinetics, it can be calculated

dx.doi.org/10.1021/bm3012727 | *Biomacromolecules* 2012, 13, 3805−3813

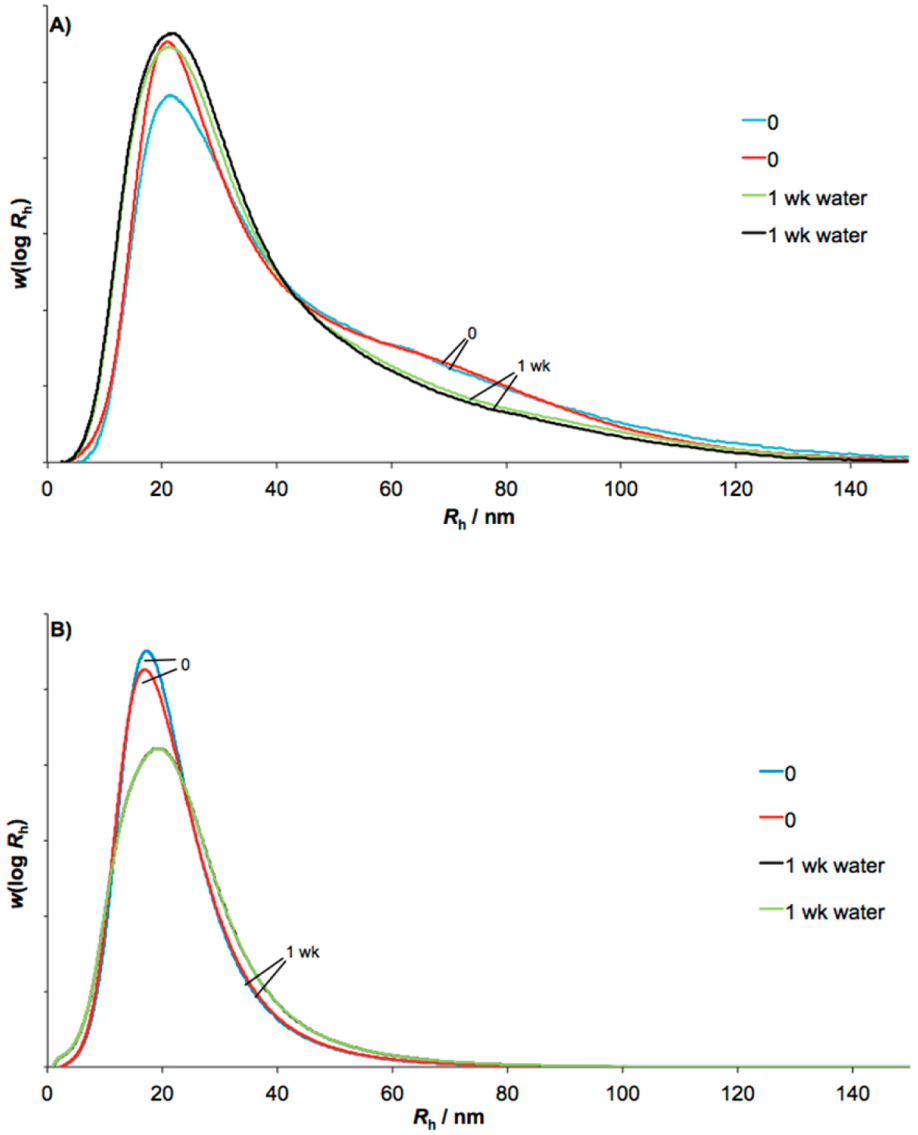

Figure 6. Pig-liver (A) and oyster glycogen (B) dissolved directly in SEC eluent (time zero) and after being heated at 80 °C in deionized water for 1 week (curves overlap entirely in panel B). Curves are normalized to equal areas.

that after 7 days ~1.2% of peptide bonds will have been hydrolyzed; given the covalently linear nature of protein, this should be sufficient to sever many of the links between β particles. Consistent with this approximate calculation, Figure 6A shows how α particles are hydrolyzed when heated to 80 °C in deionized water for 7 days, a result consistent with the hypothesis that protein holds α particles together.

***α* Particles Exposed to a Variety of Conditions.** Comparing the z-average diameter (obtained with DLS) of pig-liver to oyster glycogen (which essentially contains only β particles)[50] for each treatment suggests whether or not α particles are degraded into β particles. While there is a significant amount of overlap between the oyster and the pig-liver glycogen size distributions (see Figure 1C), the intensity of scattered light measured in DLS is proportional to the sixth power of the diameter, making it highly sensitive to higher molecular sizes.

Exposing β particles to the same procedure as the liver glycogen gives the apparent z-average diameter of β particles in each solvent. This allows us to infer whether α particles break up under a range of solvents and reagents, in which case the apparent z-average size would be similar to that of the oyster glycogen. Because β particles from oyster glycogen may be slightly different from those in pig liver, only large differences in the z-average diameter between the liver and oyster glycogen can be used to infer whether α particles are or are not broken apart. Because β and α particles have different dynamical properties in solution,[51] the degradation of α particles to β particles would have large effects not only on center-of-mass motion but also on all but the shortest local modes.

The results in Figures 7 and 8 show that β particles (typically ~30 nm in diameter) gave a large range of apparent z-average diameters in different solvents, ranging from 56 to 171 nm. Because it is unconceivable that a β particle could swell to a size of 171 nm or preferentially form aggregates in the much more solvating LiBr/DMSO (which is not seen in SEC when β particles are dissolved in this solvent), it is very likely that the varied apparent sizes are artifacts arising from DLS being sensitive to local motion at high angles. These results emphasize that DLS of complex branched molecules can give artifactual results.

dx.doi.org/10.1021/bm3012727 | *Biomacromolecules* 2012, 13, 3805−3813

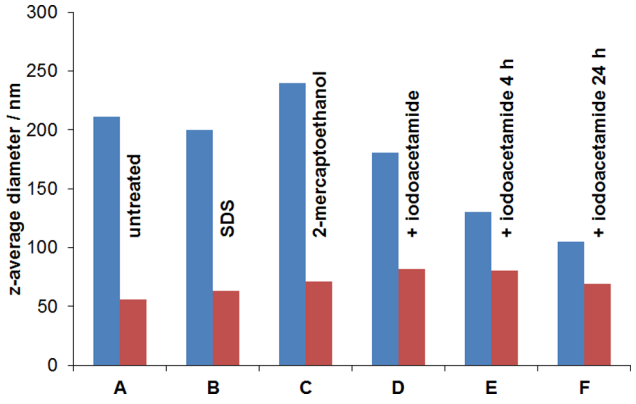

Figure 7. Apparent z-average diameter of untreated liver (blue) and oyster (red) glycogen (A); glycogen treated with 2 wt % SDS (B); glycogen treated with 2-mercaptoethanol (C); glycogen treated with 2-mercaptoethanol and iodoacetamide (D); glycogen treated with 2-mercaptoethanol, and iodoacetamide after 4 (E) and 24 h (F).

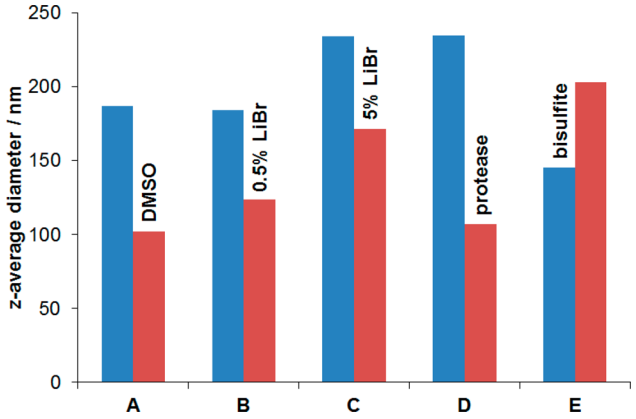

Figure 8. Apparent z-average diameter of pig-liver (blue) and oyster (red) glycogen in DMSO (A); glycogen in DMSO with 0.5 wt % LiBr (B); glycogen in DMSO with 5 wt % LiBr (C); glycogen in DMSO with 0.5 wt % LiBr treated with protease (D); and glycogen in DMSO with 0.5 wt % LiBr treated with protease and reducing agent bisulfite (E).

Figure 7 shows that there is a moderate time-dependent decrease in the apparent (DLS) size of glycogen treated with 2-mercaptoethanol and iodoacetamide (D–F), whereas 2-mercaptoethanol without iodoacetamide gave a moderate increase (C). Figure 7B shows that the introduction of the surfactant SDS, introduced to disrupt any hydrophobic interactions, has no significant effect on the apparent size of the glycogen (consistent with past experiments).[9]

Figure 8 shows the apparent size of untreated glycogen in DMSO with two LiBr concentrations, treated with protease and treated with both protease and bisulfite. In agreement with previous results,[13] 5% LiBr caused a slight increase in apparent size. Protease-treated liver glycogen also showed a moderate increase in apparent size. When treated with protease and bisulfite, a reducing agent that disrupts disulfide bonds, the apparent particle size decreased slightly for the liver glycogen. When treated with protease and bisulfite, the oyster glycogen formed aggregates: there were two peaks in the apparent size distribution obtained from the DLS software, at 100 and ~3000 nm. Whereas one must be extremely cautious with distribution reported by the DLS manufacturer's software, because there are major assumptions involved in inferring them from the raw data, they are suggestive. Consistent with this, after centrifugation this apparent 3000 nm peak was not present in the supernatant, with just a single peak at ~100 nm being observed using DLS. This aggregate formation of β particles, given that the α particles did not under the same conditions, suggests a difference in the nature of the surfaces of β and α particles. It should be noted, however, that it is possible that this difference is not between β and α particles per se but is instead a species-specific difference.

These results in Figure 7 show that α particles are not held together by disulfide bonds, as once reported by Chee and Geddes.[8] A possible reason for that reported degradation of glycogen particles may be that the byproduct hydroiodic acid caused hydrolysis.[18] We confirmed the possibility that the size diminution reported by Chee and Geddes[8] was caused by adventitious hydroiodic acid by testing the pH after the introduction of iodoacetamide, with the pH dropping from 8.5 to ~1, while the apparent size changed from 170 to 105 nm after 24 h.

Treatment with protease does not lead to a significant change in apparent size (Figure 8), consistent with past experiments.[10] Whereas the formation of free β particles from liver glycogen α particles upon protease incubation would have been strong evidence of a protein link between β particles, we suspect that the protease would not be able to diffuse within the glycogen α-particle structure because of steric hindrance.

CONCLUSIONS

Liver glycogen, a glucose polymer functioning as a blood-sugar reservoir in animals, comprises small β particles that are linked together to form larger, more complex α particles. It has recently been found that liver glycogen in diabetic mice contains fewer and smaller α particles than found in healthy mice,[12] and thus understanding the nature of the binding between β particles has significance for diabetes. The present study investigates the changes in overall size and size distribution (using static light scattering, DLS, and SEC) when glycogen is subjected to a range of reagents and conditions that should selectively break the bonds that are possible candidates for this binding. The results presented here show that the link joining β particles together, within an α particle, is more susceptible to acid hydrolysis than glycogen's inherent glycosidic α-(1→4) and α-(1→6) linkages. Hydrolytic degradation of α particles at neutral pH is also observed, with the rate of hydrolysis more consistent with protein, not glycosidic, linkages being degraded. While having to be careful when interpreting high-angle DLS data, it is clear that α particles are not degraded by disulfide-bond-disrupting 2-mercaptoethanol or hydrophobic-interaction-disrupting SDS. Whereas protease treatment did not result in the breaking apart of α particles, it is quite possible that steric hindrance prevented the protease from accessing the proteins between the particles. The data are therefore most consistent with proteinaceous links between the β particles to form α rosettes. One possibility is for this protein to be glycogenin-1, believed to be located within the glycogen core, but recently this was shown to be an abundant protein associating with the surface of liver glycogen particles.[22] Proteomics work directed at the question of whether glycogenin-1 is as prevalent on the surface of liver glycogen from diabetic mice may help explain their inability to form as many large α particles as healthy mice. This knowledge is of potential interest in improved understanding of Type 2 diabetes.

■ ASSOCIATED CONTENT

Supporting Information

Replicate SEC distributions of acid hydrolysis experiments, batch MALLS Berry plots, and calculation of the rate constant for the uncatalyzed hydrolysis of acetylglycylglycine *N*-methylamide at 80 °C. This material is available free of charge via the Internet at http://pubs.acs.org.

■ AUTHOR INFORMATION

Corresponding Author

*E-mail: b.gilbert@uq.edu.au.

Notes

The authors declare no competing financial interest.

■ ACKNOWLEDGMENTS

We thank Drs. Barbara Williams and Helen Keates for help with the sample collection and Mr. Richard Webb for help with TEM analysis. The staff at the University of Queensland Centre for Advanced Animal Science are gratefully acknowledged for their assistance with the pig studies. Electron microscopy was carried out in the Centre for Microscopy and Microanalysis at the University of Queensland, a node of the Australian Microscopy and Microanalysis Research Facility (AMMRF). Sarah Chung is gratefully acknowledged for her skill and technical assistance with SEC measurements.

■ REFERENCES

(1) Takeuchi, T.; Iwamasa, T.; Miyayama, H. *J. Electron Microsc.* **1978**, *27*, 31.
(2) Roach, P. J.; Depaoli-Roach, A. A.; Hurley, T. D.; Tagliabracci, V. S. *Biochem. J.* **2012**, *441*, 763.
(3) Childress, C. C.; Sacktor, B.; Grossman, I. W.; Bueding, E. *J. Cell Biol.* **1970**, *45*, 83.
(4) Calder, P. C.; Geddes, R. *Carbohydr. Res.* **1985**, *135*, 249.
(5) Besford, Q. A.; Sullivan, M. A.; Zheng, L.; Gilbert, R. G.; Stapleton, D.; Gray-Weale, A. *Int. J. Biol. Macromol.* **2012**, *51*, 887–891.
(6) Towfighi, J.; Yoss, B. S.; Wasiewski, W. W.; Vannucci, R. C.; Bentz, M. S.; Mamourian, A. *Hum. Pathol.* **1989**, *20*, 1210.
(7) Krisman, C. R.; Barengo, R. *Eur. J. Biochem.* **1975**, *52*, 117.
(8) Chee, N. P.; Geddes, R. *FEBS Lett.* **1977**, *73*, 164.
(9) Orrell, S. A.; Bueding, E. *J. Biol. Chem.* **1964**, *239*, 4021.
(10) Matsuda, K.; Hata, K. *J. Jpn. Soc. Starch Sci.* **1985**, *32*, 118.
(11) Drochmans, P. *J. Ultrasctruct. Res.* **1962**, *6*, 141.
(12) Sullivan, M. A.; Li, J.; Li, C. Z.; Vilaplana, F.; Stapleton, D.; Gray-Weale, A. A.; Bowen, S.; Zheng, L.; Gilbert, R. G. *Biomacromolecules* **2011**, *12*, 1983.
(13) Sullivan, M. A.; Vilaplana, F.; Cave, R. A.; Stapleton, D. I.; Gray-Weale, A. A.; Gilbert, R. G. *Biomacromolecules* **2010**, *11*, 1094.
(14) Xu, K.; Morgan, K. T.; Gehris, A. T.; Elston, T. C.; Gomez, S. M. *PLoS Comput. Biol.* **2011**, *7*, 1.
(15) Pardridge, W. M.; Jefferson, L. S. *Am. J. Physiol.* **1975**, *228*, 1155.
(16) *W. H. O. Tech. Rep. Ser.* **2003**, *916*, i.
(17) Geddes, R.; Stratton, G. C. *Carbohydr. Res.* **1977**, *57*, 291.
(18) Manners, D. J. *Carbohydr. Polym.* **1991**, *16*, 37.
(19) Melendez, R.; Melendez-Hevia, E.; Mas, F.; Mach, J.; Cascante, M. *Biophys. J.* **1998**, *75*, 106.
(20) Lichti, G.; Hawkett, B. H.; Gilbert, R. G.; Napper, D. H.; Sangster, D. F. *J. Polym. Sci., Polym. Chem. Ed.* **1981**, *19*, 925.
(21) Smythe, C.; Villar-Palasi, C.; Cohen, P. *Eur. J. Biochem.* **1989**, *183*, 205.
(22) Stapleton, D.; Nelson, C.; Parsawar, K.; McClain, D.; Gilbert-Wilson, R.; Barker, E.; Rudd, B.; Brown, K.; Hendrix, W.; O'Donnell, P.; Parker, G. *Proteomics* **2010**, *10*, 2320.
(23) Gibbons, B. J.; Roach, P. J.; Hurley, T. D. *J. Mol. Biol.* **2002**, *319*, 463.
(24) Wyatt, P. J. *Anal. Chim. Acta* **1993**, *272*, 1.
(25) Wanson, J. C.; Drochman., P. *J. Cell Biol.* **1968**, *38*, 130.
(26) *Transmission Electron Microscopy*; Williams, D. B., Carter, C. B., Eds.; Springer: New York, 2009.
(27) Huang, L.; Yao, Y. A. *Carbohydr. Polym.* **2011**, *83*, 1665.
(28) Ryu, J.-H.; Drain, J.; Kim, J. H.; McGee, S.; Gray-Weale, A.; Waddington, L.; Parker, G. J.; Hargreaves, M.; Yoo, S.-H.; Stapleton, D. *Int. J. Biol. Macromol.* **2009**, *45*, 478.
(29) Cave, R. A.; Seabrook, S. A.; Gidley, M. J.; Gilbert, R. G. *Biomacromolecules* **2009**, *10*, 2245.
(30) Schmitz, S.; Dona, A. C.; Castignolles, P.; Gilbert, R. G.; Gaborieau, M. *Macromol. Biosci.* **2009**, *9*, 506.
(31) Syahariza, Z. A.; Enpeng, L.; Hasjim, J. *Carbohydr. Polym.* **2010**, *82*, 14.
(32) Vilaplana, F.; Gilbert, R. G. *Macromolecules* **2010**, *43*, 7321.
(33) Galinsky, G.; Burchard, W. *Macromolecules* **1997**, *30*, 6966.
(34) Yang, C.; Meng, B.; Chen, M.; Liu, X.; Hua, Y.; Ni, Z. *Carbohydr. Polym.* **2006**, *64*, 190.
(35) Dona, A.; Yuen, C.-W. W.; Peate, J.; Gilbert, R. G.; Castignolles, P.; Gaborieau, M. *Carbohydr. Res.* **2007**, *342*, 2604.
(36) Graham, T. E.; Yuan, Z.; Hill, A. K.; Wilson, R. J. *Acta Physiol.* **2010**, *199*, 489.
(37) Sterling, C. *Biopolymers* **1970**, *9*, 891.
(38) Melendez, R.; Melendez-Hevia, E.; Cascante, M. *J. Mol. Evol.* **1997**, *45*, 446.
(39) Melendez-Hevia, E.; Waddell, T. G.; Shelton, E. D. *Biochem. J.* **1993**, *295*, 477.
(40) Young, A. H. In *Starch: Chemistry and Technology*, 2nd ed.; Whistler, R. L., BeMiller, J. N., Paschall, E. F., Eds.; Academic Press: London, 1984, p 249.
(41) Everett, W. W.; Foster, J. F. *J. Am. Chem. Soc.* **1959**, *81*, 3459.
(42) Rodriguez, I. R.; Fliesler, S. J. *Arch. Biochem. Biophys.* **1988**, *260*, 628.
(43) Capon, B. *Chem. Rev.* **1969**, *69*, 407.
(44) Banks, W. *Starch/Staerke* **1973**, *25*, 405.
(45) Kim, H. Y.; Lee, J. H.; Kim, J. Y.; Lim, W. J.; Lim, S. T. *Starch/Staerk* **2012**, *64*, 367.
(46) Mikkola, S.; Oivanen, M. *ARKIVOC* **2009**, 39.
(47) Lawrence, L.; Moore, W. J. *J. Am. Chem. Soc.* **1951**, *73*, 3973.
(48) Downs, F.; Pigman, W. *Int. J. Protein Res.* **1970**, *2*, 27.
(49) Radzicka, A.; Wolfenden, R. *J. Am. Chem. Soc.* **1996**, *118*, 6105.
(50) Calder, P. C. *Int. J. Biochem.* **1991**, *23*, 1335.
(51) Wary, C.; Desvaux, H.; Van Cauteren, M.; Vanstapel, F.; Carlier, P. G.; Jehenson, P. *Carbohydr. Res.* **1998**, *306*, 479.

2.2 Outcomes

This study has provided strong evidence that glycogen α particles are held together via a linkage more acid labile than glycosidic linkages. This has led to the hypothesis of a protein "glue" that is capable of linking β particles together. If this suspected protein is proven to exist, any regulator that decreases its expression may become a promising inhibitory drug target for diabetes management, based on the impaired α-particle formation found in diabetic mice[98].

While the experiments here do not conclusively rule out long glucan chains that are more reactive to acid hydrolysis than the glucan chains within a glycogen β particle acting as the glue that holds α particles together, it is unlikley that chain length would have a significant, if any effect on the acid hydrolysis rate of the glycosidic linkages. The results presented in Chapter 5 provide further evidence that the linkages holding β particles together to form larger α particles are not glycosidic.

We also demonstrated that past studies observing the effect of 2-mercaptoethanol on glycogen structure, with the addition of iodoacetamide, did indeed result in low pHs (as Manners suggested[3]) and that it is the acidic environment, not the reducing effect of 2-mercaptoethanol that resulted in the reported degradation of glycogen α particles.

Chapter 3: Changes in Glycogen Structure over Feeding Cycle Sheds New Light on Blood-Glucose Control

3.1 Introduction

While the previous chapter has indicated the potential of a protein "glue" in holding α particles together, it is still unclear when during the glycogen cycle these particles are formed. One significant limitation to our previous study that compared the structure of liver glycogen from

healthy and diabetic mice[38], is that all of the mice were sacrificed at approximately the same time during the day (~9 am), instead of taking into account the whole diurnal cycle of glycogen metabolism.

As described in section 1.2.4 above, there have been discrepencies in the literature regarding the metabolism of glycogen in terms of structure, with some studies[32] seeing the structure varying significantly during glycogen synthesis and others seeing little difference[59]. This chapter analyzes the glycogen content and structure at various times over a diurnal cycle, with the aim being to characterize any structural changes that occur during synthesis and degradation. The Supporting Information is given in Appendix 2.

Article

pubs.acs.org/Biomac

Changes in Glycogen Structure over Feeding Cycle Sheds New Light on Blood-Glucose Control

Mitchell A. Sullivan,[†,‡] Samuel T. N. Aroney,[‡] Shihan Li,[†,‡] Frederick J. Warren,[‡] Jin Suk Joo,[§] Ka Sin Mak,[∥] David I. Stapleton,[⊥] Kim S. Bell-Anderson,[§] and Robert G. Gilbert*[,†,‡]

[†]Tongji School of Pharmacy, Huazhong University of Science and Technology, Wuhan, Hubei 430030, China

[‡]The University of Queensland, Centre for Nutrition and Food Sciences, Queensland Alliance for Agriculture and Food Innovation, Brisbane, Queensland 4072, Australia

[§]School of Molecular Bioscience, University of Sydney, Sydney, New South Wales 2006, Australia

[∥]School of Biotechnology and Biomolecular Sciences, University of New South Wales, Kensington, New South Wales 2033, Australia

[⊥]Department of Physiology, The University of Melbourne, Parkville, Victoria 3052, Australia

Supporting Information

ABSTRACT: Liver glycogen, a highly branched polymer of glucose, is important for maintaining blood-glucose homeostasis. It was recently shown that *db*/*db* mice, a model for Type 2 diabetes, are unable to form the large composite glycogen α particles present in normal, healthy mice. In this study, the structure of healthy mouse-liver glycogen over the diurnal cycle was characterized using size exclusion chromatography and transmission electron microscopy. Glycogen was found to be formed as smaller β particles, and then only assembled into large α particles, with a broad size distribution, significantly after the time when glycogen content had reached a maximum. This pathway, missing in diabetic animals, is likely to give optimal blood-glucose control during the daily feeding cycle. Lack of this control may contribute to, or result from, diabetes. This discovery suggests novel approaches to diabetes management.

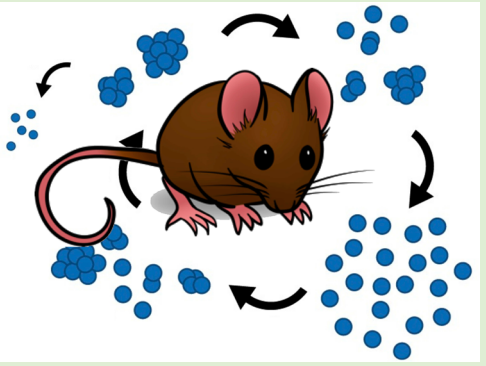

INTRODUCTION

Glycogen, a hyperbranched glucose polymer, is found in a number of organisms; in the case of animals, including humans, it is present in a variety of different tissues. Liver glycogen acts as a blood-glucose buffer, helping the body maintain blood-glucose homeostasis. Glycogen particles range from smaller β particles (~20−30 nm in diameter) to composite α particles as large as 300 nm.[1,2]

Size exclusion chromatography (SEC) has recently been used to compare the structure of nondiabetic liver glycogen with that in *db*/*db* mice, a model for type 2 diabetes.[3] The results show that the size distribution of nondiabetic liver glycogen varies, with a wide range of sizes in a given animal, but with a predominance of very large glycogen α particles in many individuals. However, liver glycogen in "diabetic" *db*/*db* mice has relatively little size variation between mice, with all glycogen consisting predominantly of β particles within a fairly narrow size distribution, plus some small α particles. This is consistent with the observation that *db*/*db* mice had fewer "heavy particles", as inferred using sucrose density centrifugation.[4] If this is a general phenomenon, then there are potential implications for elucidation of the molecular mechanisms underlying diabetes and its management in humans.

The first step in understanding why *db*/*db* mice are unable to form larger α particles is to gain a better understanding of the formation and degradation of these particles in healthy, nondiabetic mice.

Liver glycogen in mice, like many animal species,[5−8] follows a daily rhythm. This rhythm in rodents has been studied in some detail during a 12 h light/12 h dark cycle, with glycogen content peaking during the dark period and decreasing during the light (due to their nocturnal nature).[5,6,9−11] Previous results and conclusions for glycogen structural changes during synthesis and degradation have been conflicting. In 1967, Parodi reported[12] that, while glycogen content increased significantly after administering glucose to overnight-fasted mice, the glycogen size distributions (using sucrose gradient centrifugation) remained almost unchanged. However, Geddes in 1971[13] found that sucrose-density-centrifugation size distributions varied significantly with glycogen content in refed rabbits after 4 days of starvation.

Moreover, liver-glycogen contents after the refeeding of starved rats[14] and rabbits[13] were significantly higher than those of normal livers with an overproduction of low molecular weight glycogen in rabbits. Thus, a starvation/refeeding

Received: November 20, 2013
Revised: December 27, 2013
Published: December 28, 2013

method may not accurately reflect the process occurring during a normal feeding cycle.

To better understand the dynamics of liver glycogen formation, we characterized liver glycogen structure by SEC and transmission electron microscopy (TEM), from mice sacrificed at various times of the day, exploiting the natural diurnal rhythms of feeding patterns in mice.

EXPERIMENTAL SECTION

Animals. Approval for the use of animals was from the University of Sydney Animal Care and Ethics Committee. Male mice on an FVB/NJ background were bred in-house and housed in standard cages (2−6 mice/cage). Temperature was controlled at 22° ± 1 °C with a 12 h dark-light cycle (lights on at 6 am). Mice were given ad libitum access to water and standard chow (6% kcal from fat, 14.3 MJ kg^{-1}, Glen Forest Specialty Feeds WA, Australia) until age 12 weeks.

At termination, 12 week old mice were anaesthetized with sodium pentobarbitone (150 mg kg^{-1} intraperitoneal). Liver was rapidly excised, snap frozen in liquid nitrogen, and stored at −80 °C.

Glycogen Extraction. Glycogen was extracted similarly to previous studies.[15,16] Approximately 200 mg of mouse liver was homogenized in 3.2 mL of glycogen isolation buffer (50 mM Tris, pH 8, 150 mM NaCl, 2 mM EDTA, 50 mM NaF, and 5 mM sodium pyrophosphate). A total of 200 μL of this homogenate was removed for glycogen content analysis. Samples were centrifuged at 6000 *g* for 10 min at 4 °C. The supernatants were then centrifuged at 300000 *g* for 1 h at 4 °C. The pellet was then resuspended in glycogen isolation buffer and layered over a 3 mL, stepwise sucrose gradient (37.5 and 75% in glycogen isolation buffer). These samples were then centrifuged at 488300 *g* for 2 h at 4 °C. The pellet of glycogen at the bottom of the tube was resuspended in 500 μL of water. Samples were mixed with four parts absolute ethanol to precipitate glycogen. The samples were centrifuged at 4000 *g* for 10 min and the pellets were redissolved in 1 mL of deionized water and lyophilized (freeze-dried; VirTis, Benchtop K). A small amount of sample was put aside for TEM.

Size-Exclusion Chromatography. As shown previously in refs 17 and 18, mouse-liver glycogen was dissolved directly into the SEC eluent, dimethyl sulfoxide (DMSO; HPLC grade, Sigma-Aldrich) with 0.5 wt % LiBr (ReagentPlus) on a thermomixer at 80 °C for 6 h, giving complete molecular dissolution. The size separation method follows that performed previously.[17] Samples were injected into an Agilent 1100 Series SEC system (PSS, Mainz, Germany) using a GRAM preColumn, 30 and 3000 columns (PSS) in a column oven at 80 °C and a flow rate of 0.3 mL min^{-1}. This flow rate was employed to minimize shear scission of the molecules.[19] SEC weight distributions were determined by using a refractive index detector (RID; Shimadzu RID-10A, Shimadzu, Japan).

A universal calibration curve was obtained using pullulan standards (PSS), with a molar mass range of 342 to 2.35 × 10^6 Da, which were directly dissolved into the DMSO/LiBr eluent. This allowed the conversion of elution volume into hydrodynamic radius (R_h).[19] It is noted that the IUPAC definition of hydrodynamic radius[20] depends on the technique used, and thus, R_h as defined by the SEC separation parameter is a (hopefully only slightly) different quantity to that for, for example, dynamic light scattering. While there are obvious problems with this definition, it is the one that is internationally agreed upon. It could be supplanted by adding a further subscript indicating the technique in question, but to do that here, where only a single type of R_h is under discussion, would introduce an unnecessary clutter in notation. The Mark−Houwink parameters for pullulan in DMSO/LiBr (0.5 wt %) at 80 °C are $K = 2.427 \times 10^{-4}$ dL g^{-1} and $\alpha = 0.6804$ (Kramer and Kilz, PSS, private communication); this gives an R_h upper limit of accurate calibration of ∼60 nm, with the size scale above this being only semiquantitative.

Transmission Electron Microscopy. TEM images of glycogen were obtained using a similar method to that employed previously.[21] One glycogen sample from each of the mice sacrificed at 9 pm, 4 am, 12 noon, 4 pm, and after 16 h of starvation was dissolved into deionized water (∼0.5 mg mL^{-1}). This was then diluted 10-fold and applied to a glow discharged 100 mesh copper grid (ProSciTech). After 1 min, excess sample was drawn off with filter paper and 2−3 drops of 2% uranyl acetate was added to stain the sample. Excess uranyl acetate was removed using filter paper after 45 s. The preparations were then analyzed using a JEOL 1010 transmission electron microscope (JEOL, Tokyo, Japan) operating at 100 kV. The images were recorded digitally with a SIS Veleta CCD camera (Olympus, Münster, Germany) and reports and measurements were prepared using the AnalySiS image management software.

Glycogen Content Assays. The method employed, using amyloglucosidase to degrade glycogen to individual glucose units and then glucose oxidase/peroxidase (GOPOD) reagent to quantify the amount of glucose, was similar to that used elsewhere.[22] A total of 5 μL of amyloglucosidase (Megazyme), 20 μL of homogenate (from Glycogen Extraction), and 100 μL of sodium acetate buffer (pH 6) was made up to 0.5 mL with deionized water and incubated on a thermomixer at 50 °C for 30 min. A control, with everything except amyloglucosidase, was also analyzed. A 300 μL aliquot of each sample was then added to 1 mL of glucose oxidase/peroxidase reagent (GOPOD, Megazyme) and incubated for a further 30 min at 50 °C on a thermomixer. The absorbance (510 nm) of each sample was then analyzed on a UV-1700 PharmaSpec UV−vis spectrophotometer (Shimadzu). The glycogen content was then calculated based on a calibration curve (constructed by reacting D-glucose of various concentrations with the same GOPOD reagent). All samples and controls were run in duplicate with the absorbance values averaged.

RESULTS AND DISCUSSION

As shown in Figure 1, the amount of liver glycogen in the mice followed a diurnal pattern, being synthesized during the dark

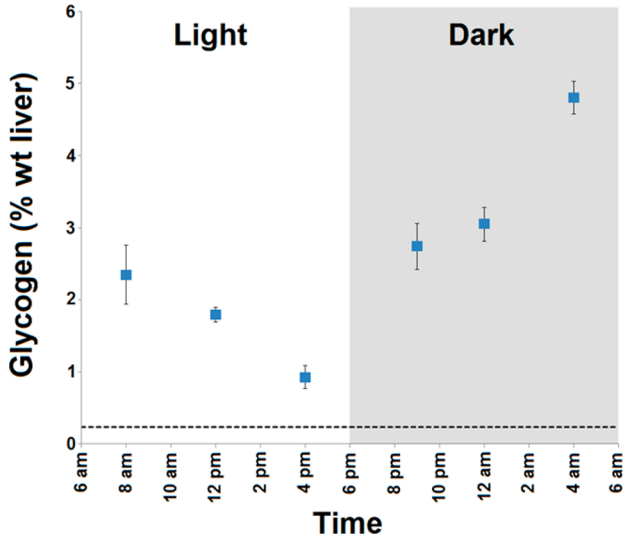

Figure 1. Liver-glycogen content of ad libitum fed wild-type mice at various stages of a day/night cycle; shading represents night/feeding period. Values shown are the mean ± SEM of 3−9 mice. The dashed line represents the mean glycogen content of 7 mice starved for 16 h.

(feeding) period and subsequently degraded during the light hours. This resembles the pattern reported in previous studies.[5,23,24] Glycogen structure was characterized at various phases of this cycle, to examine changes during glycogen synthesis, degradation, and after starvation.

SEC weight distributions of glycogen, as functions of molecular size (the hydrodynamic radius R_h) at various time points of the diurnal cycle, are given in Figure 2. The areas of the curves were normalized to unity, to give an indication of the relative structural changes. Distributions of glycogen are also

dx.doi.org/10.1021/bm401714v | Biomacromolecules 2014, 15, 660−665

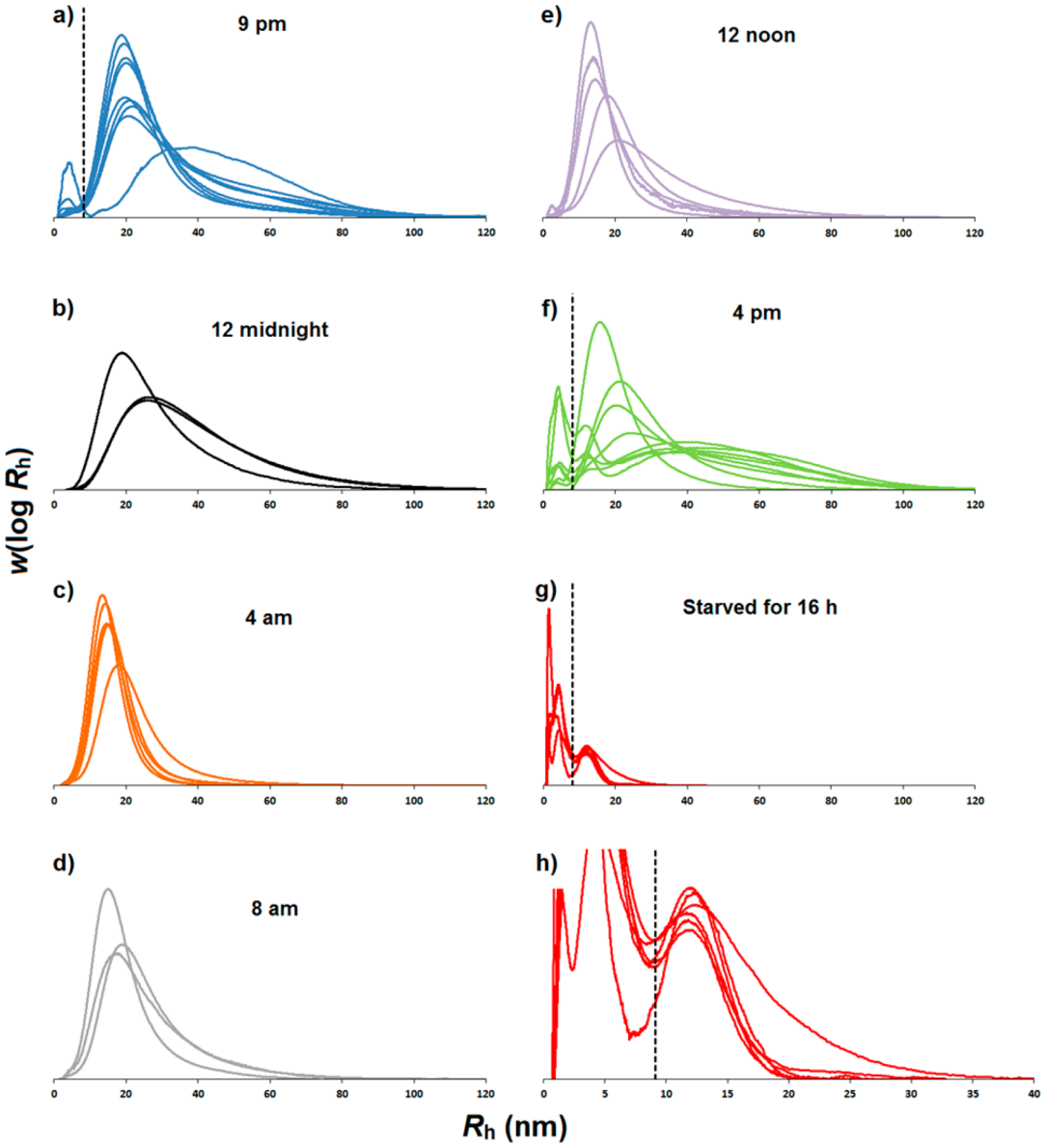

Figure 2. SEC weight distributions, $w(\log R_h)$; normalized to equal areas) as functions of molecular size (the hydrodynamic radius R_h) for wild-type mice sacrificed at various stages of the day/night cycle: 9 pm, blue (a); midnight, black (b); 4 am, orange (c); 8 am, gray (d); 12 noon, purple (e); 4 pm, green (f); after 16 h starvation, red (g); and a magnified version of (g), (h). The multiple distributions for each time point represent replicates with each distribution being from one mouse. A dashed line is added in a, f, g, and h to separate the glycogen peaks from the contamination peaks (which are much more prominent when glycogen concentrations are low) of small molecules. Note the x axis is linear in R_h, not logarithmic as normal for SEC weight distributions; the linear axis enables particular features to be distinguished for the present system. The mean values (and SEM bars) for the R_h at which the maximum occurs and the average R_h are given in the SI (Figure S1a and S1b, respectively).

normalized to their concentration in Figure 3, with the synthesis and degradation phases represented in Figure 3a and b, respectively.

Surprisingly, when glycogen reaches a maximum concentration at 4 am (Figure 1), it consists almost entirely of β particles, as seen in Figures 2c and 3a. This decrease in the average size of glycogen particles between 4 pm and 4 am is statistically significant (Figure S1 in Supporting Information). The micrographs from TEM (Figure 4b) support the suggestion that glycogen forms initially as separate β particles, which later in some way form α particles.

It cannot be confirmed whether these mice were ever going to form α particles, as approximately half of the distributions at later time points during degradation (8 am and 12 noon) also did not contain a significant population of α particles. Further studies are required to properly understand the synthesis of liver glycogen in terms of structure.

Figure 2f shows the glycogen size distributions of mice sacrificed at 4 pm, toward the end of degradation. Interestingly, large glycogen α particles still remain, with a greater proportion of the smaller molecules having been degraded. This increase in the average particle size from 12 to 4 pm is statistically significant (Figure S1 in Supporting Information). TEM was used to visualize these α particles (Figure 4d).

Where Parodi reported that the molecular weight of glycogen did not significantly change after fasting,[12] the mice were only fasted for 5 h after sacrificing the controls early in the morning, and the glycogen content decreased by ~62%. If the highest

dx.doi.org/10.1021/bm401714v | Biomacromolecules 2014, 15, 660−665

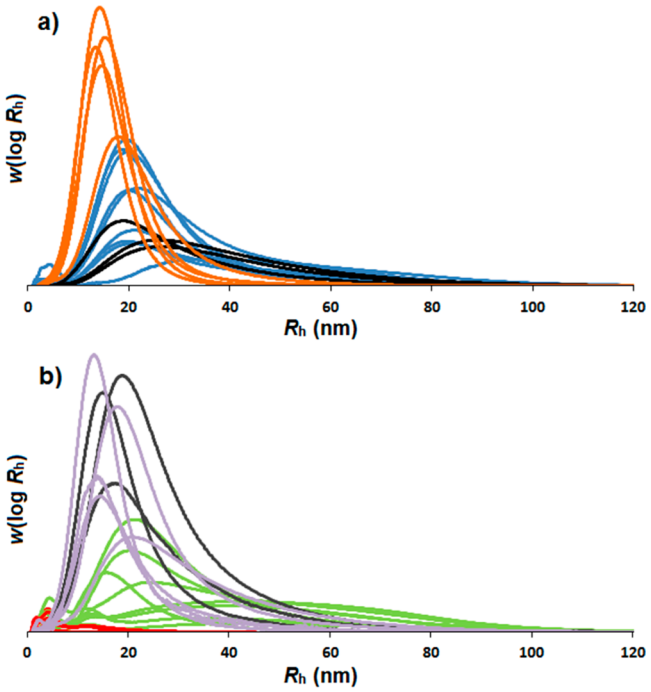

Figure 3. Same SEC weight distributions of liver glycogen from Figure 2. These are separated into the phases of glycogen synthesis (a) and degradation (b) with mice being sacrificed at 9 pm, blue (a); midnight, black (a); 4 am, orange (a); 8 am, gray (b); 12 noon, purple (b); 4 pm, green (b); after 16 h starvation, red (b). The multiple distributions represent replicates with each distribution being from one mouse. All distributions are now normalized to have an area equal to their calculated concentration.

glycogen content in the present study (~5%, see Figure 1) were to decrease by the same amount, there would be a glycogen content of ~2% (roughly that of mice sacrificed at 12 noon). It can be seen from Figure 2e that this glycogen would more likely have a distribution similar to the glycogen during the synthesis phase, but Figure 2f shows that one only has significantly different distributions at a glycogen content as low as ~1%. This suggests that if the past study had been for mice fasted for longer, the results might have been very different.

Our results agree with Geddes'[25] finding of a significant differences in sucrose-density-centrifugation distributions of liver glycogen at different times after starvation, with no large glycogen molecules remaining after 16 h of fasting (Figure 2g,h); it is noted that one can only make qualitative inferences from data obtained from sucrose-density centrifugation.

While liver glycogen reaches low levels after starvation, this glycogen can persist for up to 72 h of starvation.[26] Microscopy studies on frog hepatocytes demonstrate that starved frogs only have β particles as opposed to the α particles found in hepatocytes of fed frogs.[27] This is consistent with Figure 2g,h, where only small β particles remain during the starvation phase. These smaller β particles were visualized using TEM (Figure 4e). It is important to note that these small β particles (R_h ~12 nm) started to form during fasting (Figure 2f) when there were still large α particles present (which eventually degrade away). This, as well as the fact these molecules are narrowly distributed, suggests that they are more resistant to degradation and are not just persisting because glycogen degradation pathways are switched off.

Altogether, the size distributions of glycogen being synthesized, degraded and after starvation have revealed a number of interesting insights into glycogen metabolism, leading to the proposed "recycling" model of glycogen metabolism in terms of the tertiary structure (β and α particles) presented in Figure 5.

When glycogen reaches its maximum concentration ("Late synthesis" in Figure 5), it appears to consist almost entirely of β particles. This result, which at first is surprising, shows that α particles are formed following the formation of individual β particles.

This pathway makes evolutionary sense, with the need to rapidly synthesize large amounts of glycogen (when blood sugar is rising from the digestion of food) being aided by the higher surface area to volume ratio of the smaller β particles. Indeed it has been shown in vitro with rabbit-liver glycogen that, in the direction of synthesis, glycogen phosphorylase has a higher activity for smaller glycogen molecules.[28] Further support for this hypothesis comes from a study demonstrating a tendency for radiolabeled glucose to be incorporated more readily into lower molecular weight material.[25] Our data also suggest that α particles remaining from the previous day/night cycle appear to be degraded during glycogen synthesis (arrows 1 and 2 in Figure 5). If this were not the case, glycogen α particles that were not degraded in one diurnal cycle would continually grow during the following synthetic phase, making even larger α particles than the previous cycle. This would result in the average size of glycogen particles becoming larger from one day to the next.

During fasting, however, it is desirable to have a slower, more controlled, release of glucose back into the blood, which is aided by the transformation of many β particles into larger α particles. As stated, our results show an initial, preferential degradation of smaller molecules in the liver (arrow 4 in Figure 5), which is consistent with past studies that show glycogen phosphorylase is more associated with,[29] and has a higher in vitro activity for,[30] lower molecular weight glycogen. A radioactivity study also hinted that larger molecules may be metabolized more slowly.[13] These results and preliminary rate

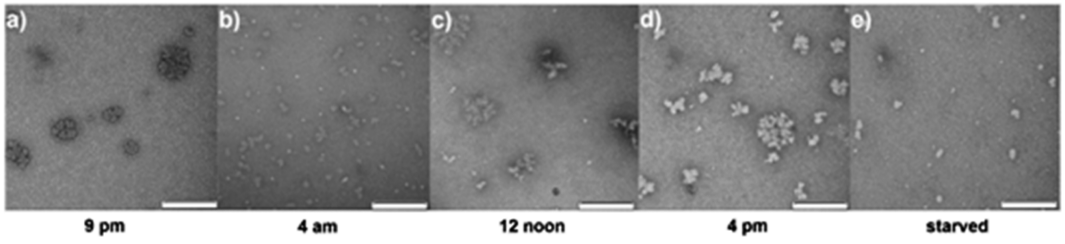

Figure 4. TEM images of liver glycogen at various stages of the day/night cycle: 9 pm (a); 4 am (b); 12 pm (c); 4 pm (d); and after 16 h of starvation (e). Scale bar represents 200 nm.

dx.doi.org/10.1021/bm401714v | Biomacromolecules 2014, 15, 660−665

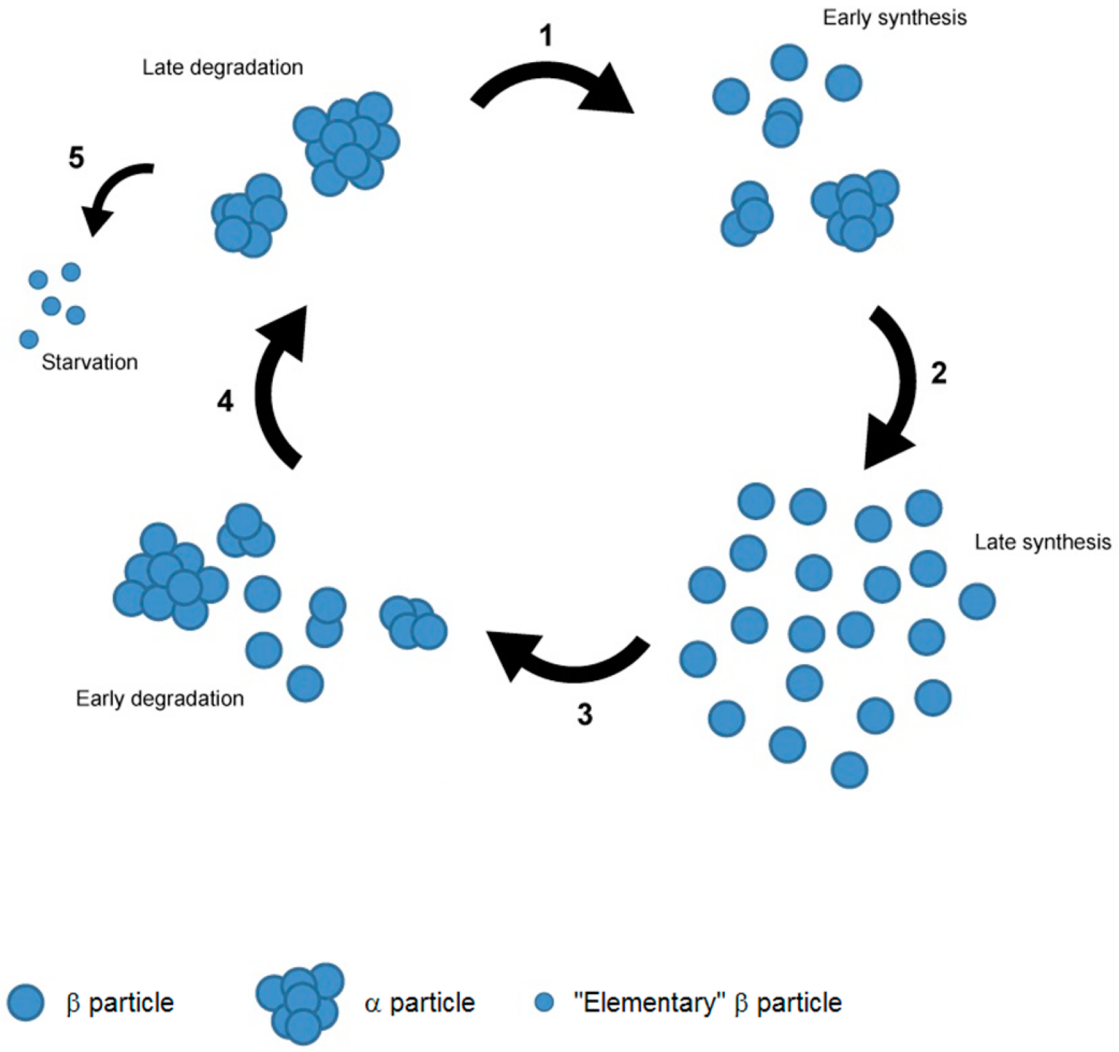

Figure 5. Proposed "recycling" model for the structural changes of glycogen over a diurnal cycle and after starvation.

data from our laboratories (showing populations of large glycogen particles degrading much slower than populations of smaller β particles; see Figure S3 in SI) support the inference that the rates of degradation per mass of glycogen of small glycogen molecules are faster than those of large molecules, consistent with the hypothesis that glycogen degradation is controlled by surface area. The observation that diabetic mice are unable to form as many large α particles as healthy mice[3] therefore suggests that these smaller molecules are more vulnerable to enzymatic degradation due to their lower ratio of surface area to volume.[3,31]

Another interesting feature of our data is the narrowly distributed small β particles that remain after starvation. An evolutionary advantage of this resistant glycogen is clear, as synthesizing a new glycogen molecule from the beginning (involving the production of more initiating protein, glycogenin) would require more energy, and be much slower, than building glycogen from this resistant "elementary" glycogen molecule. While the mechanism for the resistance of these molecules is unclear, it has been suggested that this remaining liver glycogen may be denser, impeding the access of degradative enzymes.[13,32,33] Whether this glycogen bears any relation to the proglycogen referred to in previous publications[34−36] is hard to determine due to the different glycogen-extraction methods employed; however, it has been suggested[37] that the "proglycogen" inferred in these past studies were artifacts of the extraction methods.

CONCLUSION

Size distributions of glycogen being synthesized, degraded, and after starvation have revealed a number of interesting insights into glycogen metabolism. When glycogen reaches its maximum concentration it appears to consist almost entirely of β particles. This surprising result suggests that α particles may be formed after the formation of separate β particles. A very important new discovery (consistent with past studies that suggested this may be the case) is that as glycogen degrades the larger α particles persist longer than the smaller particles and that this glycogen is degraded to a more stable molecule with an R_h of ∼12 nm. Given the lack of large α particles in diabetic animals, these findings have potential application in drug targets for diabetes management, through drugs which affect different steps in the pathway of Figure 5, a pathway whose existence was never previously suspected.

dx.doi.org/10.1021/bm401714v | *Biomacromolecules* 2014, 15, 660−665

■ ASSOCIATED CONTENT

Supporting Information

Statistical analysis of differences between the mean hydrodynamic radii at which the maximum occurs and the average hydrodynamic radii of glycogen extracted at various time points, as well as, preliminary kinetics data. This material is available free of charge via the Internet at http://pubs.acs.org.

■ AUTHOR INFORMATION

Corresponding Author

*Fax: +61 7 3365 1188. Tel.: +61 7 3365 4809. E-mail: b.gilbert@uq.edu.au.

Notes

The authors declare no competing financial interest.

■ ACKNOWLEDGMENTS

We thank Ms. Thillini Jayasinghe for assistance with the transport of tissue samples. The authors also gratefully thank Ms. Sarah Chung and Ms. Kai Wang for their technical assistance with SEC analysis. Electron microscopy was carried out in the Centre for Microscopy and Microanalysis at the University of Queensland, a node of the Australian Microscopy and Microanalysis Research Facility (AMMRF). The authors would also like to thank Professor Ling Zheng, Ms. Jiong Li, and Dr. Chuanzhou Li for their assistance with the mice used for the kinetics studies presented in the Supporting Information. We also gratefully acknowledge Ms. Thea Darnell's design skills used to create Figure 5.

■ REFERENCES

(1) Drochmans, P. *J. Ultrastruct. Res.* **1962**, *6*, 141−63.
(2) Rybicka, K. K. *Tissue Cell* **1996**, *28*, 253−265.
(3) Sullivan, M. A.; Li, J.; Li, C. Z.; Vilaplana, F.; Stapleton, D.; Gray-Weale, A. A.; Bowen, S.; Zheng, L.; Gilbert, R. G. *Biomacromolecules* **2011**, *12*, 1983−1986.
(4) Roesler, W. J.; Pugazhenthi, S.; Khandelwal, R. L. *Mol. Cell. Biochem.* **1990**, *92*, 99−106.
(5) Roesler, W. J.; Khandelwal, R. L. *Int. J. Biochem.* **1985**, *17*, 81−85.
(6) Mukerjea, R.; Robyt, J. F. *Carbohydr. Res.* **2013**, *372*, 55−59.
(7) Kim, H. J.; White, P. J. *J. Agric. Food Chem.* **2013**, *61*, 3270−3277.
(8) Cohn, C.; Joseph, D. *Proc. Soc. Exp. Biol. Med.* **1971**, *137*, 1303−1306.
(9) Halberg, F.; Albrecht, P. G.; Barnum, C. P. *Am. J. Physiol.* **1960**, *199*, 400−402.
(10) Ishikawa, K.; Shimazu, T. *Life Sci.* **1976**, *19*, 1873−1878.
(11) Philippens, K. M. H.; Vonmayersbach, H.; Scheving, L. E. *J. Nutr.* **1977**, *107*, 176−193.
(12) Parodi, A. J. *Arch. Biochem. Biophys.* **1967**, *120*, 547−&.
(13) Geddes, R.; Stratton, G. C. *Carbohydr. Res.* **1977**, *57*, 291−9.
(14) Maddaiah, V. T.; Madsen, N. B. *Can. J. Biochem.* **1968**, *46*, 521.
(15) Parker, G. J.; Koay, A.; Gilbert-Wilson, R.; Waddington, L. J.; Stapleton, D. *Biochem. Biophys. Res. Commun.* **2007**, *362*, 811−815.
(16) Ryu, J.-H.; Drain, J.; Kim, J. H.; McGee, S.; Gray-Weale, A.; Waddington, L.; Parker, G. J.; Hargreaves, M.; Yoo, S.-H.; Stapleton, D. *Int. J. Biol. Macromol.* **2009**, *45*, 478−482.
(17) Zhou, Z. K.; Cao, X. H.; Zhou, J. Y. H. *Starch-Starke* **2013**, *65*, 509−516.
(18) Sullivan, M. A.; O'Connor, M. J.; Umana, F.; Roura, E.; Jack, K.; Stapleton, D. I.; Gilbert, R. G. *Biomacromolecules* **2012**, *13*, 3805−3813.
(19) Cave, R. A.; Seabrook, S. A.; Gidley, M. J.; Gilbert, R. G. *Biomacromolecules* **2009**, *10*, 2245−53.
(20) Jones, R. G.; Kahovec, J.; Stepto, R.; Wilks, E. S.; Hess, M.; Kitayama, T.; Metanomski, W. V., *Compendium of Polymer Terminology and Nomenclature, IUPAC Recommendations 2008*; Royal Society of Chemistry: Cambridge, 2009.
(21) Ryu, J.-H.; Drain, J.; Kim, J. H.; McGee, S.; Gray-Weale, A.; Waddington, L.; Parker, G. J.; Hargreaves, M.; Yoo, S.-H.; Stapleton, D. *Int. J. Biol. Macromol.* **2009**, *45*, 478−482.
(22) Roehrig, K. L.; Allred, J. B. *Anal. Biochem.* **1974**, *58*, 414−21.
(23) Roesler, W. J.; Helgason, C.; Gulka, M.; Knandelwal, R. L. *Horm. Metab. Res.* **1985**, *17*, 572−575.
(24) Chen, C. B.; Williams, P. F.; Cooney, G. J.; Caterson, I. D. *Int. J. Obesity* **1992**, *16*, 913−921.
(25) Geddes, R. *Int. J. Biochem.* **1971**, *2*, 657−&.
(26) Cardell, R. R.; Larner, J.; Babcock, M. B. *Anat. Rec.* **1973**, *177*, 23−37.
(27) Baic, D.; Ladewski, B. G.; Frye, B. E. *J. Exp. Zool.* **1979**, *210*, 381−405.
(28) Stetten, M. R.; Stetten, D. *J. Biol. Chem.* **1958**, *232*, 489−504.
(29) Barber, A. A.; Orrell, S. A.; Bueding, E. *J. Biol. Chem.* **1967**, *242*, 4040−&.
(30) Orrell, S. A.; Bueding, E. *J. Biol. Chem.* **1964**, *239*, 4021−6.
(31) Besford, Q. A.; Sullivan, M. A.; Zheng, L.; Gilbert, R. G.; Stapleton, D.; Gray-Weale, A. *Int. J. Biol. Macromol.* **2012**, *51*, 887−91.
(32) Brammer, G. L.; Rougvie, M. A.; French, D. *Carbohydr. Res.* **1972**, *24*, 343−354.
(33) Geddes, R. *Carbohydr. Res.* **1968**, *7*, 493−497.
(34) Alonso, M. D.; Lomako, J.; Lomako, W. M.; Whelan, W. J. *FASEB J.* **1995**, *9*, 1126−1137.
(35) Lomako, J.; Lomako, W. M.; Whelan, W. J. *FEBS Lett.* **1991**, *279*, 223−228.
(36) Lomako, J.; Lomako, W. M.; Whelan, W. J. *Eur. J. Biochem.* **1995**, *234*, 343−349.
(37) James, A. P.; Bames, P. D.; Palmer, T. N.; Fournier, P. A. *Metab., Clin. Exp.* **2008**, *57*, 535−543.

3.2 Outcomes

The structural characterization of glycogen at various time points across a diurnal cycle has led to several interesting insights. First, when glycogen was at its peak concentration, it consisted almost entirely of β particles, indicating that glycogen is initially created as separate β particles which can later combine to form α particles. This was unexpected, it being hypothesized that most α particles would be present when the glycogen content was at a maximum. However, this unexpected result yielded important new insights. In evolutionary terms the prevalence of small β particles when glycogen content is high would be a strategy optimal with an animal's need to quickly synthesize glycogen after food digestion. Assuming that the enzymatic kinetics of both synthesis and degradation of β particles are surface-area controlled (the enzymes are different, but both are much larger than the accessible spaces within a glycogen particle), rapid synthesis would be assisted by the greater surface area to volume ratio of the smaller molecules. An *in vitro* study[101] with rabbit-liver glycogen supports this hypothesis, with glycogen phosphorylase having a higher activity for smaller glycogen particles in the direction of glycogen synthesis. In 1971 Geddes[32] also found that glucose tended to be incorporated more into lower-weight material, which is consistent with smaller molecules being synthesized more rapidly.

The second major insight resulting from the structural study of glycogen across a diurnal cycle, is that towards the end of glycogen degradation, there is a much greater proportion of large α particles remaining. This is consistent with the hypothesis that α particles degrade relatively slowly due to their decreased surface area to volume ratio; our preliminary *in vitro* kinetics data given in Appendix 2 and a past kinetics study[31] support this hypothesis. Indeed we have suggested[38] that this is why α particles have evolved; to give a slower, more controlled release of glucose back into the blood. It has also been observed[102] that glycogen phosphorylase is more associated with lower-molecular-weight glycogen, again being consistent with the idea

of larger molecules being more resistant to degradation because of their lower surface area to volume ratio.

The final insight into glycogen metabolism gained from this study is that after 16 hours of starvation, the liver glycogen of mice consisted of narrowly distributed, very small β particles, with a hydrodynamic radius R_h of ~12 nm. These particles started to form while there were still large α particles remaining, indicating that their persistence is attributable to the particles being resistant to degradation, as opposed to the degradative enzymes being "switched off". Past studies have noted that glycogen can persist long after starvation, when no high molecular weight material remained[103,104] and it has been suggested that perhaps these molecules have a high molecular density, impeding enzymatic access[32]. The synthetic pathway to create these small resistant molecules may have evolved as a more efficient mechanism for glycogen metabolism, with particles not having to be created completely *ab initio*, which involves the synthesis of the glycogen-initiating protein, glycogenin.

Chapter 4: Improving size-exclusion chromatography separation for glycogen

4.1 Introduction

Given the pivotal role SEC has played in the analysis of glycogen structure, any improvements in the resolution and effectivness of this technique will benefit further research associated with the importance of glycogen structure on glycaemic control. While our past studies that have obtained size distributions of native glycogen using SEC have employed a dimethyl sulfoxide/lithium bromide (DMSO/LiBr) eluent, it has recently been shown for synthetic branched polysaccharides (with similar size ranges to glycogen) that aqueous SEC results in significantly improved resolution[105]. There are several other advantages to using an

aqueous system: water is cheaper, safer, easier to dispose of and is more physiologically relevant than DMSO. In this chapter we compare the size distributions of glycogen obtained from DMSO- and aqueous-SEC, and also analyze the effect of flow rate and column pore-size. The Supporting Information is given in Appendix 3.

Journal of Chromatography A, 1332 (2014) 21–29

Contents lists available at ScienceDirect

Journal of Chromatography A

journal homepage: www.elsevier.com/locate/chroma

Improving size-exclusion chromatography separation for glycogen

Mitchell A. Sullivan[a,b], Prudence O. Powell[a,b], Torsten Witt[a,b], Francisco Vilaplana[b,c], Eugeni Roura[b], Robert G. Gilbert[a,b,*]

[a] Tongji School of Pharmacy, Huazhong University of Science and Technology, Wuhan, Hubei 430030, China
[b] The University of Queensland, Centre for Nutrition and Food Sciences, Queensland Alliance for Agriculture and Food Innovation, Brisbane, Queensland 4072, Australia
[c] Division of Glycoscience, School of Biotechnology and Wallenberg Wood Science Centre (WWSC), KTH Royal Institute of Technology, AlbaNova University Centre, SE-106 91 Stockholm, Sweden

ARTICLE INFO

Article history:
Received 12 September 2013
Received in revised form
23 December 2013
Accepted 20 January 2014
Available online 25 January 2014

Keywords:
Size-exclusion chromatography (SEC)
Glycogen
Structural characterization
Improved resolution

ABSTRACT

Glycogen is a hyperbranched glucose polymer comprised of glycogen β particles, which can also form much larger composite α particles. The recent discovery using size-exclusion chromatography (SEC) that fewer, smaller, α particles are found in diabetic-mouse liver compared to healthy mice highlights the need to achieve greater accuracy in the size separation methods used to analyze α and β particles. While past studies have used dimethyl sulfoxide as the SEC eluent to analyze the molecular size and structure of native glycogen, an aqueous eluent has not been rigorously tested and compared with dimethyl sulfoxide. The conditions for SEC of pig-liver glycogen, phytoglycogen and oyster glycogen were optimized by comparing two different eluents, aqueous 50 mM NH_4NO_3/0.02% NaN_3 and dimethyl sulfoxide/0.5% LiBr, run through different column materials and pore sizes at various flow rates. The aqueous system gave distinct size separation of α- and β-particle peaks, allowing for a more detailed and quantitative analysis and comparison between liver glycogen samples. This greater resolution has also revealed key differences between the structure of liver glycogen and phytoglycogen.

1. Introduction

Glycogen functions as a glucose storage molecule in a wide range of organisms, ranging from bacteria to animals, while some plant varieties have a structurally similar glucan termed phytoglycogen (which may also play a role in starch biosynthesis).

Both glycogen and phytoglycogen consist of linear chains of α-(1 → 4)-linked D-glucose residues, with branching points being connected via α-(1 → 6) glycosidic linkages. Glycogen comprises smaller molecules, termed β particles (~20 nm in diameter with molecular weights ~10^6–10^7) [1,2] that can also form much larger molecules, termed α particles (anywhere between 40 and 300 nm in diameter with molecular weights reaching over 10^8) [3,4]. In animals, glycogen is found in a number of organs, performing various functions. Liver glycogen is essential in maintaining blood-glucose homeostasis [5], whereas muscle glycogen provides rapid energy during muscular activity [6]. While muscle glycogen consists of β particles, liver [7] and cardiac [8] glycogen has been shown to contain α particles. These larger molecules are also seen in phytoglycogen [9]. It is also noted that glycogen is not simply a polysaccharide, as there is extensive evidence that all glycogens contain small but significant amounts of protein [10,11].

Insight can be gained into the biosynthesis and degradation of glycogen by analyzing glycogen's macromolecular structure. Size-exclusion chromatography (SEC) has been successfully used to determine size distributions of starch and glycogen, as recently reviewed [12–15], which has resulted in the discovery that db/db mice (a model for type 2 diabetes) have impaired α particle formation [16]. Given the greater ratio of surface area to volume of smaller molecules, it has been hypothesized that impaired α-particle formation, all other things being equal, may impact on blood–glucose homeostasis [8,16].

While dimethyl sulfoxide (DMSO)/LiBr has been used as the SEC solvent in these past studies to characterize glycogen structure, to date aqueous-SEC has not been employed for native liver glycogen, although some encouraging analysis has been performed on commercial oyster and rabbit-liver glycogen [17]. The DMSO/LiBr system has been employed in the past because it has been shown that this dissolves amylose and amylopectin (the two types of glucans in starch, with the same glycosidic linkages as in glycogen) molecularly and without aggregation [18]. However, there are a number of potential benefits of using an aqueous system: the lower

* Corresponding author at: The University of Queensland, Centre for Nutrition and Food Sciences, Queensland Alliance for Agriculture and Food Innovation, Brisbane, Queensland 4072, Australia. Tel.: +61 412215144.
E-mail address: b.gilbert@uq.edu.au (R.G. Gilbert).

0021-9673/$ – see front matter © 2014 Elsevier B.V. All rights reserved.
http://dx.doi.org/10.1016/j.chroma.2014.01.053

viscosity of water should lead to better resolution and reduction of shear scission; the characterization is more physiologically relevant as glycogen is in an aqueous solvent *in vivo*; and water is a much cheaper and safer solvent than DMSO. Aqueous SEC has recently been successfully used for synthetic branched polysaccharides (with similar size ranges to glycogen), where better separation was found compared to a DMSO setup [19]. Additionally, the presence of small amounts of proteins in glycogen will affect the solubility of this molecule in water- and DMSO-based systems; if, as is usually the case, the proteins are predominantly hydrophilic on the surface, water solubilization will be increased. In this present study, the size separation of glycogen from pig liver, *sugary-1* (*su-1*) mutant maize grain (termed phytoglycogen) and oyster glycogen were analyzed using both aqueous (50 mM NH_4NO_3/0.02% NaN_3) and DMSO/LiBr SEC. Differential refractive index detection was used alone, as the objective of improved separation is not aided by further knowledge (which would be useful for mechanistic interpretation) that would result from having additional detectors.

2. Method

2.1. Glycogen extraction and purification

2.1.1. Pig-liver glycogen

Pig-liver glycogen was extracted as previously described [20]. A sample from the central lobe of the liver (~25 g) from a 106-day old male pig (Large White breed), reared at the University of Queensland Centre for Advanced Animal Science, was immediately frozen in dry ice and kept at −80 °C for 6 weeks prior to glycogen extraction. Liver (~4 g) was homogenized with 5 volumes of glycogen isolation buffer (50 mM Tris, pH 8, 150 mM NaCl, 2 mM EDTA, 50 mM NaF, 5 mM sodium pyrophosphate, and phenylmethanesulfonylfluoride (PMSF)). The homogenate was centrifuged at 6000 × *g* for 10 min at 4 °C with the resulting supernatant then being centrifuged at 50,000 × *g* for 30 min at 4 °C. The pellet was resuspended in glycogen isolation buffer (3 mL) and layered over an 18 mL, stepwise sucrose gradient (25%, 50%, and 75% in glycogen isolation buffer). The gradient was then centrifuged at 300,000 × *g* for 2 h at 4 °C. The supernatant was discarded and the pellet was resuspended in 1 mL of 80% ethanol. The sample was then centrifuged at 4000 × *g* for 10 min at 4 °C and the supernatant was discarded. This ethanol precipitation step was repeated once more and the pellet was dissolved in 1 mL of deionized water and then lyophilized (freeze-dried; VirTis, Benchtop K).

2.1.2. Phytoglycogen

Extraction of phytoglycogen was performed following a technique developed in our laboratories, as done previously [21]. Kernels of *su-1* mutant maize, obtained from Prof. Ian D. Godwin (The University of Queensland, Brisbane, Australia), were ground into a fine powder using a cryo-mill (Freezer/Mill 6870, SPEC CertiPrep, Metuchen, NJ, USA) that used a 1 min precooling step followed by 5 min grinding. This technique is used to minimize mechanical and thermal damage and has been shown to be effective for starch extraction [22]. After grinding, 100 mg of kernel flour was incubated in 2.5 mL of tricine buffer for 30 min at 37 °C with protease (2.5 units mL^{-1}; bacterial type XIV, Sigma-Aldrich). An additional 2.5 mL of ice-cold tricine buffer was added to the sample, followed by centrifugation at 4000 × *g* for 10 min. The supernatant was precipitated with 4 volumes of absolute ethanol and centrifuged for an additional 10 min at 4000 × *g*. The pellet was dissolved in 1 mL of deionized water and then lyophilized (freeze-dried; VirTis, Benchtop K).

Table 1
Column information.

Solvent	Column	Particle size (μm)
Aqueous	Suprema 30	5
	Suprema 1000	5
	Suprema 3000	5
	Suprema 10,000	10
DMSO	GRAM 30	10
	GRAM 1000	10
	GRAM 3000	10
	GRAM 10,000	10

2.1.3. Oyster glycogen

Oyster type II glycogen was purchased from Sigma-Aldrich. This was used as a comparative tool as it consists only of β particles [20].

2.2. Size-exclusion chromatography using dimethyl sulfoxide (DMSO)/LiBr as an eluent

Pig-liver glycogen, phytoglycogen and oyster glycogen were dissolved (2 g L^{-1}) in DMSO with 0.5 wt% LiBr on a thermomixer at 80 °C and 350 rpm overnight.

Samples were injected into an Agilent 110 Series SEC system (PSS, Mainz, Germany) using two different column setups: GRAM preColumn, 30 and 3000 columns (PSS); and GRAM preColumn, 1000 and 10,000 (PSS) (see Table 1 for column information). The columns were kept at 80 °C using a column oven and 3 different flow rates were tested (0.3, 0.6 and 0.9 mL min^{-1}). A refractive index detector (RID) (Shimadzu RID-10A, Shimadzu, Japan) was used to determine the SEC weight distributions. The detector temperature was 45 °C. Because SEC weight distributions are based on the relative amount of DRI signal, any small difference in the refractive index between the eluent in the column and in the detector due to a temperature difference will remain constant.

Universal calibration curves were obtained for each column setup and flow rate using pullulan standards (PSS), with a molar mass range of 1080 Da to 2.35×10^6 Da, which were directly dissolved into eluent. This allowed elution volumes to be converted into hydrodynamic volumes (V_h), or equivalently the hydrodynamic radius (R_h), where $V_h = 4/3\pi R_h^3$ [23], using the Mark-Houwink relationship (see Eq. (1)).

$$V_h = \frac{2}{5}\frac{KM^{1+\alpha}}{N_A} \quad (1)$$

The hydrodynamic radius here is defined by IUPAC as the volume of a hydrodynamically equivalent sphere [24], and thus the meaning is dependent on the particular technique used: for example, hydrodynamic radius in dynamic light scattering is a different quantity to that for SEC.

The use of universal calibration in this study is based on the assumption that SEC separates solely on hydrodynamic size, an assumption which has been shown to be valid for molecules with widely varied shapes [25–27]. As this study is aimed at improving the separation of α and β particles and very accurate values of size are not necessary for this goal, the universal calibration assumption is used here with the caveat that calibration is not absolute and may not be completely reliable for glycogen.

The Mark-Houwink parameters for pullulan in DMSO/LiBr (0.5 wt%) at 80 °C are $K = 2.427 \times 10^{-4}$ dL g^{-1} and $\alpha = 0.6804$ (Kramer and Kilz, PSS, private communication; the number of significant figures is that provided by Kramer and Kilz, and are given in full to avoid the possibility of sensitivity of the data processing to these values). No uncertainty (or rather, joint confidence interval) is known for the two Mark-Houwink parameters. These values give an R_h upper limit of accurate calibration of ~58 nm for this solvent.

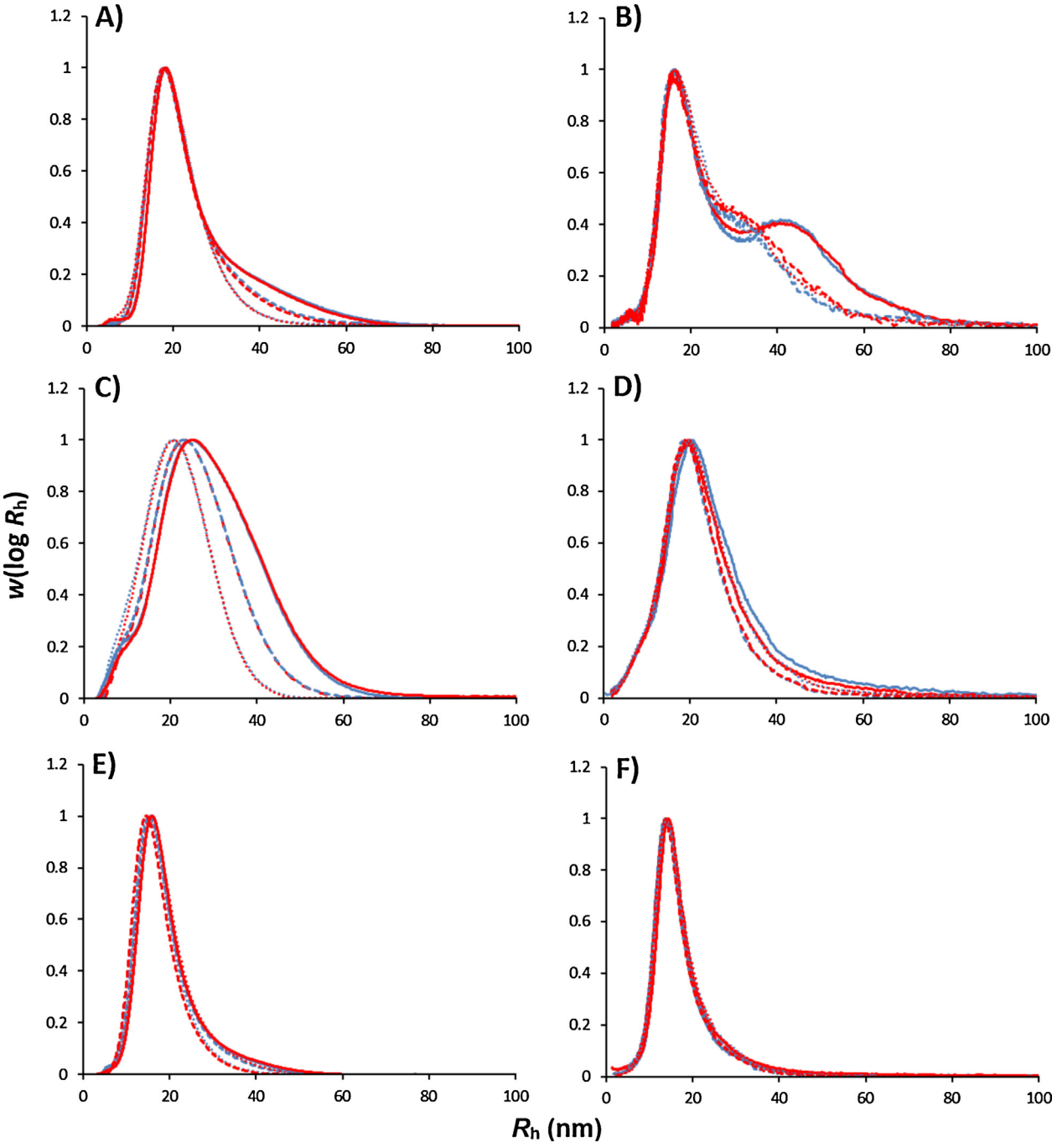

Fig. 1. A comparison of aqueous and DMSO systems at different flow rates for larger pore columns (10,000 and 1000). SEC weight distributions of pig-liver glycogen (A and B), phytoglycogen (C and D) and oyster glycogen (E and F) using a DMSO/LiBr (A, C and E) and an aqueous (B, D and F) eluent system. Each sample was run in duplicate (red and blue) and at 3 different flow rates (0.3 mL min^{-1}, full line; 0.6 mL min^{-1}, dashed line; 0.9 mL min^{-1}, broken line). The concentration of all samples were ~2 g L^{-1}. The normalization of these distributions is arbitrary and for convenience is chosen to have a maximum of 1.

2.3. Size-exclusion chromatography using aqueous (ammonium nitrate) eluent

Pig-liver glycogen, phytoglycogen and oyster glycogen were dissolved (2 g L^{-1}) in 50 mM NH_4NO_3 with 0.02% sodium azide (antimicrobial agent) in a thermomixer at 80 °C and 350 rpm overnight. The ammonium nitrate was used to increase the ionic strength of the solution, minimizing any potential interactions between the glycogen and the column [28].

Dissolved samples were injected into an AF2000 SEC setup (Postnova Analytics, Landsberg-Lech, Germany), with 2 different columns setups being tested: SUPREMA preColumn, 30 and 3000 (PSS); and SUPREMA preColumn, 1000 and 10,000 (PSS) (see Table 1 for column information). The temperature was set at 80 °C and 3 flow rates (0.3, 0.6 and 0.9 mL min^{-1}) were tested.

The same pullulan standards used for the DMSO SEC setup were used to create universal calibration curves for each column setup and flow rate. The Mark-Houwink parameters used were the same as those used for an aqueous SEC set up that used pullulan in 50 mM $NaNO_3$ with 0.02% NaN_3 at 50 °C [19], as differences between the two solvent setups were unable to be determined beyond experimental error (see supporting

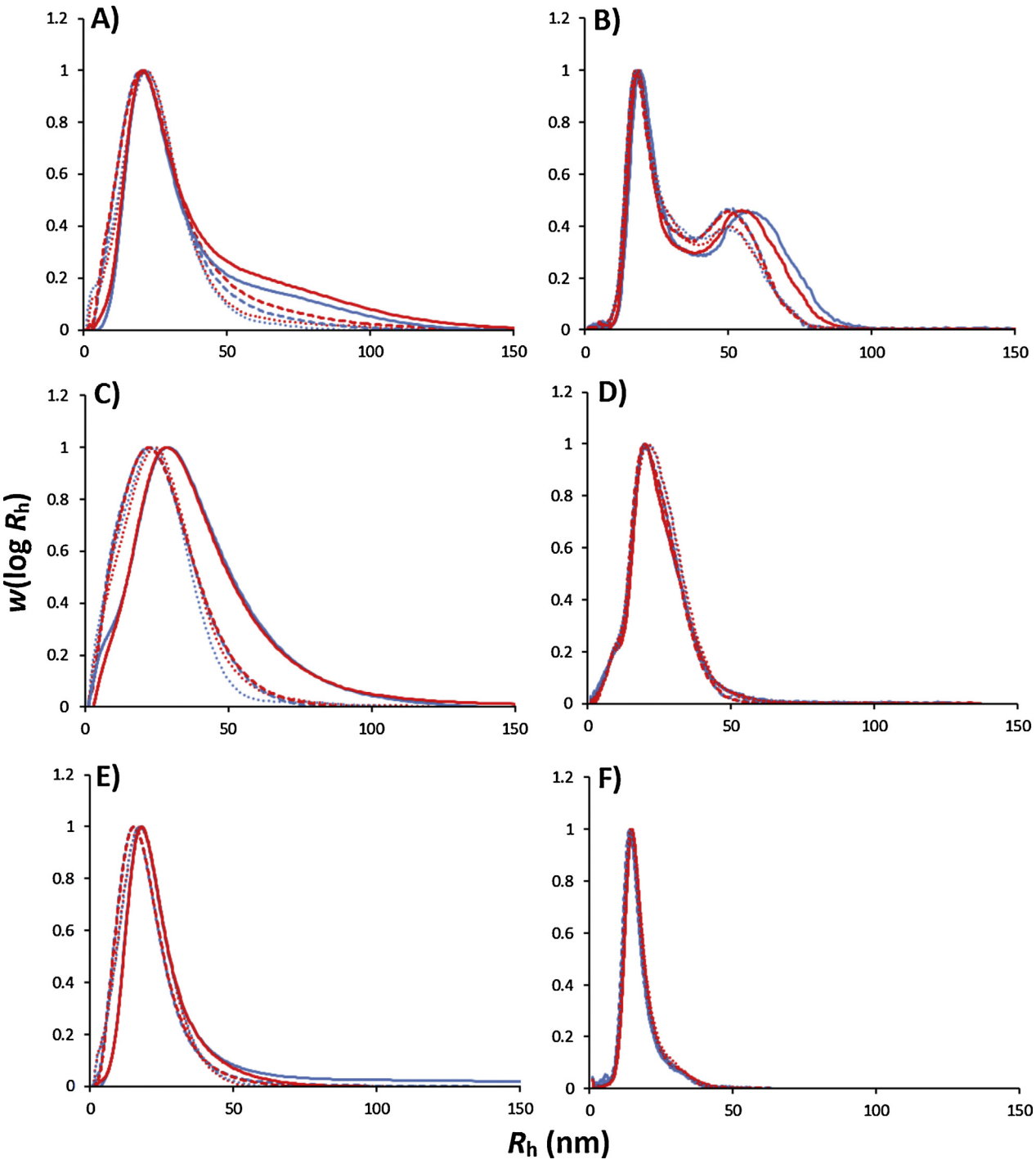

Fig. 2. A comparison of aqueous and DMSO systems at different flow rates for smaller pore columns (3000 and 30). SEC weight distributions of pig-liver glycogen (A and B), phytoglycogen (C and D) and oyster glycogen (E and F) using a DMSO/LiBr (A, C and E) and an aqueous (B, D and F) eluent system. Each sample was run in duplicate (red and blue) and at 3 different flow rates (0.3 mL min^{-1}, full line; 0.6 mL min^{-1}, dashed line; 0.9 mL min^{-1}, broken line). The concentration of all samples were ~2 g L^{-1}. The normalization of these distributions is arbitrary and for convenience is chosen to have a maximum of 1.

information Figure S1). The Mark-Houwink parameters (Prof. Katja Loos, private communication) for pullulan in both these solvents are $K = 1.0176 \times 10^{-3}$ dL g^{-1} and $\alpha = 0.525$, giving an R_h upper limit of calibration of ~44 nm.

Pig-liver glycogen (a different pig sample from the same trial, extracted exactly the same way as the previous sample) was also tested at various concentrations (5, 2, 1, 0.5 mg mL^{-1}) using a SUPREMA preColumn, 30 and 3000 (PSS) setup at 80 °C and a flow rate of 0.3 mL min^{-1}.

3. Results and discussion

3.1. Transmission electron microscopy (TEM) images of glycogen

While this study focuses on optimizing SEC for glycogen, TEM images were obtained to visualize the glycogen being tested. Typical images have been presented in previous publications [2,4,20]. Similar images of α and β particles were also obtained in the present work.

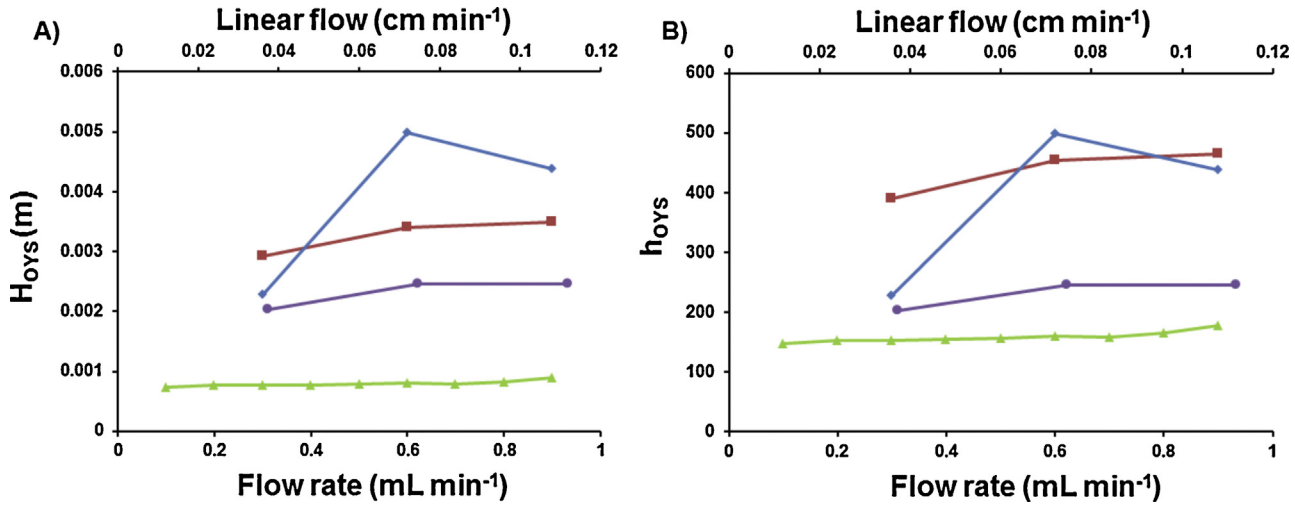

Fig. 3. The calculated plate height (A) and reduced plate height (B) using oyster glycogen peaks at various flow rates for larger pore DMSO columns (purple circles), smaller pore DMSO columns (blue diamonds), larger pore aqueous columns (red squares), and smaller pore aqueous columns (green triangles). While the dispersity of the oyster glycogen leads to the calculation of lower plate heights, using this peak gives the relative column efficiency of the columns at different flow rates.

3.2. SEC of glycogen

SEC weight distributions of pig-liver glycogen, phytoglycogen and oyster glycogen were obtained for both DMSO/LiBr and aqueous (50 mM NH_4NO_3/0.02% NaN_3) setups with large (10,000 and 1000) and small (3000 and 30) column pores at three different flow rates (0.3, 0.6 and 0.9 mL min^{-1}) (Figs. 1 and 2). While SEC elutes approximately linearly in log *R*h, we have found that features are more easily distinguished for α particles with a linear size axis. Each SEC distribution is also provided in the supporting information with a logarithmic *X*-axis to aid in the visual observation of any differences at lower R_h values.

3.3. Comparing different solvents and flow rates

Figs. 1 and 2 compare the SEC weight distributions of glycogen obtained using DMSO/LiBr and aqueous (50 mM NH_4NO_3/0.02% NaN_3) setups for the larger (Fig. 1) and smaller (Fig. 2) pore columns at three different flow rates. There is a striking difference between the distributions of pig-liver glycogen from DMSO/LiBr (Figs. 1A and 2A) and aqueous (Figs. 1B and 2B) SEC setups. In the aqueous systems there are two distinct peaks, each corresponding to the sizes of α and β particles. This represents greatly improved separation over the DMSO/LiBr system, where there is only one peak corresponding to the size of β particles (with only a shoulder being present in the α particle region). While the differences between pig-liver glycogen, phytoglycogen and to a lesser extent oyster glycogen are less obvious when analyzed using SEC with DMSO/LiBr (Figs. 1A, C and E and 2A, C and E), it is clear, using aqueous SEC, that pig-liver glycogen is unique in having two distinct peaks. This explains why this difference was not seen in a recent paper comparing pig-liver glycogen to phytoglycogen, as a DMSO/LiBr system was employed [21].

The resolution of SEC for a polymer with a given size distribution depends both on the intrinsic separation capacity of the stationary phase under the specific elution conditions (determined by the calibration curve) and the peak variance (related to band broadening). This dependence of the SEC resolution on both the calibration curve and the peak variance can be mathematically described using Eq. (2) [29,30]:

$$R_{sp} \propto \frac{1}{\sigma \times b \times \sqrt{L}} \tag{2}$$

Here R_{sp} is the specific SEC resolution, *b* the slope of the calibration curve (as approximated by a linear expression $\log M = \log a - bVel$, *L* the length of the column set, and σ is the peak variance (band broadening).

The quantity σ is related to the plate number, *N*, a dimensionless quantity [30] indicative of the system efficiency. Assuming the elution peak is Gaussian, their relation is described by Eq. (3):

$$\sigma = V_R \sqrt{\frac{p}{N}} \tag{3}$$

Here *p* is the fraction of solute in the stationary phase and V_R is the peak retention volume.

To determine the relative contribution of σ for each column set, the number of theoretical plates, *N*, were calculated from the elution profiles of oyster glycogen at each of the 3 flow rates. As the peaks were close to being symmetrical and Gaussian-shaped, Eq. (4) can be employed [30]:

$$N = 5.54\left(\frac{V_R}{W_{1/2}}\right)^2 \tag{4}$$

Here $W_{1/2}$ is the width of the peak at one-half the height.

While this leads to a greatly reduced calculated *N* due to the disperse oyster glycogen (the true *N* would be calculated using a mono-disperse sample), the use of oyster glycogen allows a direct comparison of the relative broadening effect experienced by glycogen in each column. The calculated values for *N* could then be converted to the theoretical plate height, *H*, which is simply *N* divided by the added length of the columns in the setup. Fig. 3, which is effectively a van Deemter analysis, gives the theoretical plate height, H_{OYS} (Fig. 3A), and reduced plate height, h_{OYS} (Fig. 3B), calculated using oyster glycogen elution peaks for the four different column setups at the three different flow rates. For the aqueous-SEC SUPREMA 3000 and 30 setup, nine flow rates ranging from 0.1 to 0.9 mL min^{-1} were employed, confirming that the longitudinal diffusion (commonly referred to as the B-term of the van Deemter equation) was insignificant, as is generally the case with SEC [30]. Therefore resolution will improve gradually as the flow rate is decreased. It should be noted however that these improvements are very small, with very little flow-rate effects being observed for oyster glycogen (see Figs. 1E and F and 2E andF). Therefore, the main consideration for choosing a flow rate is to minimize shear scission, while maintaining a flow rate that allows reasonable throughput of samples. The plate height, Fig. 3A, is lowest for

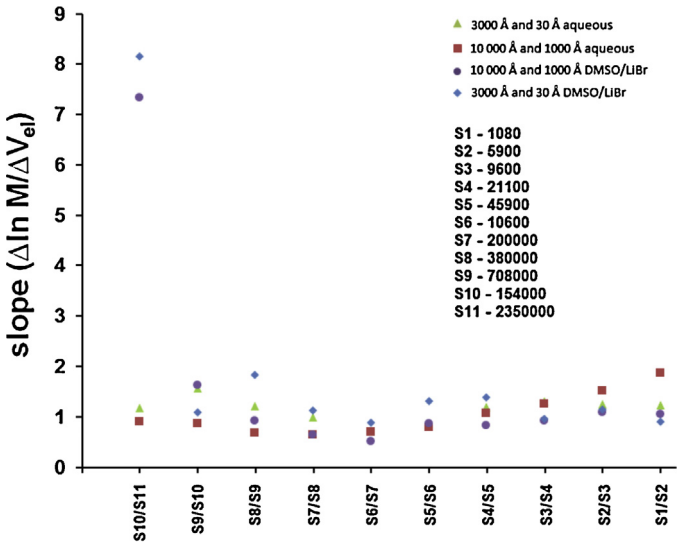

Fig. 4. The slope between each consecutive two points in the calibration curve of the larger pore DMSO columns (purple circles), smaller pore DMSO columns (blue diamonds), larger pore aqueous columns (red squares) and smaller pore aqueous columns (green triangles).

the aqueous 3000 and 30 setup; however when adjusting for the particle size of the column packing material (given in Table 1), the reduced plate height (Fig. 3B) is more similar to that of the DMSO 10,000 and 1000 setup. The least efficient column setup at a flow rate of 0.3 mL min^{-1} is the aqueous 10,000 and 1000. This indicates that the better resolution obtained in aqueous columns is not due to the column efficiency, or the peak variance of the column.

Given the length of all column setups is equal, any difference in the resolution is therefore most likely due to *b*, the slope of the calibration curve. A comparison of the calibration curves for each setup is given in supporting information (Figure S2A). A plot of the derivation of the calibration plot is also given in the supporting information (Figure S2B); however because the larger pullulan standards deviate substantially from the calibration curve, this plot does not adequately represent the effectiveness of the columns at these larger sizes.

To properly compare the separation of the larger standards in the different column setups, the slope *b* between each two consecutive pullulan standards was calculated (see Fig. 4). The slope of the calibration curve is dramatically higher in the DMSO setups for larger sized molecules, indicating that the largest pullulan standard is approaching the exclusion limit of the columns. However with the aqueous setups, the slopes of the calibration curves remain low, indicating that the columns are still separating effectively at these sizes. This key difference between DMSO and aqueous setups explains the significantly improved separation of β- and α-particle peaks observed in the aqueous systems. One reason for this difference in exclusion limits (other than the possibility that a GRAM column of a particular pore size is not equivalent to the corresponding SUPREMA column) is that pullulan of the same molecular weight will have a larger hydrodynamic radius in the DMSO setups (~58 nm) then in the aqueous setups (~44 nm). This difference in hydrodynamic volume (and intrinsic viscosity) may also affect glycogen in a similar manner, leading to a higher proportion of the molecules being larger than the exclusion limit in DMSO/LiBr.

This would also have the effect of increasing the amount shear scission, as larger molecules experience more shear [23].

Another factor that influences the amount of shear scission is the viscosity of the solvent, with the more viscous solvents resulting in a higher shear force. The viscosity of DMSO at 80 °C is ~0.8 mPa s (as estimated in a previous publication [23] from an Arrhenius fit to literature viscosity data), while the viscosity of water at 80 °C is ~0.36 mPa s [31,32], meaning glycogen will be less susceptible to shear scission in aqueous SEC. It can be seen in Figs. 1 and 2 that this appears to be the case; however there still seems to be some shear scission of molecules in the aqueous setups at higher flow rates, emphasizing the risk of using high flow rates when looking at macromolecules such as glycogen.

One of the concerns when using aqueous-based solvents for the analysis of large polysaccharides is the effect of aggregation. There is the possibility that the separate peak representing the α particles in the pig-liver glycogen is due to aggregation, which is then broken in higher shear environments. This was tested using a variety of concentrations of pig-liver glycogen; those with higher concentrations should display higher aggregation, and therefore a greater proportion of large molecules. As seen in Fig. 5, this is not the case, indicating that the α particle peak is not due to aggregation. This is consistent with a light scattering study of glycogen at different concentrations in water, with aggregation only becoming obvious at a concentration of around 8% (w/v) [33].

Furthermore, the observation that phytoglycogen has some particles that correspond to the size of small α particles, but remains mono-modal, is strong evidence that this second peak present in pig-liver glycogen is not due to anomalous separation at this size range. An overlay of all pullulan standard peaks is given in the supporting information (Figure S7) to highlight that all peaks are symmetrical, indicating normal SEC separation.

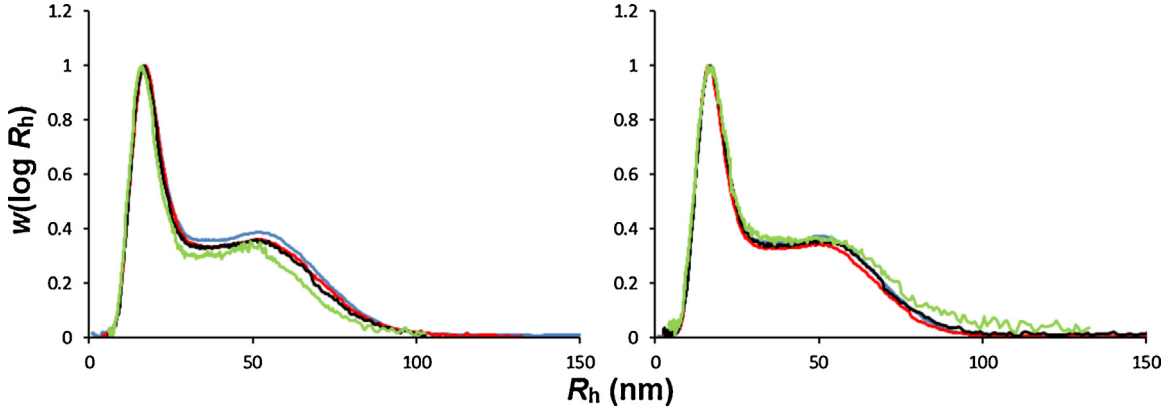

Fig. 5. Pig-liver glycogen samples at different concentrations (5 mg mL^{-1}, blue; 2 mg mL^{-1}, red; 1 mg mL^{-1}, black; 0.5 mg mL^{-1}, green) in the aqueous 3000 and 30 columns. These were done in duplicate from the same glycogen sample. The normalization of these distributions is arbitrary and for convenience is chosen to have a maximum of 1.

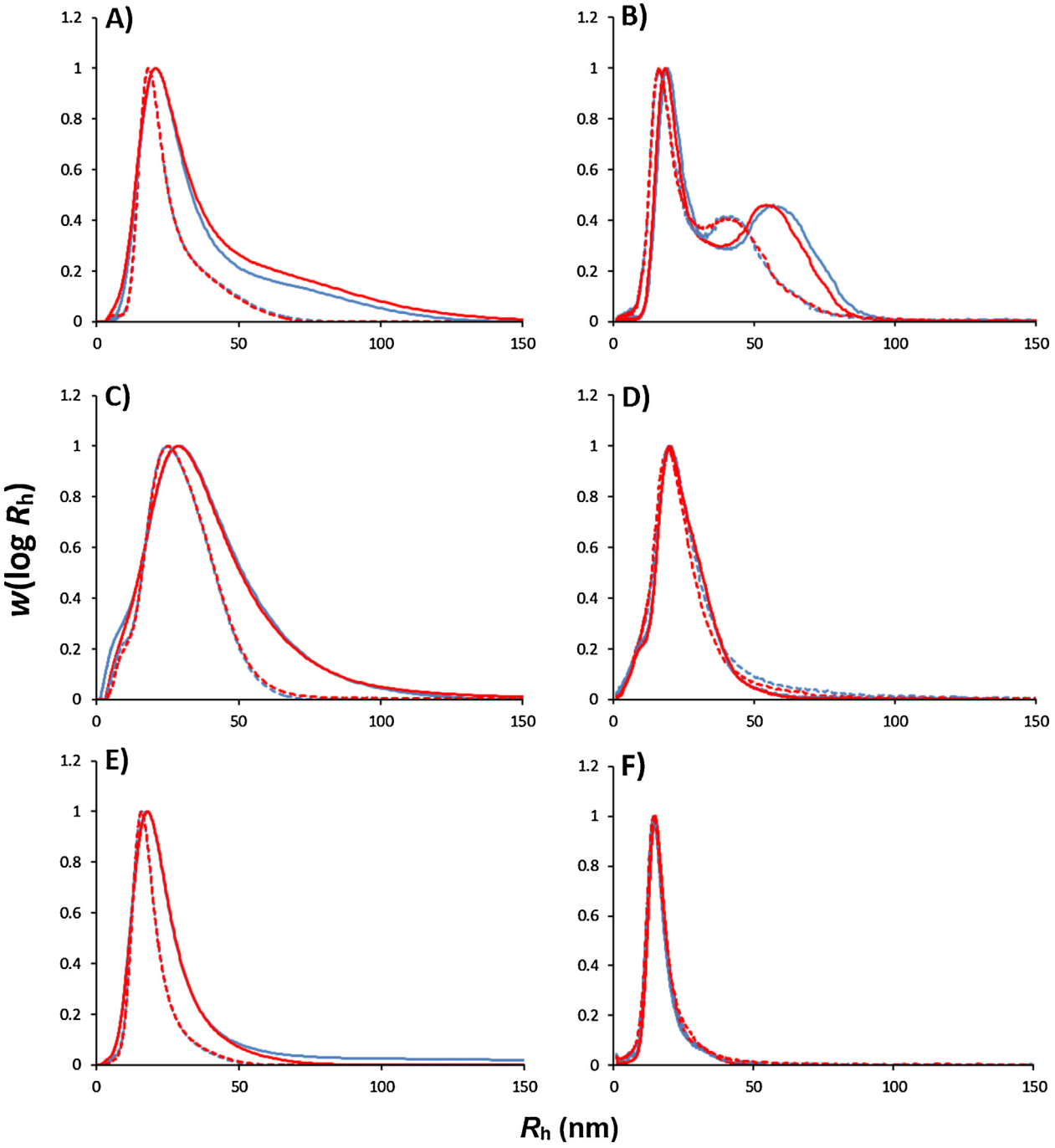

Fig. 6. Comparison of SEC weight distributions (3000 and 30, complete line; 10,000 and 1000, dashed line) using a DMSO/LiBr (A, C and E) and an aqueous (B, D and F) eluent system of pig-liver glycogen (A and B), phytoglycogen (C and D) and oyster glycogen (E and F). Each sample was run in duplicate (red and blue). The normalization of these distributions is arbitrary and for convenience is chosen to have a maximum of 1.

3.4. Comparing columns with different pore sizes

A comparison of large- and small-pore column setups is given in Fig. 6. For all glycogen types in the DMSO/LiBr column setups (Fig. 6A, C and E), the larger pore columns (10,000 and 1000) result in a narrower distribution with smaller R_h values. In the aqueous setups the resolution is qualitatively similar between the SUPREMA 10,000 and 1000 and SUPREMA 3000 and 30; however, with the pig-liver glycogen, the α particle peak in the SUPREMA 10,000 and 1000 is shifted down to lower sizes. Because a greater proportion of the distribution for the aqueous SUPREMA 10,000 and 1000 is below the calibration upper limit ($R_h \sim 44$ nm), it is probably more accurate than the SUPREMA 3000 and 30 setup. For example, the α particle peak maximum is within the calibration upper limit for the SUPREMA 10,000 and 1000 setup, but is significantly outside this limit in the SUPREMA 3000 and 30 setup, causing problems of inaccurate extrapolation (see Figure S3 in supporting information). For all types of glycogen however, the column pore-size does not significantly change the shape of the distribution.

3.5. Parameterization of distributions

While information can be gained by looking at qualitative differences between curves when comparing SEC distributions

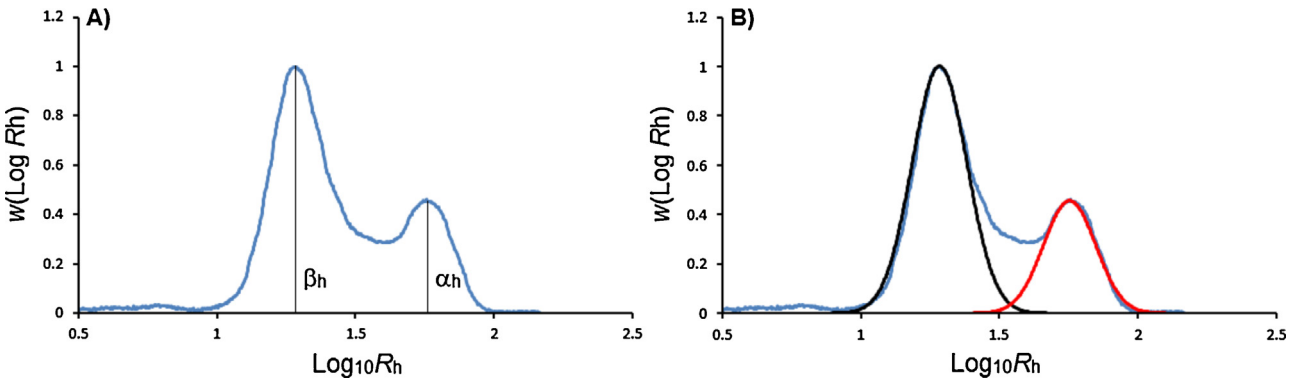

Fig. 7. Useful parameters that can be obtained from the aqueous SEC distributions of pig-liver glycogen: (A) peak heights allowing the determination of α_h/β_h; (B) α and β particles fitted with Gaussian distributions (red and black, respectively) allowing the proportion of α and β particles to be estimated.

(for example the observation that there are more α particles in healthy mice than diabetic [16]), having the ability to reduce the distributions to meaningful parameters is beneficial, especially when looking for statistical relevance between samples. Parameterization of distributions obtained using DMSO/LiBr for liver glycogen is very limited, with the most obvious parameter being the R_h at which the maximum occurs. The average, $\bar{R}_h$, can also be calculated [34] as given in Eq. (5):

$$\log \bar{R}_h = \frac{\int_{-\infty}^{\infty} w(\log R_h) \mathrm{d}\log R_h}{\int_{-\infty}^{\infty} (w(\log R_h)/\log R_h)\, \mathrm{d}\log R_h} \quad (5)$$

While these parameters are useful, they do not necessarily give a good indication of the relative amount of α and β particles in a sample. Although there is no clear distinction seen under electron microscopy of small particles always being individual β particles, it is useful to have an approximate metric. The improved separation obtained using aqueous SEC allows for the determination of a number of useful parameters regarding the proportion of α to β particles. The ratio of the peak heights (Fig. 7A), here denoted α_h/β_h, is a useful way to get insight into the relative amount of α particles, if any, in a sample. Another useful parameter is the area under the curve (AUC) of the α-particle peak as a proportion of the total area (Fig. 7B), α_{area}, with the α-particle peak being fitted with a Gaussian distribution (here done using Fityk software). Similarly the proportional AUC of the estimated β-particle peak, β_{area}, can be calculated. It should be noted that there is still a significant proportion of the SEC distribution lying between the α- and β-particle peaks that is not included in either estimated Gaussian curves. While this also creates the possibility of another parameter, that being the proportional AUC in this intermediate region, this is perhaps excessive. An improved fit can be obtained using two exponentially-modified Gaussians, but this is merely what would be expected given the additional parameters, and such a fit has no obvious relation to physical/biological processes.

In this way, any distribution with a significant α particle peak can now be reduced to six simple, meaningful parameters: the R_h value at which the β particle peak occurs (β_{Rh}); the R_h value at which the α particle peak occurs (α_{Rh}); the average R_h ($\overline{R_h}$); the peak-height ratio of α to β particles (α_h/β_h); the estimated AUC of α particles as a proportion of the total area, α_{area}; and similarly the estimated AUC of the β-particle peak, β_{area}. This will allow for quantitative and statistical comparison between samples. The five most useful of these parameters (with β_{area} being excluded due to its strongly inverse relationship with α_{area}) have been calculated for pig-liver glycogen, phytoglycogen and oyster glycogen for both aqueous-SEC setups using the blue duplicates from Figs. 1B and 2B (see Table 2).

Table 2
Parameterization of aqueous-SEC distributions.

SUPREMA	Sample	β_{Rh} (nm)	α_{Rh} (nm)	$\bar{R}_h$ (nm)	α_h/β_h	α_{area}
10,000 and 1000	Pig	16.4	42.5	24.3	0.417	0.255
	Phyto	19.9	–	20.6	–	–
	Oys	14.2	–	15.6	–	–
3000 and 30	Pig	19.0	56.8	33.0	0.460	0.262
	Phyto	19.5	–	20.0	–	–
	Oys	14.30	–	15.0	–	–

4. Conclusion

SEC weight distributions of pig-liver glycogen, phytoglycogen and oyster glycogen were obtained using both aqueous 50 mM NH_4NO_3/0.02% NaN_3 and DMSO/0.5% LiBr setups, employing various pore columns and three flow rates. A considerable improvement in resolution, explained by differences in the slopes of the calibration curves, was obtained through the use of aqueous SEC, with pig-liver glycogen being separated into two distinct peaks. Structural differences between liver glycogen and phytoglycogen, while hard to observe in SEC-DMSO/LiBr, are clearly identifiable using SEC-50 mM NH_4NO_3/0.02% NaN_3. In contrast to pig-liver glycogen, phytoglycogen only exhibited one peak. This single peak however, still consists of some molecules that are of a similar size to small α particles, making the differences between pig-liver glycogen and phytoglycogen less obvious in TEM. The slowest flow rate employed for all columns (0.3 mL min^{-1}) was shown to be optimal, resulting in reduced shear scission and slightly better resolution. While the pore size had little effect on the shape of the distributions, the larger pores resulted in distributions having smaller R_h values. Given the results shown here, it is of benefit to employ an aqueous SEC system with a low flow rate when analyzing glycogen that may have α particles. This has potential applications in human health, given the recent observation that there are significant differences in the size distributions of α and β particles in healthy compared to diabetic animals [16].

Acknowledgements

The authors thank Drs. Barbara Williams and Helen Keates for assistance with the sample collection and the staff at the University of Queensland Centre for Advanced Animal Science for their help with the pig studies. The authors also gratefully thank Ms. Sarah Chung for her technical assistance with SEC analysis. We thank Mr. Lachlan Kann and Prof. Ian Godwin for their assistance with phytoglycogen extraction and Mr. Felipe Umana for his assistance with the extraction of pig glycogen. Electron microscopy was carried out

in the Centre for Microscopy and Microanalysis at the University of Queensland, a node of the Australian Microscopy and Microanalysis Research Facility (AMMRF).

Appendix A. Supplementary data

Supplementary data associated with this article can be found, in the online version, at http://dx.doi.org/10.1016/j.chroma.2014.01.053.

References

[1] J. Shearer, T.E. Graham, Exerc. Sport Sci. Rev. 32 (2004) 120.
[2] J.-H. Ryu, J. Drain, J.H. Kim, S. McGee, A. Gray-Weale, L. Waddington, G.J. Parker, M. Hargreaves, S.-H. Yoo, D. Stapleton, Int. J. Biol. Macromol. 45 (2009) 478.
[3] R. Geddes, G.C. Stratton, Carbohydr. Res. 57 (1977) 291.
[4] M.A. Sullivan, F. Vilaplana, R.A. Cave, D.I. Stapleton, A.A. Gray-Weale, R.G. Gilbert, Biomacromolecules 11 (2010) 1094.
[5] E.A. Newsholme, C. Start, Regulation of Metabolism, Wiley, New York, 1974.
[6] T.E. Graham, Z. Yuan, A.K. Hill, R.J. Wilson, Acta Physiol. 199 (2010) 489.
[7] P. Drochmans, J. Ultrastruct. Res. 6 (1962) 141.
[8] Q.A. Besford, M.A. Sullivan, L. Zheng, R.G. Gilbert, D. Stapleton, A. Gray-Weale, Int. J. Biol. Macromol. 51 (2012) 887.
[9] J.-L. Putaux, A. Buleon, R. Borsali, H. Chanzy, Int. J. Biol. Macromol. 26 (1999) 145.
[10] F. Meyer, L.M. Heilmeye, R.H. Haschke, E.H. Fischer, J. Biol. Chem. 245 (1970) 6642.
[11] K.K. Rybicka, Tissue Cell 28 (1996) 253.
[12] F. Vilaplana, R.G. Gilbert, J. Sep. Sci. 33 (2010) 3537.
[13] R.G. Gilbert, Anal. Bioanal. Chem. 399 (2011) 1425.
[14] AACC International, St Paul Minnesota, 1999.
[15] R.G. Gilbert, A.C. Wu, M.A. Sullivan, G.E. Sumarriva, N. Ersch, J. Hasjim, Anal. Bioanal. Chem. (2013).
[16] M.A. Sullivan, J. Li, C. Li, F. Vilaplana, L. Zheng, D. Stapleton, A.A. Gray-Weale, S. Bowen, R.G. Gilbert, Biomacromolecules 12 (2011) 1983.
[17] A. Rolland-Sabate, M.G. Mendez-Montealvo, P. Colonna, V. Planchot, Biomacromolecules 9 (2008) 1719.
[18] S. Schmitz, A.C. Dona, P. Castignolles, R.G. Gilbert, M. Gaborieau, Macromol. Biosci. 9 (2009) 506.
[19] J. Ciric, J. Oostland, J.W. de Vries, A.J.J. Woortman, K. Loos, Anal. Chem. 84 (2012) 10463.
[20] M.A. Sullivan, M.J. O'Connor, F. Umana, E. Roura, K. Jack, D.I. Stapleton, R.G. Gilbert, Biomacromolecules 13 (2012) 3805.
[21] P.O. Powell, M.A. Sullivan, M.C. Sweedman, D.I. Stapleton, J. Hasjim, R.G. Gilbert, Carbohydr. Polym. 101 (2014) 423.
[22] Z.A. Syahariza, E. Li, J. Hasjim, Carbohydr. Polym. 82 (2010) 14.
[23] R.A. Cave, S.A. Seabrook, M.J. Gidley, R.G. Gilbert, Biomacromolecules 10 (2009) 2245.
[24] R.G.K. Jones, J. Stepto, R. Wilks, Compendium of Polymer Terminology and Nomenclature IUPAC Recommendations 2008, Society of Chemistry, Cambridge, 2009.
[25] A.E. Hamielec, A.C. Ouano, J. Liquid Chromatogr. 1 (1978) 111.
[26] A.E. Hamielec, A.C. Ouano, L.L. Nebenzahl, J. Liquid Chromatogr. 1 (1978) 527.
[27] T. Kuge, K. Kobayashi, H. Tanahashi, T. Igushi, S. Kitamura, Agric. Biol. Chem. 78 (1984) 2375.
[28] E. Gomez-Ordonez, A. Jimenez-Escrig, P. Ruperez, Talanta 93 (2012) 153.
[29] W.W. Yau, J.J. Kirkland, D.D. Bly, H.J. Stoklosa, J. Chromatogr. 125 (1976) 219.
[30] A.M. Striegel, W.W. Yau, J.J. Kirkland, D.D. Bly, Modern Size-Exclusion Liquid Chromatography—Practice of Gel Permeation and Gel Filtration Chromatography, John Wiley & Sons, Hoboken, NJ, 2009.
[31] J. Kestin, M. Sokolov, W.A. Wakeham, J. Phys. Chem. Ref. Data 7 (1978) 941.
[32] R.C. Hardy, R.L. Cottington, J. Res. Nat. Bur. Stand. 42 (1949) 573.
[33] C.E. Ioan, T. Aberle, W. Burchard, Macromolecules 32 (1999) 8655.
[34] F. Vilaplana, R.G. Gilbert, J. Chromatogr. A 1218 (2011) 4434.

4.2 Outcomes

We discovered that there is a considerably enhanced resolution obtained when analyzing glycogen with aqueous-SEC compared to using DMSO, with there being a significantly improved separation of α- and β-particle peaks.

It was revealed here that the predominant reason for the differences between the SEC distributions acquired from aqueous and DMSO setups, was the superior separation of the aqueous systems for larger molecules (in the α-particle region). It was clear that the largest pullulan standard (2.35×10^6 Da) was approaching the exclusion limits of the DMSO column setups, but not for the aqueous setups. It is important to note that pullulan swells to a larger hydrodynamic size in DMSO/LiBr compared with the aqueous (50 mM NH_4NO_3/0.02 % NaN_3) solvent, with the largest pullulan standard being ~58 nm compared with ~44 nm, respectively. If glycogen also swells more in DMSO/LiBr, a larger proportion of the distribution will be excluded in these setups, given the same pore sizes in the aqueous and DMSO columns.

While size distributions of liver glycogen using DMSO-SEC are qualitatively useful, with the inability to separate α- and β-particle peaks, the parameterization and thus quantitative comparison of these distributions is limited. Two obvious parameters that can be used are the R_h at which the peak maximum occurs, β_{Rh}, as well as the average R_h ($\overline{R}_h$) given by Equation 6[106]:

$$\log \overline{R}_h = \frac{\int_{-\infty}^{\infty} w(\log R_h) \, \mathrm{d} \log R_h}{\int_{-\infty}^{\infty} \frac{w(\log R_h)}{\log R_h} \, \mathrm{d} \log R_h} \qquad 6$$

While useful, these parameters do not give a good indication of the relative amount of α-particles in a particular sample. The ideal would be if a theory were available giving the size

distribution in terms of the rate parameters of the underlying biosynthetic processes, as has been developed for the distribution of chain lengths of amylopectin[107,108]. This is work for the future, which will be spurred by the availability of more accurate data using the technique reviewed here.

With the increased resolution obtained using aqueous SEC, leading to a separation of these α- and β-particles peaks, the determination of at least six simple empirical parameters is now possible[109]. The first two parameters are the R_h values at the β-particle and α-particle peak maxima, β_{Rh} and α_{Rh}, respectively. As with DMSO-SEC, $\overline{R}_h$ can also be determined (see Equation 6). A parameter that gives a good indication of the proportion of α-particles is the ratio of the α-particle peak height to that of the β-particle peak (α_h/β_h), as seen in Figure 14.

Another parameter, α_{area}, is determined by fitting the α-particle peak with a Gaussian distribution, and then determining the area under the curve (AUC) of this peak in relation to the AUC of the whole distribution, plotted with a conventional log axis (see Figure 14, with the estimated α-particle distribution in red). Similarly, β_{area} can be calculated by fitting a Gaussian curve to the β-particle peak (black curve in Figure 14) and dividing the area under the curve (AUC) by the distribution's total AUC.

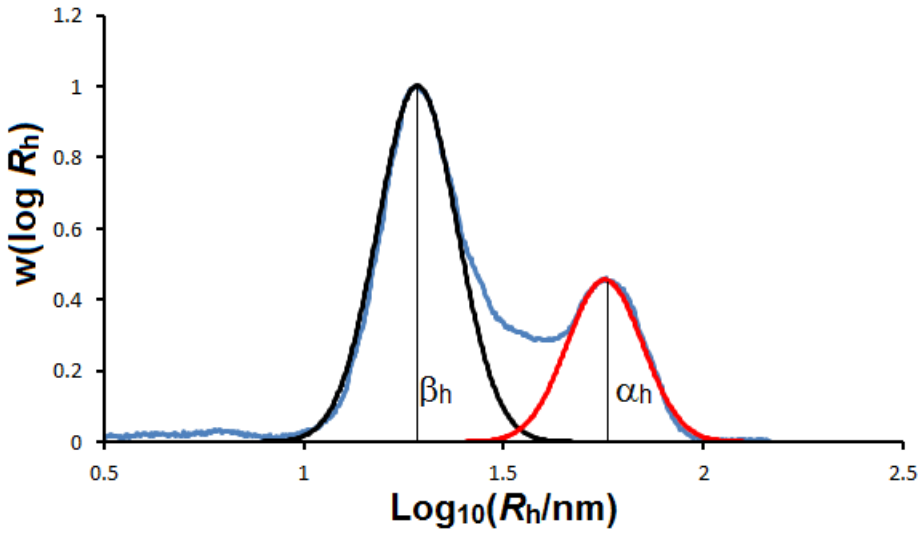

Figure 14: Parameterization of distributions by taking the ratio of peak heights and by fitting Gaussian curves to the distribution to separate the α- and β-particle components.

Unfortunately aqueous-SEC, which has been shown here to be superior to a DMSO-SEC setup, was not available for the experiments carried out in Chapter 2 and Chapter 3. It may be interesting to repeat the experiments performed in these chapters with the new system, as the improved resolution between the α- and β-particle peaks may provide greater insight into the nature of what is holding α particles together and the formation and degradation of these particles across a diurnal cycle.

Chapter 5: A Rapid Extraction Method for Glycogen from Formalin-fixed Liver

5.1 Introduction

While the use of mouse models is an extremely useful way of studying the metabolism of glycogen in terms of structure, the translation of this research into human liver-tissues will automatically enhance the physiological relevance of any further discoveries. Given pathology

laboratories' routine method of chemically fixing human liver samples with formalin, the development of a method to extract glycogen from formalin-fixed tissue would allow for the analysis of these human samples. In this chapter we compare the size distributions of glycogen extracted from frozen liver tissue via sucrose gradient centrifugation to that extracted from formalin fixed tissues. We also assess the potential for doing mass spectroscopy (MS) proteomics on glycogen extracted via both methods. The Supporting Information is given in Appendix 4.

A Rapid Extraction Method for Glycogen from Formalin-fixed Liver.

Mitchell Anthony Sullivan[1,2], Shihan Li[1,2], Samuel Theodore Nicholas Aroney[2], Bin Deng[1], Cheng Li[1,2], Eugeni Roura[2], Benjamin Luke Schulz[3], Brooke Elyse Harcourt[4], Josephine Maree Forbes[4,5], Robert Goulston Gilbert[1,2]*

[1]Tongji School of Pharmacy, Huazhong University of Science and Technology, Wuhan, Hubei 430030, China

[2]The University of Queensland, Centre for Nutrition and Food Sciences, Queensland Alliance for Agriculture and Food Innovation, Brisbane, QLD 4072, Australia

[3]School of Chemistry and Molecular Biosciences, The University of Queensland, Brisbane, QLD 4072, Australia

[4]Glycation and Diabetes Complications, Mater Research-UQ, Translational Research Institute, Woolloongabba, QLD 4102, Australia

[5]Mater Clinical School, University of Queensland, Brisbane, QLD 4072, Australia

*corresponding author: Professor Robert Gilbert, University of Queensland (83/S434), Brisbane, Queensland 4072, Australia.

Email: b.gilbert@uq.edu.au Phone: +61 41 2215 144. Fax +61 7 3365 1188

Running Head: **Formalin-fixed Liver: Glycogen Extraction**

Number of Pages: 20

Number of Figures: 3

Number of Tables: 3

BLS is supported by an NHMRC Career Development Fellowship APP1031542. JMF is an NHMRC Senior Research Fellow. MAS is supported by an Australian Postgraduate Award. RGG is supported by the 1000-Talents Program of the Chinese Foreign Experts Bureau.

Abstract

Liver glycogen is necessary for maintaining glucose homeostasis. It has recently been discovered that diabetes alters hepatic glycogen structure in mice, but it is not known if this is also the case for human liver glycogen. While past structural studies have extracted glycogen from fresh or frozen tissue using a cold-water, sucrose-gradient centrifugation technique, a method for the extraction of glycogen from formalin-fixed liver would allow the analysis of glycogen from human tissues that are routinely collected in pathology laboratories. In this study, both sucrose-gradient and formalin-fixed extraction techniques were carried out on piglet livers, with the yields, purities and size distributions (using size exclusion chromatography) compared. The formalin extraction technique, when combined with a protease treatment, resulted in higher yields (but lower purities) of glycogen with size distributions similar to the sucrose gradient centrifugation technique. This formalin extraction procedure was also significantly faster, allowing glycogen extraction throughput to increase by an order of magnitude. Both extraction techniques were compatible with mass spectrometry proteomics, with SWATH-MS analysis showing the two techniques were highly complementary. This new procedure can thus be used to examine differences in glycogen molecular structure in healthy and diabetic human livers.

Introduction

Glycogen is a highly branched glucose polymer which functionally stores energy in a state which can be rapidly mobilized in response to hypoglycaemia. The highest concentration of glycogen is present in the liver; glycogen is also found in skeletal muscle,[1] heart,[2] adipose[3] and brain tissues.[4] Liver glycogen consists of glucose units that are attached to form linear chains via α-(1→4) linkages. These chains are connected via α-(1→6)-linked branch points to form

highly branched glycogen "β" particles (~20 nm in diameter) that can further join to form much larger "α" particles (~100 – 200 nm).[5]

Glycogen was first isolated by Claude Bernard in 1857 from dog liver, employing a method of heating liver tissue in an alkaline solution.[6] This method was shown to degrade the glycogen, making the exploration of milder techniques advantageous.[7] Later methods employing cold trichloroacetic acid (TCA)[8] isolated glycogen with less degradation. Since then extraction methods have become progressively milder, with a cold water extraction method coupled with ultracentrifugation being shown to extract much larger, intact glycogen α particles.[9,10]

More recent cold-water extraction techniques have used a Tris buffer,[11-13] which is a potent inhibitor of glucosidase activity.[14] These techniques have also used sucrose-density gradient centrifugation to aid in the separation of the glycogen particles from the contaminating microsomal layer.

Liver glycogen undergoes rapid enzymatic degradation post-mortem under ambient conditions.[15] Therefore unless glycogen can be immediately extracted from fresh liver tissue, which is usually an unfeasible arrangement for human samples, characterization requires a method for preserving the tissue. Two common ways to do this are by rapidly freezing the samples or by chemically fixing them in a solution such as formalin. However, it is important to ensure that it is possible to extract glycogen from samples that have been so preserved without significant loss or degradation of the glycogen (and any glycogen-bound proteins), compared to the parent glycogen from the liver extracted immediately after sacrifice.

A method employing formalin (which can dissolve glycogen and precipitate protein) to extract liver glycogen, while initially promising,[16] was shown to be inferior to the cold-water extraction techniques, with a product of lower purity being obtained.[17] It was however noted that this method may be useful for recovering glycogen from tissues already stored in formalin.

It was shown that the formalin method extracts glycogen with larger particle sizes than the alkali and TCA methods (as inferred from having higher sedimentation coefficients), indicating less degradation; however, a comparison with the cold-water extraction technique has not yet been performed. One potential problem with the formalin technique is the acidity of formaldehyde;[17] however the use of neutral-buffered formalin (NBF), a common reagent used today for fixing tissue samples, can avoid potential acid degradation.

A comparison of glycogen extracted from modern cold-water extraction techniques that utilize Tris buffers, ultracentrifugation and sucrose density gradients with a formalin method that uses NBF would determine the potential of extracting glycogen from formalin-fixed tissues, allowing for the analysis of glycogen from the vast source of human tissues currently fixed with NBF in pathology laboratories.[18] The extension of this work into human samples would allow for a more detailed study of liver glycogen and its role in type 2 diabetes. This is especially relevant given the discovery[19] that liver glycogen from healthy and diabetic mouse livers shows significant molecular structural differences, from which a number of deductions can be made[5,20] of potential relevance to diabetes in humans. For example, the prevalence of α particles comprising tightly bound β particles in healthy livers is likely to cause slower glucose release under glycolysis, which would lead to better control of blood sugar; elucidating the nature of the structural difference between healthy and diabetic α particles might then suggest novel drug targets for diabetes management.

The efficacy of different glycogen extraction techniques, with and without formalin, is explored here, using liver from healthy piglets. Efficacy is judged by comparing the molecular size distributions from the various extraction techniques using size-exclusion chromatography, which can show if there is a systematic loss of particles of different sizes. Mass spectroscopy proteomics was also performed on mouse-liver glycogen, confirming the ability to identify

glycogen-associating proteins from glycogen extracted via both cold-water sucrose-gradient centrifugation and formalin techniques.

Materials and Methods

Animals

Glycogen was extracted from two piglet livers following a procedure similar to that used previously[20] (The University of Queensland animal ethics approval certificate CNFS/217/11/PORK CRC). Two male, 34 day-old piglets (Large White breed), reared at the UQ Gatton piggery, were sedated and euthanized prior to sample extraction. The piglets were fed a standard nursery diet consisting of wheat (68.6%); fishmeal (6.8%); whey powder (5.0%), soybean meal (4.0%) and soy protein concentrate (4.0%). A sample of liver from each (~10 g) was obtained from the central lobe of the liver and immediately frozen in liquid nitrogen and stored at −80 °C. Each following procedure was first performed with one liver sample and then repeated 2 days later with the other, acting as an experimental replicate.

For the proteomics analysis, one male 24-week old, non-fasted C57BL6/J mouse was euthanazed via CO_2 inhalation. Following this, the liver was divided into two and either immediately snap frozen for the sucrose method or placed in 10% NBF for ~48 h. Small animal studies were performed in accordance with guidelines from the University of Queensland Ethics Committee and the National Health and Medical Research Council of Australia.

Cold-water extraction using sucrose density ultracentrifugation ("sucrose method")

The procedure for liver-glycogen extraction and purification using sucrose density ultracentrifugation was similar to that used previously.[5] Approximately 1.2 g of frozen liver was homogenized in 18.2 mL of glycogen isolation buffer, an inhibitor of glucosidase activity (50 mM Tris, pH 8, 150 mM NaCl, 2 mM EDTA, 50 mM NaF, 5 mM sodium pyrophosphate,

and protease-inhibiting cocktail (Roche)). Then 200 μL of the homogenate was removed and frozen at −20 °C for glycogen content analysis. The remaining homogenate was divided into six equal portions and was centrifuged at 6000 *g* for 10 min at 4 °C with the resulting supernatants centrifuged further at 488 300 *g* for 1 h at 4 °C. The pellets were resuspended in 400 μL of glycogen isolation buffer and layered over a 3-mL stepwise sucrose gradient (37.5% and 75% in glycogen isolation buffer). The samples were then centrifuged at 488 300 *g* for 2 h at 4 °C. The supernatants were discarded and the resulting pellets were resuspended in 200 μL of deionized water. 1 mL of absolute ethanol was added to the samples and centrifuged at 4000 *g* for 10 min, with the supernatants being discarded. The pellets were resuspended in 500 μL of deionized water and then lyophilized (freeze-dried; VirTis, Benchtop K).

Preparation of 10% neutral-buffered formalin

While technically 3.7% formaldehyde, historically the preparation of this fixative chemical has been achieved by diluting commercial-grade stock formaldehyde (37-40% formaldehyde, generally referred to as formalin when in solution) 10-fold in a phosphate buffer; hence the name 10% neutral-buffered formalin (NBF). A 10% NBF solution (pH 7) was prepared by diluting 37% formaldehyde (formalin) 10-fold and adding 4% sodium dihydrogenphosphate monohydrate and 6.5% anhydrous sodium hydrogenphosphate.

Extraction of glycogen from formalin-fixed tissue ("formalin method")

The method used was modified from that employed previously.[16] Approximately 1.2 g of frozen liver was divided into 6 portions (~200 mg each). These samples were taken from the same piglets as for the "Cold-water extraction using sucrose density ultracentrifugation" section. To these samples, 2 mL of 10% NBF was added, with the liver tissues being fully immersed. These samples were left at room temperature for ~48 h, which has been shown to be an adequate time to form protein crosslinks when using NBF at ~25 °C,[21] and then

homogenized. The homogenate was subsequently centrifuged at 4000 *g* for 10 min. The supernatant of each sample was added to 10 mL of absolute ethanol and the samples were centrifuged at 4000 *g* for 10 min. The pellet was resuspended in 500 μL of deionized water and then lyophilized (freeze-dried; VirTis, Benchtop K).

Measuring the liver-glycogen content

The glycogen content of the liver was determined using a glucose oxidase/peroxidase (GOPOD) assay procedure, similar to that used previously.[5,22] Firstly, six 20 μL aliquots of liver-glycogen homogenate (from Cold-water extraction using sucrose density ultracentrifugation ("sucrose method")) were separated, allowing for a more accurate determination of the liver-glycogen content and determination of the statistical error in the analysis. To each of these 6 samples was added 5 μL of amyloglucosidase (3260 U mL^{-1}, Megazyme) and 100 μL of sodium acetate buffer (pH 6), with the solution being made up to 500 μL with deionized water and incubated on a thermomixer (50 °C) for 30 min. A control for each of the samples, containing everything except amyloglucosidase, and a blank containing everything except the glycogen homogenate, were also analyzed. A 300 μL aliquot of each sample was added to 1 mL of GOPOD reagent (Megazyme) and incubated at 50 °C for a further 30 min on the thermomixer. The absorbance (510 nm) of each sample was analyzed on a UV-1700 PharmaSpec UV-vis spectrophotometer (Shimadzu). The glycogen content was determined by constructing a calibration curve that analyzed the absorbance of various concentrations of D-glucose that had been reacted with the same GOPOD reagent. All samples including controls were run in duplicate. Various concentrations of sucrose (up to a concentration of 1 mg mL^{-1}) were also tested, showing no reaction with GOPOD, confirming that there is no additional absorbance resulting from sucrose contamination.

The liver glycogen content, given in Table 1, is presented as the mean ± standard error of the mean (SEM) of the 6 samples.

Measuring crude glycogen yield

The crude yield from both of the glycogen extraction methods, given in Table 1, was determined by weighing the amount of sample remaining after being freeze-dried. There were 6 samples from each method, allowing the yield to be presented as the mean ± standard error of the mean (SEM).

Measuring glycogen purity

The purity of glycogen can also be determined using the same assay used to measure the glycogen content of the liver. Briefly, 100 μL of extracted-glycogen solution (~0.006 mg mL^{-1}) was added to 5 μL of amyloglucosidase (3260 U mL^{-1}, Megazyme) and 100 μL of sodium acetate buffer (pH 6), with the solution being made up to 500 μL with deionized water. The rest of the procedure is identical to that in the section "Measuring the liver-glycogen content", with the glycogen purity being calculated as a percentage of the determined glycogen content to that of the intial amount of sample used in the assay. Because there were 6 samples for each extraction procedure, the glycogen purity is given as the mean ± standard error of the mean (SEM); see Table 1.

Protease treatment of formalin-extracted glycogen ("formalin/protease method")

Approximately 3 mg of the glycogen extracted using the formalin-extraction method was subjected to protease treatment as follows. Glycogen was dissolved in 0.5 mL of protease solution (2.5 U mL^{-1}; bacterial type XIV, Sigma-Aldrich) in tricine buffer (pH 7.5, 250 mM) and incubated at 37 °C for 4 h. Samples were then lyophilized (freeze-dried; VirTis, BTP-9EL).

Size-exclusion chromatography (SEC) of glycogen

An aqueous SEC setup similar to that recently employed for glycogen characterization was used here.[23] Glycogen samples were dissolved in a thermomixer overnight at 25 °C in 50 mM ammonium nitrate/0.02% sodium azide at ~2 g L^{-1}. The effect of heating the samples overnight at 80 °C in a thermomixer was also tested. As previously stated,[23] the ammonium nitrate is used to minimize any potential interactions between the glycogen and the column by increasing the solution's ionic strength. Sodium azide acts as an antimicrobial agent.

Dissolved glycogen samples were injected into an Agilent 1260 infinity SEC system (Aglient, Santa Clara, CA, USA) using a column setup of SUPREMA pre-column, 1000 and 10000 columns (Polymer Standard Service, Mainz, Germany). The columns were kept at 80 °C using a column oven and the flow rate was set to 0.3 mL min^{-1}. A refractive index detector (RID) (Optilab UT-rEX, WYATT, Santa Barbara, CA, USA) was used to determine the SEC weight distributions.

Pullulan standards (PSS), with a molar mass range of 342 Da to 2.35×10^6 Da, were dissolved into the 50 mM ammonium nitrate/0.02% sodium azide solution and run through the SEC system, allowing the construction of a universal calibration curve. While this assumes that the SEC is separating solely on hydrodynamic size, a valid assumption shown for molecules with widely varied shapes,[24,25] the purpose of this study was to compare the relative structure of glycogen obtained from different extraction methods, with any inaccuracies in calibration being equal for all of the samples as they were run consecutively.

Mass Spectrometry

Mouse-liver glycogen was extracted via both the sucrose and formalin methods, as was performed with the piglet livers (see Cold-water extraction using sucrose density ultracentrifugation ("sucrose method") and Extraction of glycogen from formalin-fixed tissue

213 ("formalin method")). For glycogen extracted from the formalin method, two treatments that
214 have been previously employed for formalin-fixed tissue were trialled.[26] 2 mg mL^{-1} of
215 glycogen was treated with either 6 M guanidine-HCl or 2% SDS, then heated at 100 °C for 1
216 h. Samples without either treatment were also tested as a control. Glycogen extracted from the
217 sucrose method also did not undergo these additional treatments.

218 Extracted glycogen samples containing ~50 μg protein were resuspended in 50 mM Tris HCl
219 buffer (pH 7.5) and 10 mM DTT with 1 μg trypsin (proteomics grade, Sigma-Aldrich) and
220 incubated at 37 °C with constant mixing for 16 h. Insoluble material was removed by
221 centrifugation at 18 000 *g* for 10 min, and peptides were desalted with C18 ZipTips (Millipore).
222 Peptides were analyzed as described previously[27] by LC-ESI-MS/MS using a Prominence
223 nanoLC system (Shimadzu) and TripleTof 5600 mass spectrometry with a Nanospray III
224 interface (AB SCIEX). Identical LC conditions were used for SWATH-MS, with an MS-TOF
225 scan from an *m/z* of 350-1800 for 0.05 s followed by high sensitivity information-independent
226 acquisition with 26 *m/z* isolation windows with 1 *m/z* window overlap each for 0.1 s across an
227 *m/z* range of 400 – 1250. Collision energy was automatically assigned by Analyst software (AB
228 SCIEX) based on *m/z* window ranges.

229 Peptides were identified essentially as described.[28] using ProteinPilot (AB SCIEX), searching
230 the UniProt database (downloaded from www.uniprot.org/ as at 4th March 2014) with standard
231 settings: Sample type, identification; Instrument, TripleTof 5600; Species, Mouse with
232 common contaminants; ID focus, biological modifications; Enzyme, Trypsin; Search effort,
233 thorough ID. False discovery rate analysis using ProteinPilot was performed on all searches,
234 and peptides identified with greater than 99% confidence and with a local false discovery rate
235 of less than 1% were included for further analysis. ProteinPilot search results were used as ion
236 libraries for SWATH analyses. The abundance of proteins were measured automatically using

PeakView (AB SCIEX) with standard settings. Comparison of protein relative abundance was performed with the MSstats package in R.[29] Gene ontology analysis was performed using the DAVID bioinformatics resource.[30]

Results

The extraction of liver-glycogen using different techniques was performed on the same liver samples, allowing the direct comparison of the methods. Because the trend was the same for both pigs, the main text contains results from a single pig, with those for the corresponding size-exclusion chromatography data for the other in the SI.

The yields and purities of glycogen extracted with the sucrose and formalin methods are given in Table 1.

Table 1. Glycogen content, purity and yield.

	Liver-Glycogen Content (%)	**Crude yield (%)**	**Purity (%)**	**Glycogen Yield (%)**
Sucrose	4.31 ± 0.022	3.6 ± 0.15	55 ± 5.30	46 ± 4.65
Formalin		11.8 ± 0.45	31 ± 5.42	85 ± 16.94

Samples are given as the mean ± standard error of the mean (SEM), n = 6.

While the purity of the glycogen extracted using the formalin method is lower than that of the sucrose method (~31% compared to ~55%), the amount of glycogen extracted (the glycogen yield) is significantly higher with the formalin method, which extracted ~85% of the glycogen present in the liver (as calculated in "Measuring the liver-glycogen content"), compared to the ~46% from the sucrose method. Because the formalin/protease method consists of taking

formalin-extracted glycogen and adding protease, the glycogen yield is the same as for the formalin method. The crude yield and purity will change as a direct result of how much protease is added to the samples.

Size distributions of the glycogen extracted by the sucrose method, the formalin method and the formalin/protease method are given in Figure 1.

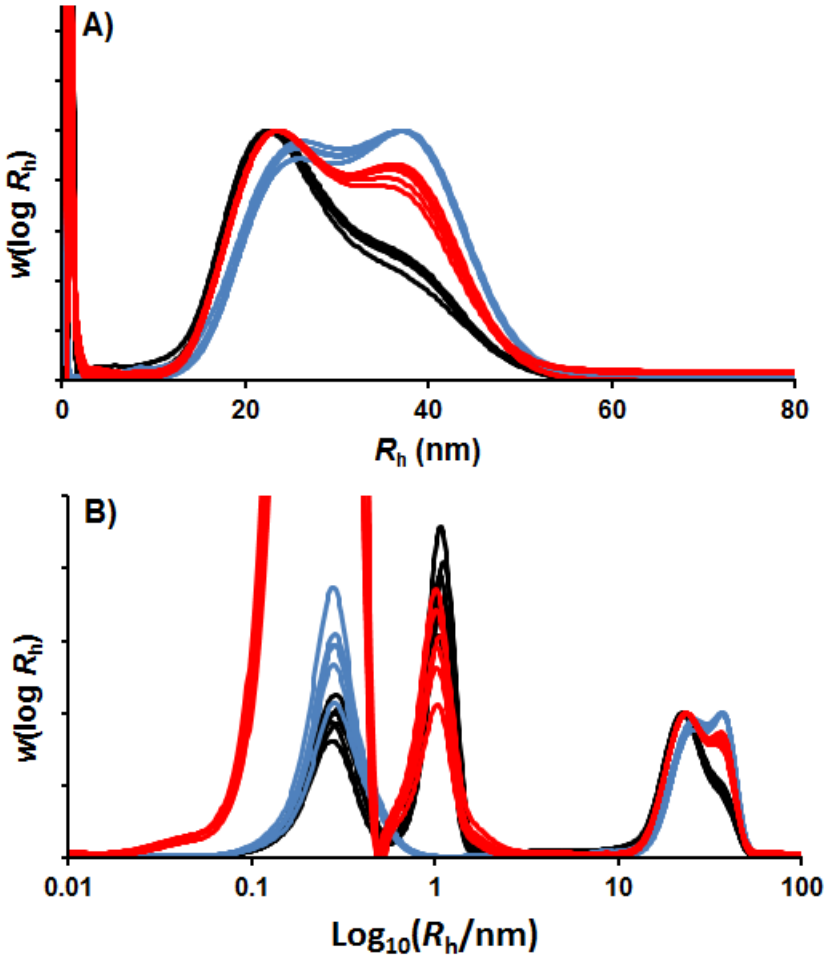

Figure 1. SEC weight distributions, $w(\log R_h)$; normalized to have equal heights for the maximum glycogen peak) as a function of molecular size (the hydrodnamic radius R_h) for pig-liver glycogen extracted via the sucrose method (blue), formalin method (black) and formalin/protease method (red). The same data are provided with a linear X-axis in R_h (A) and a logarithmic X-axis (B), aiding in the visual observation of this large range of molecular sizes.

While there are 6 replicates for each extraction technique, there is significant overlap between distributions of the same method. The SEC samples were also run at a concentration 5 times more dilute, with no changes occuring in the distribution, indicating no aggregation (see SI).

As shown in Figure 1A, each of the three extraction methods have a similar and relatively good level of repeatability, with little variation between the six distributions within each extraction method. There is however some variation so care must be taken when drawing conclusions from very similar distibutions.

The effect of dissolving samples at 80 $^{\circ}$C overnight (compared to the much milder 25 $^{\circ}$C) was also tested, as this method has been employed previously.[23] As can be seen in Figure 2, glycogen from all extraction methods showed some level of degradation when dissolved at 80 $^{\circ}$C compared to 25 $^{\circ}$C.

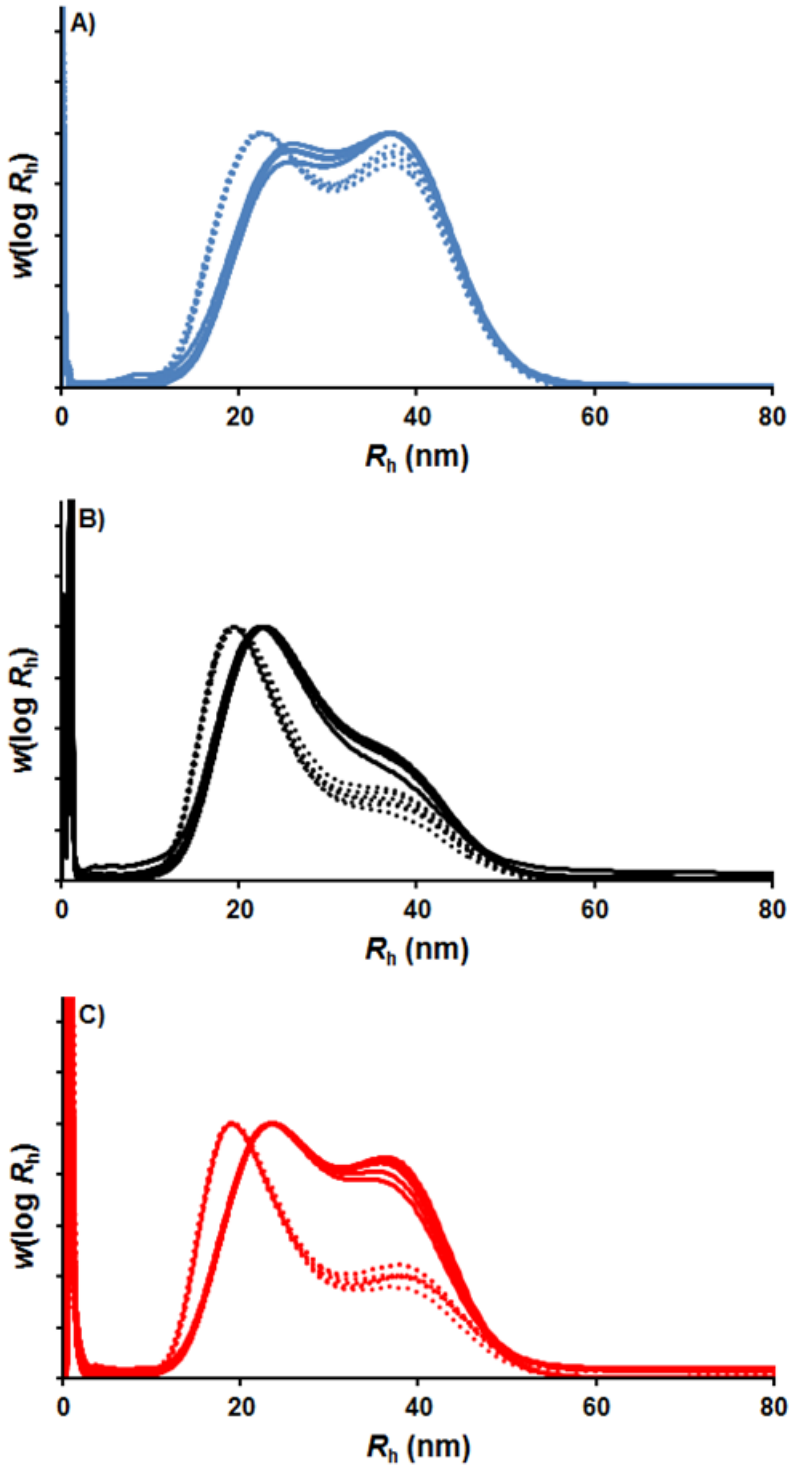

278

279 Figure 2. SEC weight distributions, $w(\log R_h)$, normalized to have equal heights for the
280 maximum glycogen peak, as a function of molecular size (the hydrodnamic radius R_h) for pig-
281 liver glycogen dissolved overnight at 25 °C (full line) and 80 °C (broken line) extracted via the
282 sucrose method (A, blue), formalin method (B, black) and formalin/protease method (C, red).

While there are 6 replicates for each extraction technique, there is significant overlap between distributions of the same method.

Mass spectroscopy (MS) proteomics was also performed on mouse-liver glycogen extracted via the sucrose and formalin methods. Proteins were digested with trypsin and detected by LC-ESI-MS/MS. This identified 147 proteins with guanidine-HCl treatment, 40 with SDS treatment and 137 with no additional treatment (Supplementary Tables 1-4). Glycogenin and glycogen phosphorylase, proteins associated with glycogen biosynthesis, were confidently identified in formalin-extracted glycogen after guanidine-HCl treatment (Table 2).

Table 2. Peptides identified from glycogen-associated proteins enriched from formalin fixed tissue.

Sequence	**ΔMass**	***m/z***	***z***	**Score**
PYGL_MOUSE				
ARPEFMLPVHFYGR	-0.0043	430.7241	4	7
DIWNMEPSDLK	0.0025	674.3174	2	8
GIVGVENVAELK	0.0006	614.3511	2	8
HLEIIYEINQK	-0.0032	467.2564	3	8
ISLSNESSNGVSANGK	0.0027	783.3694	2	10
IVALFPK	-0.0026	394.2562	2	5
LHSFVSDDIFLR	0.0017	483.5898	3	9

TFAYTNHTVLPEALER	-0.0050	621.3179	3	9
VFADYEAYVK	0.0009	602.7983	2	8
VLYPNDNFFEGK	-0.0005	721.8510	2	10
YEYGIFNQK	0.0556	581.3102	2	9
GLYG_MOUSE				
MVVLTSPQVSDSMR	0.0034	775.3909	2	13

294

295

296 However, as expected by the measured purity of the samples, many non-glycogen associated
297 proteins were also identified in these preparations. To compare formalin-extracted glycogen
298 with standard sucrose enriched glycogen, we performed semi-quantitative proteomics with
299 SWATH-MS. Proteomic analysis of glycogen enriched using the sucrose method identifyed
300 290 proteins. SWATH-MS comparison of sucrose and formalin extracted glycogen found 72%
301 of proteins had significantly different relative abundances (adjusted $P < 0.05$), suggesting that
302 these extraction methods are qualitiatively complementary (Figure 3 – volcano plot).

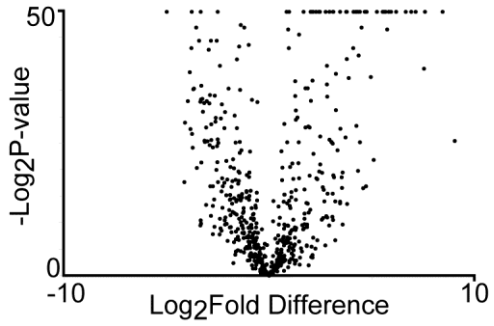

303

304

Figure 3. Volcano plot comparing differences in relative protein abundances in glycogen samples enriched via the sucrose method and the formalin method. Technical triplicates of each enrichment method were compared with SWATH-MS. Each data point represents an independent protein.

Gene ontology analysis was peformed to compare the proteins enriched by the sucrose and formalin extraction methods (see Table 3).

Table 3. Gene ontology analysis of proteins enriched by sucrose versus formalin methods

Keyword	Count	%	Adjusted P-value
Enriched in Sucrose preparation			
ribosomal protein	67	31	8.20E-18
ribonucleoprotein	71	32.9	4.80E-13
acetylation	157	72.7	7.70E-05
ribosome	17	7.9	1.50E-02
Enriched in Formalin preparation			
cytoplasm	95	47.5	2.60E-06
hydrolase	40	20	3.70E-03
Secreted	23	11.5	2.30E-02
disulfide bond	32	16	3.30E-02
metal-binding	52	26	3.80E-02

Discussion

While a cold-water extraction method that utilizes sucrose density centrifugation has been shown to be effective in extracting glycogen with minimal degradation,[11,12,31] a method that allows glycogen to be extracted from formalin-fixed tissues would permit the study of glycogen from formalin-fixed human tissues in pathology laboratories. The analysis of human glycogen would result in studies that are more physiologically relevant to human health. Given the discovery that the glycogen from diabetic (*db/db*) mice has a significantly different structure to that of the non-diabetic controls[19] and the evidence that glycogen structure may be important in its metabolism,[5] the potential impacts of having a better undertstanding of glycogen metabolism in terms of structure for humans is considerable.

Because the normalization of these distributions is arbitrary, one cannot say, for example, that one technique or other results on more or less extraction of α particles; however, comparison of *relative* amounts is meaningful.

The distributions of glycogen extracted using the formalin method (without protease) have relatively fewer α particles then the sucrose method; however, when treated with protease, there is a substantial increase in the relative height of the α particle peak (see Figure 1A). While there are still more α particles in relative terms from the sucrose method, it is possible that this is due to a loss of β particles from this method, as opposed to a loss of α particles in the formalin/protease method. Indeed, the preferential loss of β particles in the sucrose method appears to be more likely, both because the total yield is lower (see Table 1) and because, given the method's reliance on the larger, denser particles forming a pellet after the sucrose-gradient centrifugation step, it is more likely that smaller particles would be lost. The shift of the β-

particle peak from the sucrose method to higher sizes is consistent with the prefential loss of smaller particles.

One possible explanation for the increased amount of α particles in the formalin/protease method, compared to the formalin method (see Figure 1A), is that a significant amount of α particles may be left insoluble after formalin fixation, most likely due to glycogen-associating proteins being linked together to form large insoluble aggregates which can be liberated when exposed to protease. This may suggest that there are significantly more proteins on the outside of α particles than β particles; however this is only speculation. Another possibility is that there is a network of proteins that are not connected to the larger glycogen α particles, but form a physical barrier that allows smaller β particles, but not α particles, to pass into solution. Here protease would be able to destroy this barrier, allowing these glycogen α particles to be analyzed using SEC.

If the predominant aim of an experiment is to analyze the size distributions of the liver glycogen, then small contaminant molecules (such as sucrose or small proteins) that do not overlap with the glycogen in the size distribution are inconsequential. As can be seen in Figure 1B, there are a large amount of non-glycogen contaminants for all extraction methods; however these do not overlap in molecular size with the glycogen distributions. There is a large contaminant peak of small molecules in the formalin/protease extracted samples resulting from the tricine that was used in the buffer for the protease treatment.

If higher purities are required, the use of an S500 chromatography column has been shown to be effective at removing smaller particles such as free sugars and protein contaminants; however as is common with additional purification techniques, this leads to lower yields and also may affect the size distributions.[11,12]

The effect of heating samples at 80 ˚C was also analyzed, with the results showing that care must be taken when dissolving glycogen in an aqueous solvent, with lower temperatures being preferable (see Figure 2). Of particular interest is that the α particles of glycogen extracted via the formalin and formalin/protease method are much more susceptible to degradation than glycogen extracted via the sucrose method. Glycogen extracted using these methods should therefore always be dissolved at mild temperatures. The pH of the samples from all of the extraction methods was ~7, ruling out acid hydrolysis as the reason for degradation.

Inferences for bonding between β particles in α particles

The difference in degradation rates of glycogen extracted via the different methods may shed some light on the bond that holds glycogen α particles together, the nature of which there is as yet no unambiguous evidence. The fact that the formalin extraction technique leads to a significant weakening of the bonds holding α particles together provides further evidence (in addition to that reported previously[20]) that glycogen α particles are not held together via glycosidic linkages. While at room temperature protein reacts relatively quickly with formaldehyde, carbohydrates are unreactive with formaldehyde at this temperature,[32] remaining chemically unaltered unless exposed to fixation for several weeks.[33] Therefore the preferential degradation of α particles in the presence of formaldehyde is additional evidence that the bond holding them together is different to glycosidic linkages. Given the well established ability of formaldehyde to form both inter- and intra-molecular crosslinks between protein residues, it is possible that the conformation of this hypothesized protein "glue" is altered by reacting with formaldehyde. It has been shown that whether a protein maintains its native confirmation after treatment in 10% NBF depends on that protein. For example, in one study RNase A maintained a conformation almost identical to the native, untreated protein while myoglobin showed significant stuctural changes after treatment with formalin.[34] However when heated, in both cases the formalin-treated proteins behaved differently to the

untreated controls, having a broad and non-cooperative thermal transition as opposed to the cooperative, relatively sharp transitions of the native proteins. It is therefore entirely possible that any protein "glue" would be in a significantly different conformation at 80 °C when the glycogen was extracted with the formalin method as opposed to the sucrose method. How this difference would affect the ability of the protein to join the β particles together can only be speculated at this point and is beyond the scope of this study; however we will offer a brief description of two possibilities. Firstly, if there is a protein linked covalently to join together β particles, it is possible that denaturing this protein will make the protein backbone more susceptible to shear scission; given the relatively large molecular weights of β particles (10^6 – 10^7), the amount of shear scission during SEC characterization that could be subjected to a single-molecule glue holding these together may be sufficient to cleave a bond. While such shear scission is very unlikely in small molecules, it becomes increasingly likely with larger molecules, and certainly occurs with amylopectin, which is of a size commensurate with that of glycogen α particles.[35] Secondly, while the possibility of a non-covalent protein linkage has been inconsistent with a number of studies that have used powerful denaturants,[10] the presence of a highly resistant protein cannot be completely disregarded. If so, it is possible that this resistant protein is denatured to the extent of failing as a glue when treated with formalin and heated to 80 °C.

Identification of glycogen-associated proteins

Further investigations of the regulation of the structure of glycogen would require identification and measurement of the proteins physically associated with glycogen particles. Mass spectrometry proteomics would be a useful approach for this purpose. We therefore tested if formalin-extracted glycogen was compatible with MS proteomic analyses. Several sample preparation methods were tested, including denaturing proteins in formalin-extracted glycogen samples with guanidine-HCl or SDS, compared with no additional treatment. It has been shown

here that formalin-extracted glycogen can be analyzed successfully for associated proteins when using guanidine-HCl; however due to the low purity of the samples, there is a large amout of contaminating proteins. Again this problem can be largely circumvented by employing further purification with an S500 gel chromatography column. Gene ontology analysis of the differentially abundant proteins showed that the sucrose method enriched contaminating proteins from intracellular ribosomes, whereas the formalin method enriched secreted proteins, confirming the complementarity of these methods for glycogen enrichment (see Table 3). The volcano plot (Figure 3) illustrates these differences between the two methods. Future studies aimed at identifying bona fide glycogen-associated proteins would require additional purification steps to remove contaminating proteins.

Acknowledgements

The authors wish to thank Felipe Umana and Haichen Shou for their assistance with the porcine studies. We also thank Enpeng Li for his technical assistance with SEC measurments. BLS is supported by an NHMRC Career Development Fellowship APP1031542. JMF is an NHMRC Senior Research Fellow. The support of the 1000-Talents Program of the Chinese Foreign Experts Bureau is gratefully acknowledged.

References

(1) Calder, P. C.; Geddes, R. *Carb. Research* **1985**, *135*, 249.
(2) Besford, Q. A.; Sullivan, M. A.; Zheng, L.; Gilbert, R. G.; Stapleton, D.; Gray-Weale, A. *Int. J. Biol. Macromolecules* **2012**, *51*, 887.
(3) Jurczak, M. J.; Danos, A. M.; Rehrmann, V. R.; Allison, M. B.; Greenberg, C. C.; Brady, M. J. *American Journal of Physiology-Endocrinology and Metabolism* **2007**, *292*, E952.
(4) Brown, A. M. *Journal of Neurochemistry* **2004**, *89*, 537.
(5) Sullivan, M. A.; Aroney, S. T. N.; Li, S.; Warren, F. J.; Joo, L.; Mak, K. S.; Stapleton, D. I.; Bell-Anderson, K. S.; Gilbert, R. G. *Biomacromolecules* **2014**, *15*, 660.
(6) Bernard, C. *Compt. rend.* **1857**, *44*, 578.
(7) Bueding, E.; Orrell, S. A. *J. Biol. Chem.* **1964**, *239*, 4018.
(8) Stetten, M. R.; Katzen, H. M.; Stetten, D. *Journal of Biological Chemistry* **1956**, *222*, 587.

(9) Lazarow, A. *Anatomical Record* **1942**, *84*, 31.
(10) Orrell, S. A.; Bueding, E. *J. Biol. Chem.* **1964**, *239*, 4021.
(11) Parker, G. J.; Koay, A.; Gilbert-Wilson, R.; Waddington, L. J.; Stapleton, D. *Biochemical and Biophysical Research Communications* **2007**, *362*, 811.
(12) Ryu, J.-H.; Drain, J.; Kim, J. H.; McGee, S.; Gray-Weale, A.; Waddington, L.; Parker, G. J.; Hargreaves, M.; Yoo, S.-H.; Stapleton, D. *International Journal of Biological Macromolecules* **2009**, *45*, 478.
(13) Sullivan, M. A.; Vilaplana, F.; Cave, R. A.; Stapleton, D. I.; Gray-Weale, A. A.; Gilbert, R. G. *Biomacromolecules* **2010**, *11*, 1094.
(14) De Apodaca, M. A. O.; Fernandez, E.; Delafuente, G. *Journal of Inherited Metabolic Disease* **1992**, *15*, 213.
(15) Geddes, R.; Rapson, K. B. *Febs Letters* **1973**, *31*, 324.
(16) Devor, A. W.; Canowitz, D. H. *Analytical Biochemistry* **1962**, *3*, 166.
(17) Devor, A. W.; Barichie.Ro; Siddiqui, B. *Analytical Biochemistry* **1966**, *14*, 237.
(18) Thavarajah, R.; Mudimbaimannar, V. K.; Elizabeth, J.; Rao, U. K.; Ranganathan, K. *Journal of oral and maxillofacial pathology* **2012**, *16*, 400.
(19) Sullivan, M. A.; Li, J.; Li, C.; Vilaplana, F.; Zheng, L.; Stapleton, D.; Gray-Weale, A. A.; Bowen, S.; Gilbert, R. G. *Biomacromolecules* **2011**, *12*, 1983.
(20) Sullivan, M. A.; O'Connor, M. J.; Umana, F.; Roura, E.; Jack, K.; Stapleton, D. I.; Gilbert, R. G. *Biomacromolecules* **2012**, *13*, 3805.
(21) Helander, K. G. *Biotechnic & Histochemistry* **1994**, *69*, 177.
(22) Roehrig, K. L.; Allred, J. B. *Anal. Biochem.* **1974**, *58*, 414.
(23) Sullivan, M. A.; Powell, P. O.; Witt, T.; Vilaplana, F.; Roura, E.; Gilbert, R. G. *Journal of Chromatography A* **2014**, *1332*, 21.
(24) Hamielec, A. E.; Ouano, A. C. *J. Liquid Chromatography* **1978**, *1*, 111.
(25) Kuge, T.; Kobayashi, K.; Tanahashi, H.; Igushi, T.; Kitamura, S. *Agric. Biol. Chem.* **1984**, *78*, 2375.
(26) Jiang, X. G.; Jiang, X. N.; Feng, S.; Tian, R. J.; Ye, M. L.; Zou, H. F. *J Proteome Res* **2007**, *6*, 1038.
(27) Bailey, U. M.; Jamaluddin, M. F. B.; Schulz, B. L. *J Proteome Res* **2012**, *11*, 5376.
(28) Bailey, U. M.; Punyadeera, C.; Cooper-White, J. J.; Schulz, B. L. *J Chromatogr B Analyt Technol Biomed Life Sci* **2012**, *911*, 21.
(29) Choi, M.; Chang, C. Y.; Clough, T.; Broudy, D.; Killeen, T.; MacLean, B.; Vitek, O. *Bioinformatics* **2014**, *In Press, DOI 10.1093/bioinformatics/btu305*.
(30) Huang, D. W.; Sherman, B. R.; Lempicki, R. A. *Nat Protoc* **2009**, *4*, 44.
(31) Sullivan, M. A.; Vilaplana, F.; Cave, R. A.; Stapleton, D. I.; Gray-Weale, A. A.; Gilbert, R. G. *Biomacromolecules* **2010**, *11*, 1094.
(32) Eltoum, I.; Fredenburgh, J.; Myers, R. B.; Grizzle, W. E. *Journal of Histotechnology* **2001**, *24*, 173.
(33) Kiernan, J. A. *Microscopy Today* **2000**, *1*, 8.
(34) Fowler, C. B.; Evers, D. L.; O'Leary, T. J.; Mason, J. T. *J Histochem. Cytochem.* **2011**, *59*, 366.
(35) Cave, R. A.; Seabrook, S. A.; Gidley, M. J.; Gilbert, R. G. *Biomacromolecules* **2009**, *10*, 2245.

5.2 Outcomes

Liver glycogen extracted from both sucrose-gradient centrifugation and formalin-fixed techniques were carried out, comparing the yields, purities and SEC size distributions. The formalin extraction technique, when combined with an additional protease treatment step, resulted in higher yields (but lower purities) of glycogen with size distributions similar to the sucrose gradient centrifugation technique. This formalin extraction procedure was also significantly faster, allowing the throughput of glycogen samples that can be extracted to increase by an order of magnitude. Both the sucrose gradient centrifugation and formalin techniques were compatible with MS proteomics, with SWATH-MS analysis showing the two techniques to be highly complementary. This new procedure can thus be used to examine differences in glycogen molecular structure in human livers, allowing the link between diabetes and liver glycogen to be further explored.

Chapter 6: Thesis discussion and future work

6.1 Discussion

The work described in this thesis has resulted in a richer understanding of liver-glycogen metabolism in terms of structure, an aspect of glycaemic control that has often been overlooked. Given the building evidence that smaller glycogen particles: 1) have a higher association with glycogen phosphorylase[102], a key enzyme involved in glycogen degradation; and 2) are degraded more rapidly *in vitro*[31,110], the inability to form larger glycogen α particles is predicted to result in a faster, less controlled degradation into glucose. This is hypothesized to be the reason why evolution has favored the formation of large α particles in the liver, where glucose release needs to be relatively slow and tightly controlled, as opposed to the smaller β particles found in muscle tissue where glycogen needs to be broken down rapidly during

exercise. It is therefore conceivable that poor blood-glucose control is at the very least exacerbated in *db/db* mice by impaired α particle formation.

The question of what holds α particles together has proven to be difficult to resolve, with a number of past studies coming to conflicting conclusions. The possibility of hydrogen bonding has been consistently negated by experimental evidence[7,31], suggesting a covalent link. While the disulfide-disrupting reagent 2-mercaptoethanol appeared to cause α particles to break down, we have shown in Chapter 2 that this is an artifact. Another study also used 2-mercaptoethanol and iodoacetamide and reported no change in the size of liver glycogen[35]. The authors suggested that the link between β particles may just be α-(1→4) glycosidic linkages, the same bond used to connect glucose units in a glycogen chain. Again, Chapter 2 sheds light on this issue. Here, SEC was used to obtain the weight distributions of glycogen at various times after being exposed to a relatively low pH (~3.5). While it is well known that acid can hydrolyze glycogen[31,111], only when these semiquantitative distributions were obtained did it become clear that the bonds holding α particles together were degraded much faster by acid hydrolysis than the normal glycosidic linkages in glycogen. This was consistent with past sucrose density centrifugation data[112]. Furthermore, it was shown in this recent SEC study that, even at a neutral pH, α particles can degrade into β particles. The degradation rates of α particles to β particles in both acidic and neutral pHs were found to be consistent with the hydrolysis of protein[113,114]: the "glue" whereby the β particles in α particles are held together is therefore hypothesized to be proteinaceous and covalently linked to the glycogen.

One major implication of α particles being held together by protein (as suggested although not proven by experiment), as opposed to simply α-(1→4) or α-(1→6) glycosidic linkages, is a new potential target for clinical intervention. Approximately half of the orally dosed drugs used clinically are small molecules that inhibit the action of enzymes[115,116]. Therefore, any enzyme

that may be linked to impaired α particle formation (or increased α particle degradation) may potentially become a new drug target for inhibition. If a "glue" protein is found, a new drug that upregulates this protein to increase the synthesis rate and the molecular size of α particles becomes a possible intervention for diabetic patients.

It should be noted however, that there is also evidence that is not consistant with a proeteinaceous linkage, with the most obvious being that protease does not have an effect on the size of glycogen α particles. Another important consideration is the lack of reactivity of the non-reducing end of the glycogen chains, making it unlikely that any protein "glue" is able to directly react with the end of a glycogen chain. One possibility is that the phosphorylation of glycogen plays an important role in forming a covalent link with a protein glue. Another possibility (not yet tested) is that there is a direct link between β particles via phosphodiesters. While significant progress has been made in this study, future work is required to determine what links β particles together to form these larger α particles.

One important aspect of analyzing the effect glycogen structure has on glycaemic control is to determine when in the diurnal cycle of glycogen metabolism these α particles form. Equally important is to determine when these particles begin to degrade. To answer this, as given in Chapter 3, we exploited the natural diurnal cycle of glycogen metabolism in mice, sacrificing wild-type mice at various times during a 12 hour light/12 hour dark cycle. By analyzing the glycogen content and structure for each mouse we were able to form a much more detailed understanding of the role structure plays in liver-glycogen metabolism. This study revealed three key insights: 1) glycogen initially forms as separate β particles, only to be subsequently joined together to form larger α particles after the glycogen content has reached its maximum concentration; 2) during glycogen degradation the larger particles were much more resistant to glycogenolysis, persisting significantly longer than the smaller β particles; and 3) glycogen

particles are finally degraded to a small but resistant particle with a hydrodynamic radius of ~ 12 nm. Not only does this data support the theory that glycogen particle size influences the rate of glycogenolysis, but it strongly suggests that there is a mechanism in which separate β particles are able to conglomerate to form an α particle.

Given the critical role SEC plays in our understanding of glycogen structure, allowing us to probe aspects of glycogen metabolism previously unexplored due to technological limitations, any improvements made in the effectiveness of this method will be invaluable to further research into the role of glycogen structure in glycaemic control. After the recent finding that an aqueous-SEC system achieved significantly improved resolution, when compared to a DMSO-SEC system for synthetic, branched polysaccharides[105], it became clear that a comparison between our past DMSO-SEC system with the newer aqueous-SEC system could give us an improved method for analyzing glycogen's structure. While temporarily delaying the search for answers regarding glycogen structure's role in glycaemic control, an improvement in our analysis techniques could greatly increase the efficiency in which we subsequently answer these questions. Indeed, as described in Chapter 4, we found a significantly improved resolution in the SEC distributions obtained using aqueous-SEC in comparison to our previous DMSO-SEC setup. This improved resolution greatly increases the power of our SEC analyses, resulting in separation of β- and α-particle peaks. This separation is not achieved using DMSO-SEC, with the α particles forming a shoulder on the β-particle peak. As explained in greater detail in Chapter 4, there are considerable benefits to being able to separate the maxima of the β- and α-particle peaks, one being the increased ability to effectively parameterize and thus statistically compare distributions. Aqueous-SEC should therefore be used for all future work requiring glycogen SEC distributions.

Another important aspect of characterizing the structure of glycogen is being able to extract glycogen with minimal degradation. Since the initial isolation of glycogen from dog liver in 1857[117], the search for extraction techniques that result in decreased damage to the native structure has resulted in the progression of milder methods. After glycogen was shown to be degraded by both hot-alkaline[118] and cold trichloroacetic acid[31] extraction methods, the development and improvement of cold-water techniques[1,7,31,119,120] has allowed for the extraction of glycogen with minimal degradation. Given the extensive practice in pathology laboratories of chemically fixing liver tissue in a solution of dissolved formaldehyde, known as formalin[121], the development of an extraction method that can isolate glycogen from these tissues with minimal degradation would allow this vast source of human tissues to be analyzed. This extension of glycogen research into human tissues will greatly enhance the physiological relavance, in terms of human health, of further investigations into the role of glycogen structure in maintaining blood-glucose homeostasis.

Here we developed a method of extracting glycogen from formalin-fixed liver tissue. While the purity of the glycogen is lower than when compared with the cold-water sucrose gradient centrifugation method, the glycogen yield is greater. Because the impurities from both methods consist of small molecules, there is no overlap between contaminants and glycogen in the SEC distributions, making their presence irrelevant to the determination of accurate size distributions. As discussed in Chapter 5, the sucrose gradient method appears to result in the preferential loss of smaller β particles, making the formalin method preferable when needing to obtain accurate size distributions. However one disadvantage with this method is that the glycogen α particles are much more vulnerable to being degraded in water. Care must therefore be taken, with glycogen being dissolved at room temperature. This unexpected difference in susceptibilty of degradation between glycogen extracted via the formalin and sucrose gradient techniques gives us further insight into the bond holding α particles together. The preferential

degradation of α particles into β particles (compared to the degradation of β particles) following the formalin extraction method is further evidence that glycosidic linkages do not hold α particles together. Given carbohydrates are unreactive to formalin[122], but that formalin reacts rapidly with protein[123], it is possible that the inter-molecular and intra-molecular crosslinks formed during formalin fixing affect the proposed protein "glue", making it more susceptible to degradation when being heated at 80 °C. Again further research is required to test this protein "glue" hypothesis.

6.2 Future Research

While there have been a number of important advancements in our knowledge on glycogen's structure and the role this plays in its metabolism, this research is still in its infancy. There are a number of projects currently underway to further progress this research and a large amount of future projects that have been conceived to help answer the plethora of questions arising from the work presented here. In brief, here are some of the more pertinent questions remaining unanswered: What is the bond holding α particles together?; If the bond is proteinaceous, what is this protein?; Is the difference in glycogen structure seen in *db/db* mice present across the whole diurnal cycle?; Why is α-particle formation impaired in *db/db* mice?; Can a "healthy" glycogen structure be rescued in *db/db* mice with the administration of suitable type 2 diabetic drugs? and; Is this impaired α particle formation seen in other models for type 2 diabetes and most importantly, in humans?

A detailed project proposed for an NHMRC fellowship is given in Appendix 5. Below are summaries for other potential projects aimed to answer some of the above unanswered questions.

6.2.1 Proteomic analysis of fractionated glycogen

If there is a proteinaceous link holding α particles together, this protein should be able to be detected using mass-spectroscopy-based proteomics. While mass spectroscopy (MS) has been used to successful identify proteins associated on the surface of liver glycogen[19], here we propose to degrade glycogen with α-amylase and identify any proteins trapped inside the glycogen particles. Theoretically any protein "glue" should be more abundant in the α patricles than in the β particles. Therefore, by performing MS proteomics on glycogen that has been fractionated based on size and treated with α-amylase to liberate any trapped proteins, we can identify potential proteins involved in binding the larger α particles together. The absence of any suitable proteins would be strong evidence against the protein "glue" hypothesis. Fractionation of the glycogen can be performed using preparative SEC.

6.2.2 Analyzing glycogen structure across a diurnal cycle for healthy and *db/db* mice

The discovery[98] that *db/db* mice had fewer α particles than healthy mice only analyzed samples at one time point during the day (9 am). Given the diurnal nature of glycogen synthesis (discussed in Chapter 3), it is important to determine whether *db/db* mice are able to synthesize α particles at any stage across the 24 h cycle. The project proposed here is to repeat the experiments outlined in Chapter 3 but to also analyze *db/db* mice, with the wild-type mice acting as a control.

6.2.3 Analyzing glycogen structure across a diurnal cycle for healthy and high-fat diet mice

To determine whether glycogen structure plays a role in glycaemic control and diabetes, more than one dibetic model needs to be analyzed. An alternative to the *db/db* mouse as a model for type 2 diabetes is the high-fat diet mouse. While genetically identical to the controls, these mice are given a diet that has a higher fat content than the controls, causing them to become

obese and eventually insulin resistant. Again it would be ideal to analyze the glycogen content and structure over the course of a diurnal cycle.

References

(1) Ryu, J.-H.; Drain, J.; Kim, J. H.; McGee, S.; Gray-Weale, A.; Waddington, L.; Parker, G. J.; Hargreaves, M.; Yoo, S.-H.; Stapleton, D. *International Journal of Biological Macromolecules* **2009**, *45*, 478.

(2) Newsholme, E. A.; Start, C. *Regulation of Glycogen Metabolism*; Wiley: New York, **1974**.

(3) Manners, D. J. *Carbohydr. Polym.* **1991**, *16*, 37.

(4) Takeuchi, T.; Iwamasa, T.; Miyayama, H. *J. Electron Microsc.* **1978**, *27*, 31.

(5) Sullivan, M. A.; O'Connor, M. J.; Umana, F.; Roura, E.; Jack, K.; Stapleton, D. I.; Gilbert, R. G. *Biomacromolecules* **2012**, *13*, 3805.

(6) Rybicka, K. K. *Tissue Cell* **1996**, *28*, 253.

(7) Sullivan, M. A.; Vilaplana, F.; Cave, R. A.; Stapleton, D. I.; Gray-Weale, A. A.; Gilbert, R. G. *Biomacromolecules* **2010**, *11*, 1094.

(8) Manners, D. J. *Advances in Carbohydrate Chemistry & Biochemistry* **1962**, *17*, 371.

(9) Calder, P. C. *Int. J. Biochem.* **1991**, *23*, 1335.

(10) Peat, S.; Whelan, W. J.; Thomas, G. J. *Journal of the Chemical Society* **1952**, 4546.

(11) Haworth, W. N.; Hirst, E. L.; Isherwood, F. *Journal of the Chemical Society* **1937**, 577.

(12) Staudinger, H.; Husemann, E. *Annalen* **1937**, *530*, 1.

(13) Meyer, K. H.; Fuld, M. *Helvetica Chimica Acta* **1941**, *24*, 375.

(14) Larner, J.; Illingworth, B.; Cori, G. T.; Cori, C. F. *Journal of Biological Chemistry* **1952**, *199*, 641.

(15) Manners, D. *Carbohydrate Polymers* **1991**, *16*, 37.

(16) Gunja-Smith, Z.; Marshall, J. J.; Smith, E. E.; Whelan, W. J. *FEBS Letters* **1970**, *12*, 96.

(17) Marshall, J. J.; Whelan, W. J. *Archs Biochem. Biophys.* **1974**, *161*, 234.

(18) Shearer, J.; Graham, T. E. *Can. J. Appl. Physiology* **2002**, *27*, 179.

(19) Stapleton, D.; Nelson, C.; Parsawar, K.; McClain, D.; Gilbert-Wilson, R.; Barker, E.; Rudd, B.; Brown, K.; Hendrix, W.; O'Donnell, P.; Parker, G. *Proteomics* **2010**, *10*, 2320.

(20) Roach, P. J.; Depaoli-Roach, A. A.; Hurley, T. D.; Tagliabracci, V. S. *Biochemical Journal* **2012**, *441*, 763.

(21) Fontana, J. D. *Febs Letters* **1980**, *109*, 85.

(22) Tagliabracci, V. S.; Girard, J. M.; Segvich, D.; Meyer, C.; Turnbull, J.; Zhao, X. C.; Minassian, B. A.; DePaoli-Roach, A. A.; Roach, P. J. *Journal of Biological Chemistry* **2008**, *283*, 33816.

(23) Tagliabracci, V. S.; Turnbull, J.; Wang, W.; Girard, J. M.; Zhao, X.; Skurat, A. V.; Delgado-Escueta, A. V.; Minassian, B. A.; DePaoli-Roach, A. A.; Roach, P. J. *Proceedings of the National Academy of Sciences of the United States of America* **2007**, *104*, 19262.

(24) Lomako, J.; Lomako, W. M.; Kirkman, B. R.; Whelan, W. J. *Biofactors* **1994**, *4*, 167.

(25) Tagliabracci, V. S.; Heiss, C.; Karthik, C.; Contreras, C. J.; Glushka, J.; Ishihara, M.; Azadi, P.; Hurley, T. D.; DePaoli-Roach, A. A.; Roach, P. J. *Cell Metabolism* **2011**, *13*, 274.

(26) Nitschke, F.; Wang, P. X.; Schmieder, P.; Girard, J. M.; Awrey, D. E.; Wang, T.; Israelian, J.; Zhao, X. C.; Turnbull, J.; Heydenreich, M.; Kleinpeter, E.; Steup, M.; Minassian, B. A. *Cell Metabolism* **2013**, *17*, 756.

(27) Orrell, S. A.; Bueding, E. *Journal of Biological Chemistry* **1964**, *239*, 4021.

(28) Zhou, Z. K.; Cao, X. H.; Zhou, J. Y. H. *Starch-Starke* **2013**, *65*, 509.

(29) Krisman, C. R.; Barengo, R. *Eur. J. Biochem.* **1975**, *52*, 117.

(30) Chee, N. P.; Geddes, R. *FEBS Letters* **1977**, *73*, 164.

(31) Orrell, S. A.; Bueding, E. *J. Biol. Chem.* **1964**, *239*, 4021.

(32) Geddes, R.; Stratton, G. C. *Carbohydr. Res.* **1977**, *57*, 291.

(33) Geddes, R.; Harvey, J. D.; Wills, P. R. *European Journal of Biochemistry* **1977**, *81*, 465.

(34) Campbell, D. G.; Cohen, P. *European Journal of Biochemistry* **1989**, *185*, 119.

(35) Matsuda, K.; Hata, K. *Denpun Kagaku* **1985**, *32*, 118.

(36) Matsuda, K.; Hata, K. *Journal of the Japanese Society of Starch Science* **1985**, *32*, 118.

(37) Melendez, R.; Melendez-Hevia, E.; Mas, F.; Mach, J.; Cascante, M. *Biophys. J.* **1998**, *75*, 106.

(38) Sullivan, M. A.; Li, J.; Li, C.; Vilaplana, F.; Zheng, L.; Stapleton, D.; Gray-Weale, A. A.; Bowen, S.; Gilbert, R. G. *Biomacromolecules* **2011**, *12*, 1983.

(39) Smythe, C.; Villar-Palasi, C.; Cohen, P. *Eur. J. Biochem.* **1989**, *183*, 205.

(40) Roden, M.; Bernroider, E. *Best Practise & Research Clinical Endocrinology & Metabolism* **2003**, *17*, 365.

(41) Anderson, M. S.; Bluestone, J. A. *Annual Review of Immunology* **2005**, *23*, 447.

(42) Nordlie, R. C.; Foster, J. D. *Annual Review of Nutrition* **1999**, *19*, 379.

(43) Berg, J. M.; Tymoczko, J. L.; Stryer, L. *Biochemistry*; W. H. Freeman: San Francisco, **2007**; Vol. 6th.

(44) Gibbons, B. J.; Roach, P. J.; Hurley, T. D. *Journal of Molecular Biology* **2002**, *319*, 463.

(45) Mu, J.; Roach, P. *Journal of Biological Chemistry* **1998**, *273*, 34850.

(46) Lomako, J.; Lomako, W. M.; Whelan, W. J. *Biochim. Biophys. Acta, Gen. Subj.* **2004**, *1673*, 45.

(47) Skurat, A. V.; Dietrich, A. D.; Roach, P. J. *Archives of Biochemistry and Biophysics* **2006**, *456*, 93.

(48) Manners, D. J. *Academic Press, New York.* **1968**, 83.

(49) Tappy, L. *Diabetes and Metabolism* **1995**, *21*, 233.

(50) Dhital, S.; Shelat, K. J.; Shrestha, A. K.; Gidley, M. J. *Carbohydrate Polymers* **2013**, *93*, 365.

(51) Mukerjea, R.; Robyt, J. F. *Carbohydr. Res.* **2013**, *372*, 55.

(52) Kim, H. J.; White, P. J. *Journal of Agricultural and Food Chemistry* **2013**, *61*, 3270.

(53) Mikkelsen, R.; Suszkiewicz, K.; Blennow, A. *Biochemistry* **2006**, *45*, 4674.

(54) Roesler, W. J.; Khandelwal, R. L. *International Journal of Biochemistry* **1985**, *17*, 81.

(55) Higgins, G. M.; Berkson, J.; Flock, E. *American Journal of Physiology* **1932**, *102*, 673.

(56) Halberg, F.; Albrecht, P. G.; Barnum, C. P. *American Journal of Physiology* **1960**, *199*, 400.

(57) Ishikawa, K.; Shimazu, T. *Life Sciences* **1976**, *19*, 1873.

(58) Philippens, K. M. H.; Vonmayersbach, H.; Scheving, L. E. *Journal of Nutrition* **1977**, *107*, 176.

(59) Parodi, A. J. *Archives of Biochemistry and Biophysics* **1967**, *120*, 547.

(60) Mori, S.; Barth, H. G. *Size Exclusion Chromatography*; Springer: Berlin, **1999**.

(61) Jones, R. G.; Kahovec, J.; Stepto, R.; Wilks, E. S.; Hess, M.; Kitayama, T.; Metanomski, W. V. *Compendium of Polymer Terminology and Nomenclature* **2008**.

(62) *Transmission Electron Microscopy*; Williams, D. B.; Carter, C. B., Eds.; Springer, **2009**.

(63) Magliano, D. J.; Barr, E. L. M.; Zimmet, P. Z.; Cameron, A. J.; Dunstan, D. W.; Colagiuri, S.; Jolley, D.; Owen, N.; Phillis, P.; Tapp, R. J.; Welborn, T. A.; Shaw, J. E. *Diabetes Care* **2008**, *31*, 267.

(64) Yach, D.; Stuckler, D.; Brownell, K. D. *Nature Medicine* **2006**, *12*, 62.

(65) Xu, Y.; Wang, L.; He, J.; Bi, Y.; Li, M.; Wang, T.; Wang, L.; Jiang, Y.; Dai, M.; Lu, J.; Xu, M.; Yichong Li; Nan Hu; Li, J.; Shengquan Mi; Chen, C.-S.; Li, G.; Mu, Y.; Zhao, J.; Ko, L.; Chen, J.; La, S.; Wan, W.; Zhao, W.; Ning, G. *Journal of the American Medical Association* **2013**, *310*, 948.

(66) Sakuraba, H.; Mizukami, H.; Yagihashi, N.; Wada, R.; Hanyu, C.; Yagihashi, S. *Diabetologia* **2002**, *45*, 85.

(67) Butler, A. E.; Janson, J.; Bonner-Weir, S.; Ritzel, R.; Rizza, R. A.; Butler, P. C. *Diabetes* **2003**, *52*, 102.

(68) Biarnes, M.; Montolio, M.; Nacher, V.; Raurell, M.; Soler, J.; Montanya, E. *Diabetes* **2002**, *51*, 66.

(69) Fujita, Y.; Herron, A. L.; Seltzer, H. S. *Diabetes* **1975**, *24*, 17.

(70) Virally, M.; Blickle, J. F.; Girard, J.; Halimi, S.; Simon, D.; Guillausseau, P. J. *Diabetes Metab.* **2007**, *33*, 231.

(71) Kruszynska, Y. T.; Olefsky, J. M. *Journal of Investigative Medicine* **1996**, *44*, 413.

(72) DeFronzo, R. A. *Diabetes Reviews* **1997**, *5*, 177.

(73) Weyer, C.; Bogardus, C.; Mott, D. M.; Pratley, R. E. *Journal of Clinical Investigation* **1999**, *104*, 787.

(74) Orahilly, S. P.; Nugent, Z.; Rudenski, A. S.; Hosker, J. P.; Burnett, M. A.; Darling, P.; Turner, R. C. *Lancet* **1986**, *2*, 360.

(75) Kahn, S. E. *Diabetologia* **2003**, *46*, 3.

(76) Freemantle, N.; Holmes, J.; Hockey, A.; Kumar, S. *Int. J. Clin. Pract.* **2008**, *62*, 1391.

(77) Prentice, A. M.; Hennig, B. J.; Fulford, A. J. *International Journal of Obesity* **2008**, *32*, 1607.

(78) Harris, J. L.; Pomeranz, J. L.; Lobstein, T.; Brownell, K. D. In *Annual Review of Public Health* **2009**; Vol. 30, p 211.

(79) Sherry, B.; Mei, Z.; Scanlon, K. S.; Mokdad, A. H.; Grurnmer-Strawn, L. M. *Archives of Pediatrics & Adolescent Medicine* **2004**, *158*, 1116.

(80) Hummel, K. P.; Dickie, M. M.; Coleman, D. L. *Science* **1966**, *153*, 1127.

(81) Ingalls, A. M.; Dickie, M. M.; Snell, G. D. *Journal of Heredity* **1950**, *41*, 317.

(82) Dickie, M. M.; Lane, P. W. *Mouse News Lett.* **1957**, *17*, 52.

(83) Zhang, Y. Y.; Proenca, R.; Maffei, M.; Barone, M.; Leopold, L.; Friedman, J. M. *Nature* **1994**, *372*, 425.

(84) Tartaglia, L. A.; Dembski, M.; Weng, X.; Deng, N. H.; Culpepper, J.; Devos, R.; Richards, G. J.; Campfield, L. A.; Clark, F. T.; Deeds, J.; Muir, C.; Sanker, S.; Moriarty, A.; Moore, K. J.; Smutko, J. S.; Mays, G. G.; Woolf, E. A.; Monroe, C. A.; Tepper, R. I. *Cell* **1995**, *83*, 1263.

(85) Chen, H.; Charlat, O.; Tartaglia, L. A.; Woolf, E. A.; Weng, X.; Ellis, S. J.; Lakey, N. D.; Culpepper, J.; Moore, K. J.; Breitbart, R. E.; Duyk, G. M.; Tepper, R. I.; Morgenstern, J. P. *Cell* **1996**, *84*, 491.

(86) Coleman, D. L. *Nature Medicine* **2010**, *16*, 1097.

(87) Coleman, D. L.; Hummel, K. P. *American Journal of Physiology* **1969**, *217*, 1298.

(88) Coleman, D. L. *Diabetologia* **1973**, *9*, 294.

(89) Stearns, S. B.; Benzo, C. A. *Laboratory Investigation* **1977**, *37*, 180.

(90) Coleman, D. L.; Hummel, K. P. *Diabetologia* **1967**, *3*, 238.

(91) Chan, T. M.; Young, K. M.; Hutson, N. J.; Brumley, F. T.; Exton, J. H. *American Journal of Physiology* **1975**, *229*, 1702.

(92) Roesler, W. J.; Helgason, C.; Gulka, M.; Knandelwal, R. L. *Hormone and Metabolic Research* **1985**, *17*, 572.

(93) Roesler, W. J.; Khandelwal, R. L. *International Journal of Biochemistry* **1985**, *17*, 81.

(94) Soilberger, A. *Annals of the New York Academy of Sciences* **1964**, *117*, 519.

(95) Cohn, C.; Joseph, D. *Proceedings of the Society for Experimental Biology and Medicine* **1971**, *137*, 1303.

(96) Roesler, W. J.; Khandelwal, R. L. *Diabetes* **1986**, *35*, 210.

(97) Roesler, W. J.; Pugazhenthi, S.; Khandelwal, R. L. *Molecular and Cellular Biochemistry* **1990**, *92*, 99.

(98) Man, J. M.; Yang, Y.; Huang, J.; Zhang, C. Q.; Zhang, F. M.; Wang, Y. P.; Gu, M. H.; Liu, Q. Q.; Wei, C. X. *Food Chemistry* **2013**, *138*, 2089.

(99) Stetten, M. R.; Stetten, D. *Journal of Biological Chemistry* **1958**, *232*, 489.

(100) Barber, A. A.; Orrell, S. A.; Bueding, E. *Journal of Biological Chemistry* **1967**, *242*, 4040.

(101) Stetten, M. R.; Stetten Jr., D. *Journal of Biological Chemistry* **1958**, *232*, 489.

(102) Barber, A. A.; A., O. S.; Bueding, E. *Journal of Biological Chemistry* **1967**, *242*, 4040.

(103) Cardell, R. R.; Larner, J.; Babcock, M. B. *Anatomical Record* **1973**, *177*, 23.

(104) Baic, D.; Ladewski, B. G.; Frye, B. E. *Journal of Experimental Zoology* **1979**, *210*, 381.

(105) Ciric, J.; Oostland, J.; de Vries, J. W.; Woortman, A. J. J.; Loos, K. *Analytical Chemistry* **2012**, *84*, 10463.

(106) Vilaplana, F.; Gilbert, R. G. *J. Chromatography A* **2011**, *1218*, 4434.

(107) Wu, A. C.; Gilbert, R. G. *Biomacromolecules* **2010**, *11*, 3539.

(108) Wu, A. C.; Morell, M. K.; Gilbert, R. G. *PLoS ONE* **2013**, *8*, e65768.

(109) Sullivan, M. A.; Powell, P. O.; Witt, T.; Vilaplana, F.; Roura, E.; Gilbert, R. G. *J. Chromatography A* **2014**, *1332*, 21.

(110) Sullivan, M. A.; Aroney, S. T. N.; Li, S.; Warren, F. J.; Joo, L.; Mak, K. S.; Stapleton, D. I.; Bell-Anderson, K. S.; Gilbert, R. G. *Biomacromolecules* **2014**, *15*, 660.

(111) Drochmans, P. *J. Ultrastructural Res.* **1962**, *6*, 141.

(112) Mordoh, J.; Krisman, C. R.; Leloir, L. F. *Archives of Biochemistry and Biophysics* **1966**, *113*, 265.

(113) Downs, F.; Pigman, W. *Int. J. Protein Res.* **1970**, *2*, 27.

(114) Radzicka, A.; Wolfenden, R. *J. Am. Chem. Soc.* **1996**, *118*, 6105.

(115) Copeland, R. A.; Harpel, M. R.; Tummino, P. J. *Expert Opinion on Therapeutic Targets* **2007**, *11*, 967.

(116) Hopkins, A. L.; Groom, C. R. *Nature Reviews Drug Discovery* **2002**, *1*, 727.

(117) Bernard, C. *Compt. rend.* **1857**, *44*, 578.

(118) Bueding, E.; Orrell, S. A. *J. Biol. Chem.* **1964**, *239*, 4018.

(119) Lazarow, A. *Anatomical Record* **1942**, *84*, 31.

(120) Parker, G. J.; Koay, A.; Gilbert-Wilson, R.; Waddington, L. J.; Stapleton, D. *Biochemical and Biophysical Research Communications* **2007**, *362*, 811.

(121) Thavarajah, R.; Mudimbaimannar, V. K.; Elizabeth, J.; Rao, U. K.; Ranganathan, K. *Journal of oral and maxillofacial pathology* **2012**, *16*, 400.

(122) Eltoum, I.; Fredenburgh, J.; Myers, R. B.; Grizzle, W. E. *Journal of Histotechnology* **2001**, *24*, 173.

(123) Kiernan, J. A. *Microscopy Today* **2000**, *1*, 8.

Appendices

8.1 Appendix 1

New Molecular Insights into Glycogen Alpha-Particle Formation

Supporting Information

Acid hydrolysis repeat experiments

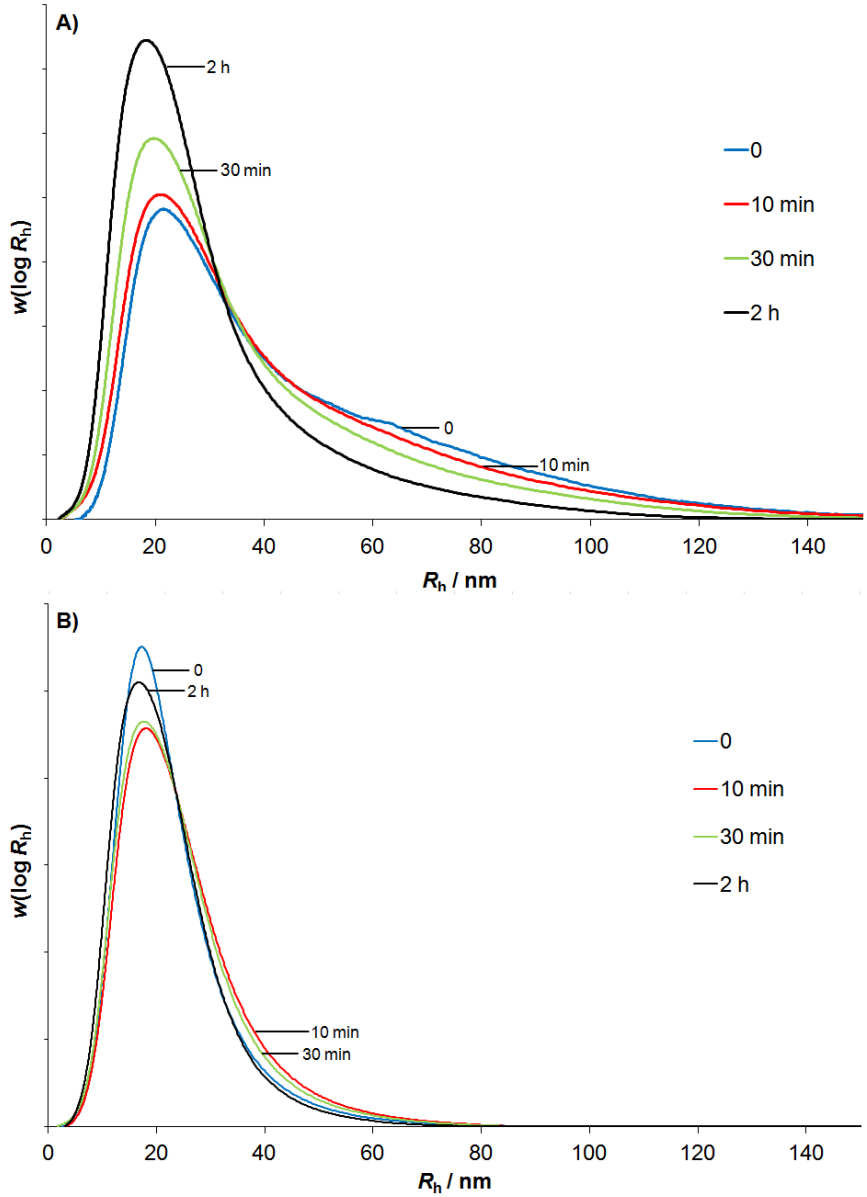

Figure 1. First 2 h of acid hydrolysis repeat; pig liver (A) and oyster (B) glycogen before acid hydrolysis (blue), and after 10 min (red), 30 min (green) and 2 h (black) of acid hydrolysis.

Shows the same trend as the figure presented in the main text.

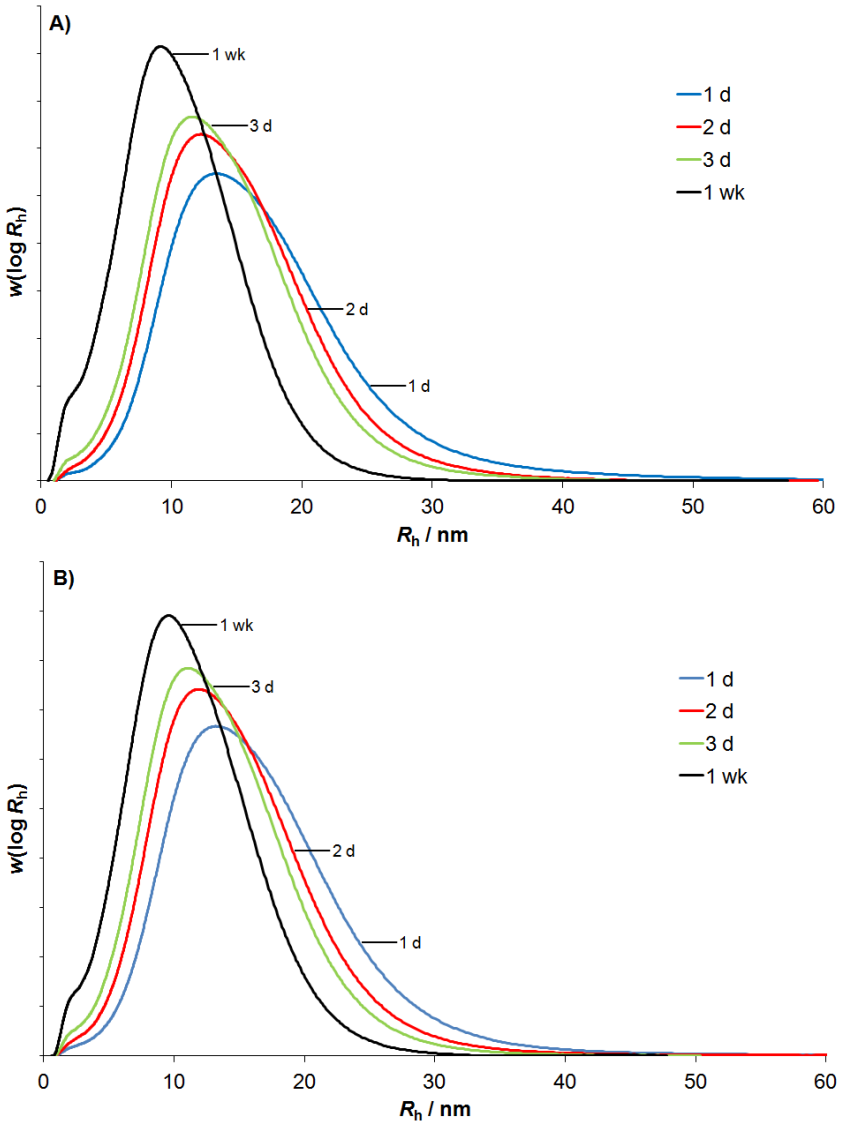

Figure 2. Final stages of acid hydrolysis repeat; pig-liver (A) and oyster (B) glycogen after 1 d (blue), 2 d (red), 3 d (green) and 1 week (black) of acid hydrolysis.

Batch MALLS Berry Plots

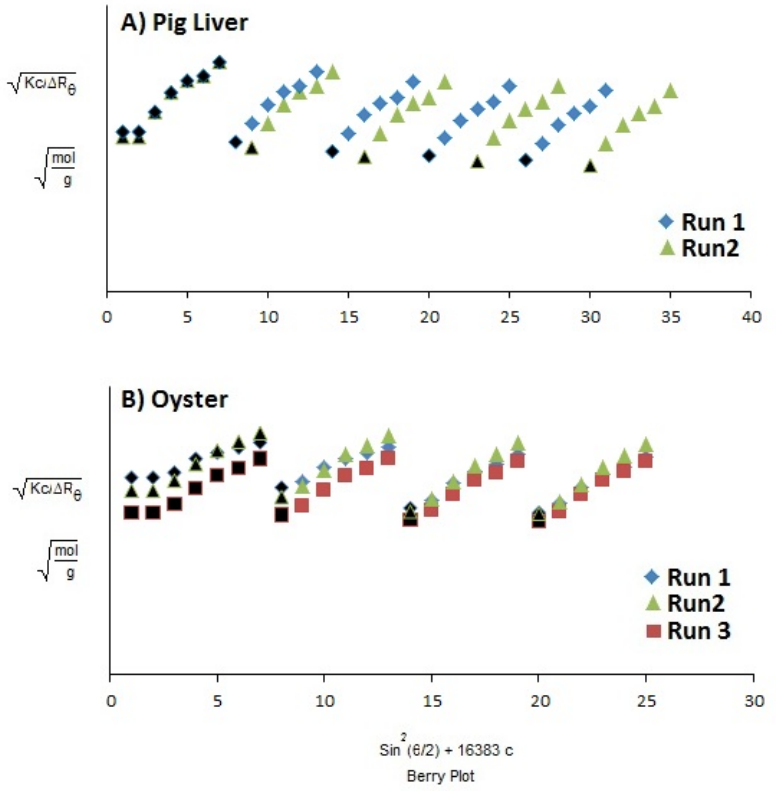

Figure 3. Replicate Berry plots of pig-liver (A) and oyster glycogen (B). Extrapolated values to zero concentration are coloured in black.

Calulation of rate constant for the hydrolysis of AcG-GNHMe at neutral pH

The following calculation uses data taken from the literature for the hydrolysis of AcG-GNHMe (representative of a protein peptide bond).[1]
By assuming the reacton rate is of Arhenius form, the rate constant of hydrolysis can be estimated at 80 ^{o}C.

At 150 ^{o}C the rate constant of AcG-GNHMe hydrolysis is 5.1×10^{-6} s^{-1}. The activation energy was calculated to be 98.3 kJ mol^{-1}.[1] The pre-exponential factor can then be calculated from the above equation to be ~ 7.1×10^{6} s^{-1} . This gives an estimated hydrolysis rate of 2.0×10^{-8} s^{-1} at 80 ^{o}C.

(1) Radzicka, A.; Wolfenden, R. *Journal of the American Chemical Society* **1996**, *118*, 6105.

8.2 Appendix 2

Supporting Information

Changes in glycogen structure over feeding cycle sheds new light on blood-glucose control

Mitchell A. Sullivan, Samuel T. N. Aroney, Shihan Li, Frederick J. Warren, Jin Suk Joo, Ka Sin Mak, David I. Stapleton, Kim S. Bell-Anderson & Robert G. Gilbert

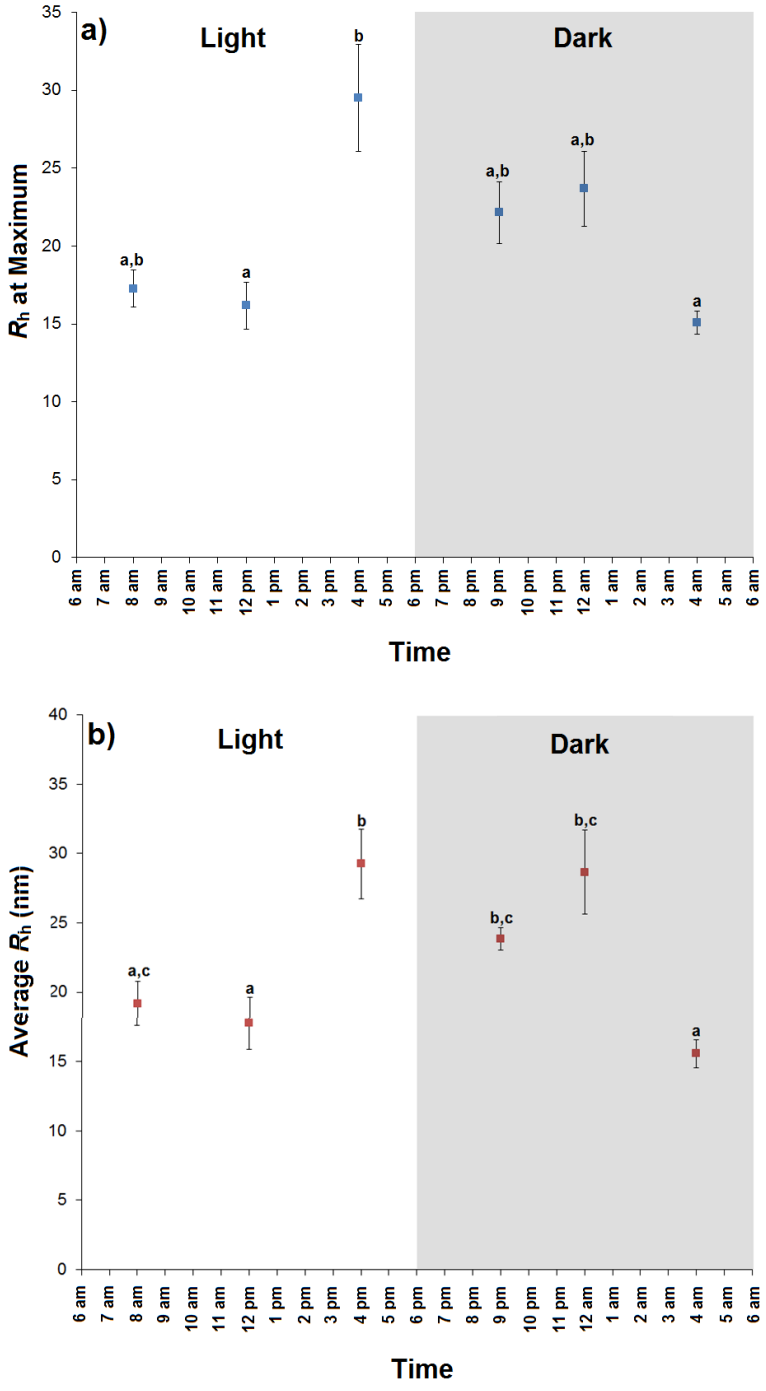

Figure S1. The mean hydrodynamic radius (R_h) at which the maximum occurs (a) and the average hydrodynamic radius (b) (calculated as previously)[1] for SEC weight distributions of glycogen at various times during a light/dark cycle. Values shown are the mean ± S.E.M. of 3–9 mice. Different letters indicate statistical significance ($p < 0.05$).

Preliminary kinetics studies

Materials

Potassium phosphate, ethylenediaminetetraacetic acid (EDTA), magnesium chloride, α-D glucose 1,6-diphosphate, β-nicotinamide adenine dinucleotide phosphate (β-NAPD), glucose-6-phosphate dehydrogenase, phosphoglucomutase, glycogen phosphorylase b from rabbit muscle and adenosine 5′-monophosphate (AMP) were purchased from Sigma-Aldrich. Diabetic C57BL/6j-db/db and wild-type female mice were sacrificed at either ~1.5 months ("young") or ~3 months ("old"). Glycogen extraction was performed using established methods.[2,3] Glycogen was extracted from the livers of eight mice with 4 non-diabetic (3 old and 1 young) and 4 diabetic (2 old and 2 young). The important factor is that there are a range of glycogen sizes to test the dependence of size on the initial rate of phosphorylase degradation; this range of sizes was achieved (see Figure S2).

Preparation of Digestion Buffer

A solution containing 500 mM potassium phosphate, 300 mM magnesium chloride and 100 mM EDTA (adjusted to pH 6.8) was prepared. The digestion buffer was obtained by mixing this solution (1.5 mL) with deionized water (10 mL), NADP 0.08 mg mL^{-1} (1 mL) and α-D glucose 1,6-diphosphate 0.08 mg mL^{-1} (30 μL).

Glycogen Phosphorylase Assay

The phosphorylase assays were performed on mouse-liver glycogen using a similar assay to a past study.[4] 0.8 mg of mouse-liver glycogen was dissolved into 0.2 mL of digestion buffer. Samples were then dissolved in a thermomixer at 80 °C and 350 rpm for 4 h. Samples were then diluted to 0.1125 mg mL^{-1} with the digestion buffer. .

A microplate reader (BMG FLUOstar OPTIMA) was used to measure the absorbance of β-NADPH, which is produced during the reaction. The following reagents were placed into each well: 180 μL glycogen solution, 6 μL of glycogen phophorylase (0.75 U mL^{-1}), 6 μL of

phosphoglucomutase (10 U mL^{-1}), 6 µL glucose-6-phosphate dehydrogenase (10 U mL^{-1}) and 2 µL of 100 mM 5 ′ AMP. Absorbance of the samples at 37 °C was measured at 340 nm every 90 s. A standard curve of known concentrations of β-NADPH was used. Initial rates for the reaction were obtained from the linear region of a plot of product concentration against time.

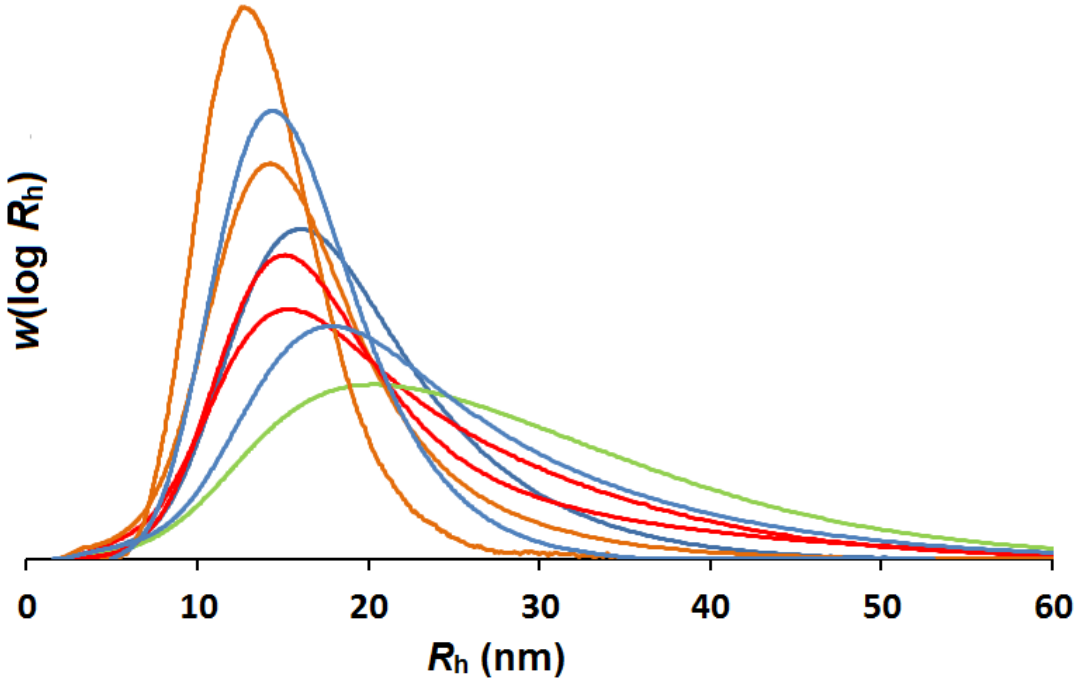

Figure S2. SEC weight distributions, $w(\log R_h)$ (normalized to equal areas) of young non-diabetic (green), old non-diabetic (blue), young diabetic (orange) and old diabetic (red) mice.

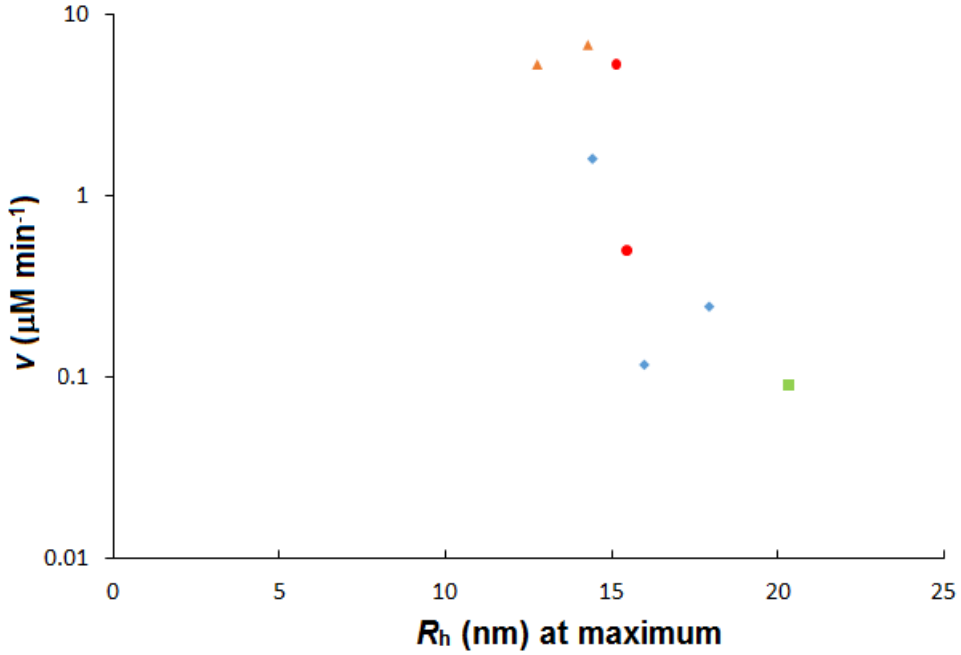

Figure S3. Initial rate *v* of glycogen phosphorylase degradation of glycogen from young non-diabetic (green square), old non-diabetic (blue diamond), young diabetic (orange triangle) and old diabetic (red circle) mice.

(1) Vilaplana, F.; Gilbert, R. G. *J. Chromatography A* **2011**, *1218*, 4434.

(2) Ryu, J.-H.; Drain, J.; Kim, J. H.; McGee, S.; Gray-Weale, A.; Waddington, L.; Parker, G. J.; Hargreaves, M.; Yoo, S.-H.; Stapleton, D. *International Journal of Biological Macromolecules* **2009**, *45*, 478.

(3) Sullivan, M. A.; Li, J.; Li, C. Z.; Vilaplana, F.; Stapleton, D.; Gray-Weale, A. A.; Bowen, S.; Zheng, L.; Gilbert, R. G. *Biomacromolecules* **2011**, *12*, 1983.

(4) Thomas, D. A.; Wright, B. E. *Journal of Biological Chemistry* **1976**, *251*, 1253.

8.3 Appendix 3

Improving size-exclusion chromatography separation for glycogen

Mitchell A. Sullivan, Prudence O. Powell, Torsten Witt, Francisco Vilaplana, Eugeni Roura, Robert G. Gilbert

Supporting Information

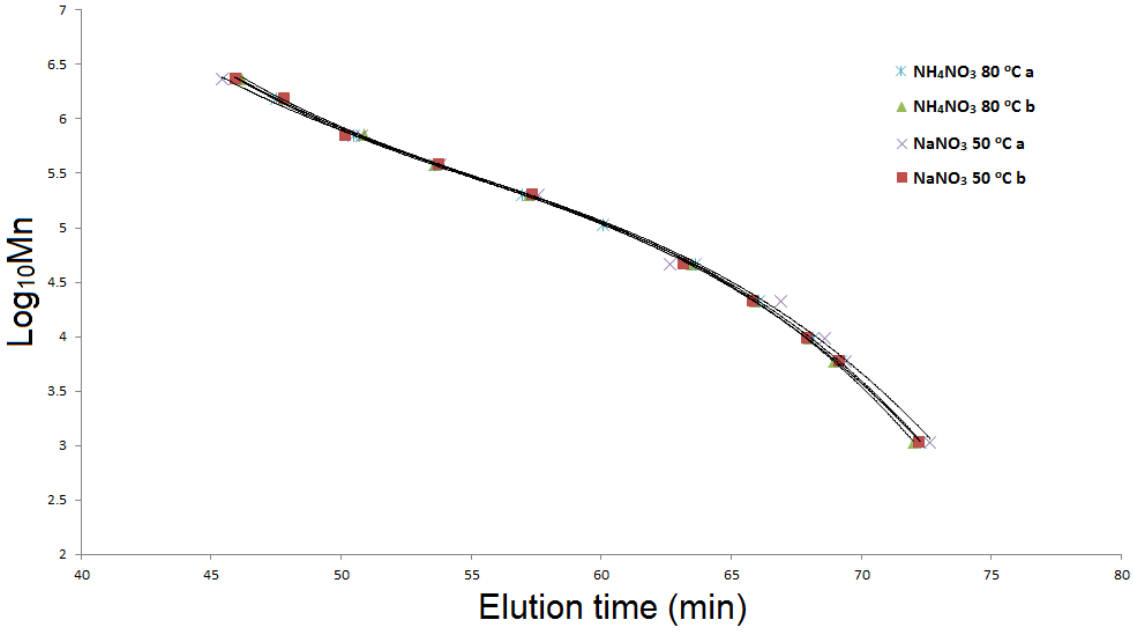

Figure S1. Calibration curves of pullulan in 50 mM NH_4NO_3/0.02% NaN_3 at 80 ^{o}C and 50 mM NaNO3/0.02% NaN3 at 50 ^{o}C. These were run in duplicate with the variation between duplicates being as large as between different solvent systems.

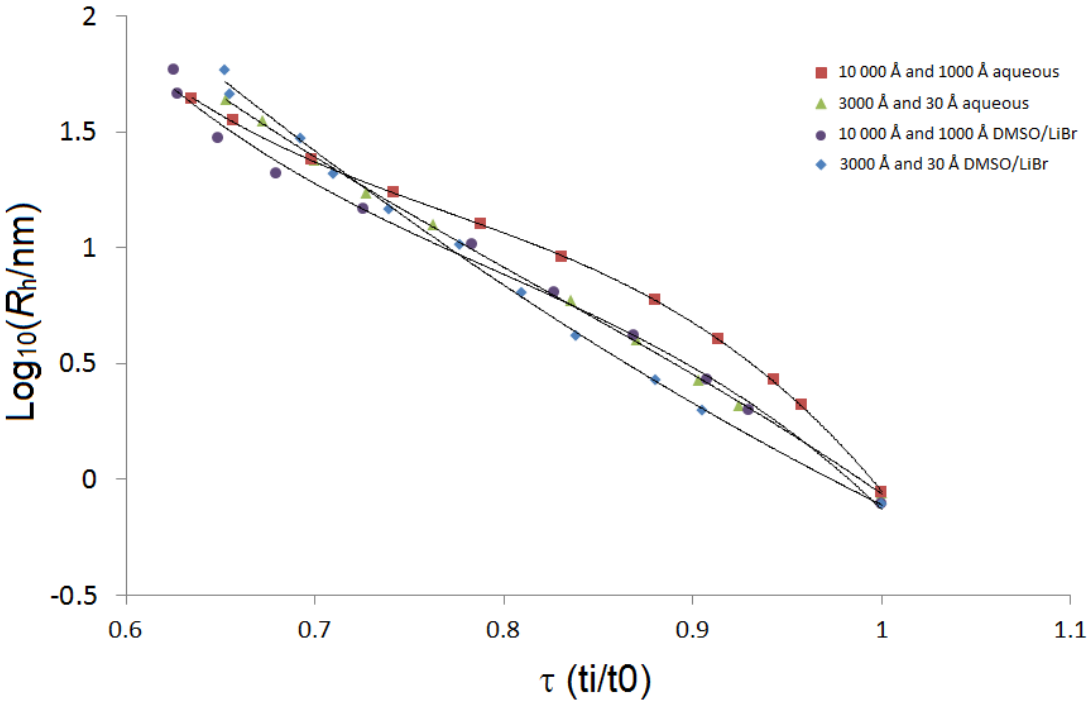

Figure S2. Comparison of calibration curves for pullulan in aqueous (50 mM NH_4NO_3/0.02% NaN_3) and DMSO/LiBr setups for the different pore sizes. τ is the elution time divided by that of the smallest standard.

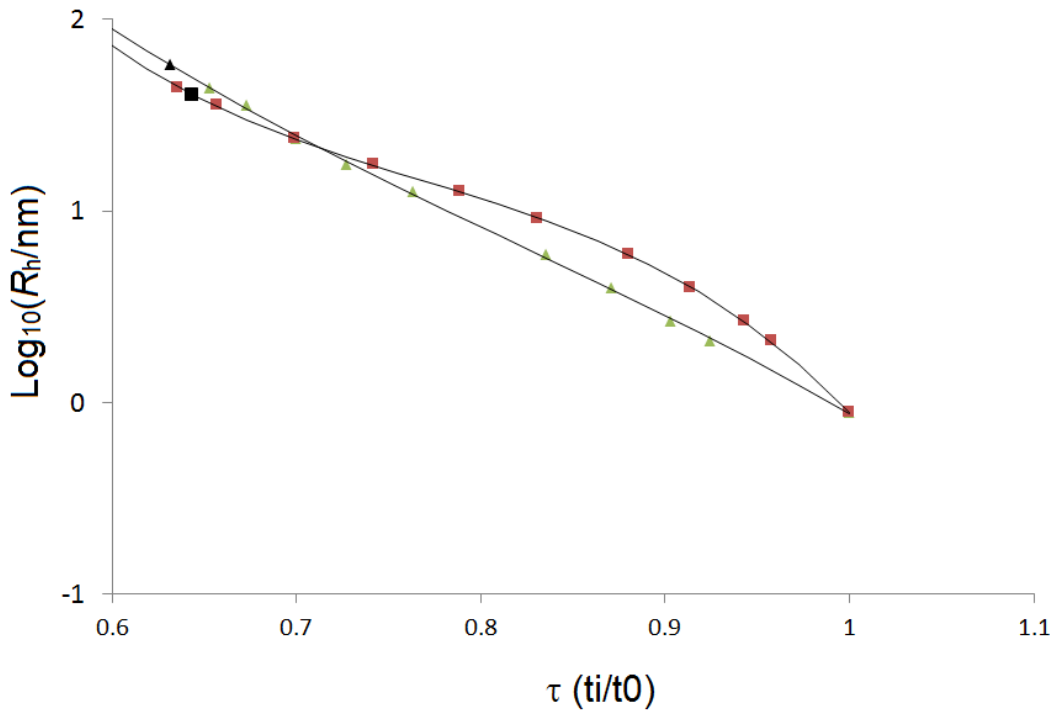

Figure S3. Comparison of aqueous calibration curves with the elution time (presented in terms of τ, where τ is the elution time divided by that of the smallest standard) corresponding to the α particle peak maxima being given (black). Trend lines have been extended.

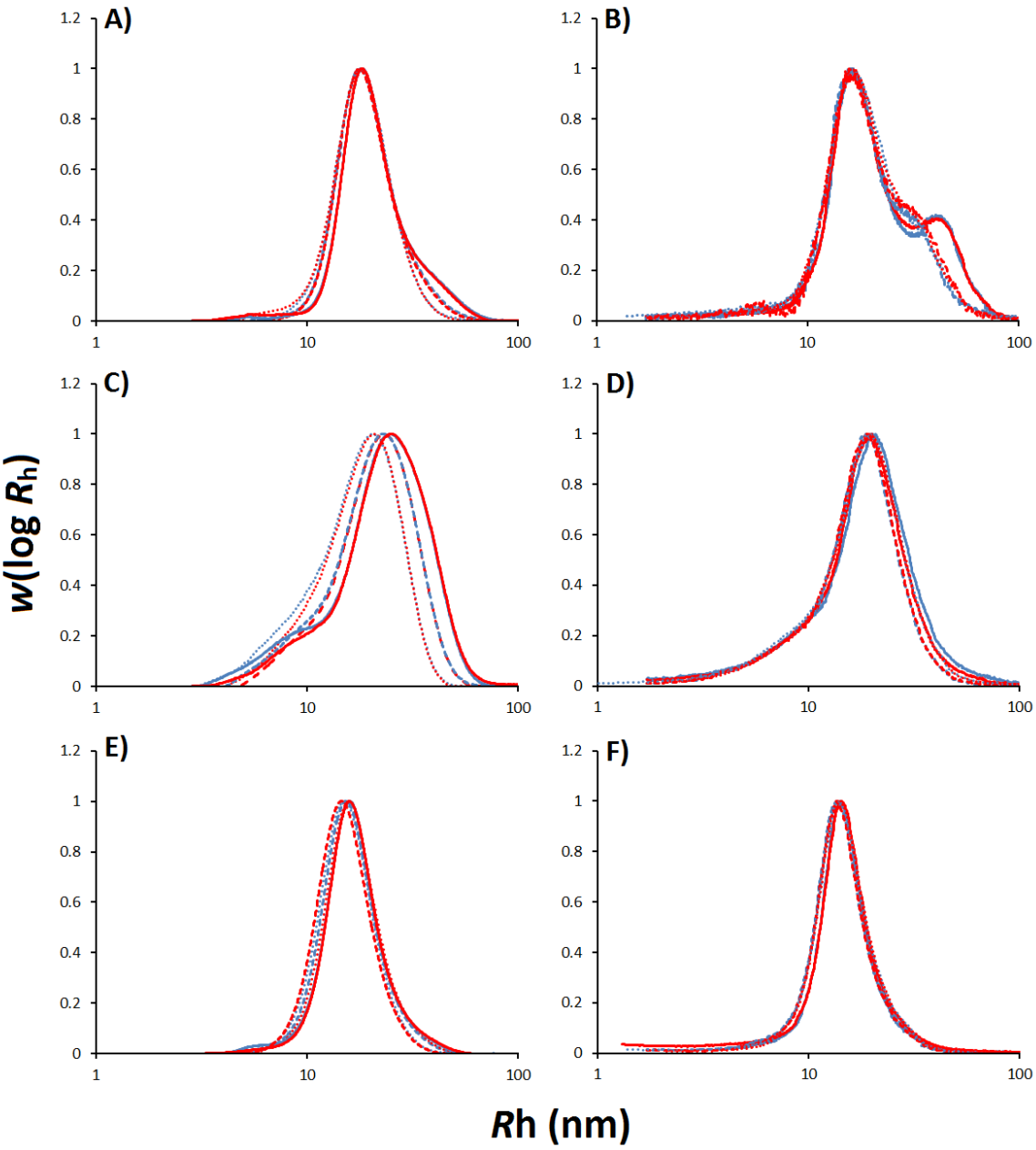

Figure S4. Equivalent to Figure 4 in main article with the X axis being changed to a logarithmic scale.

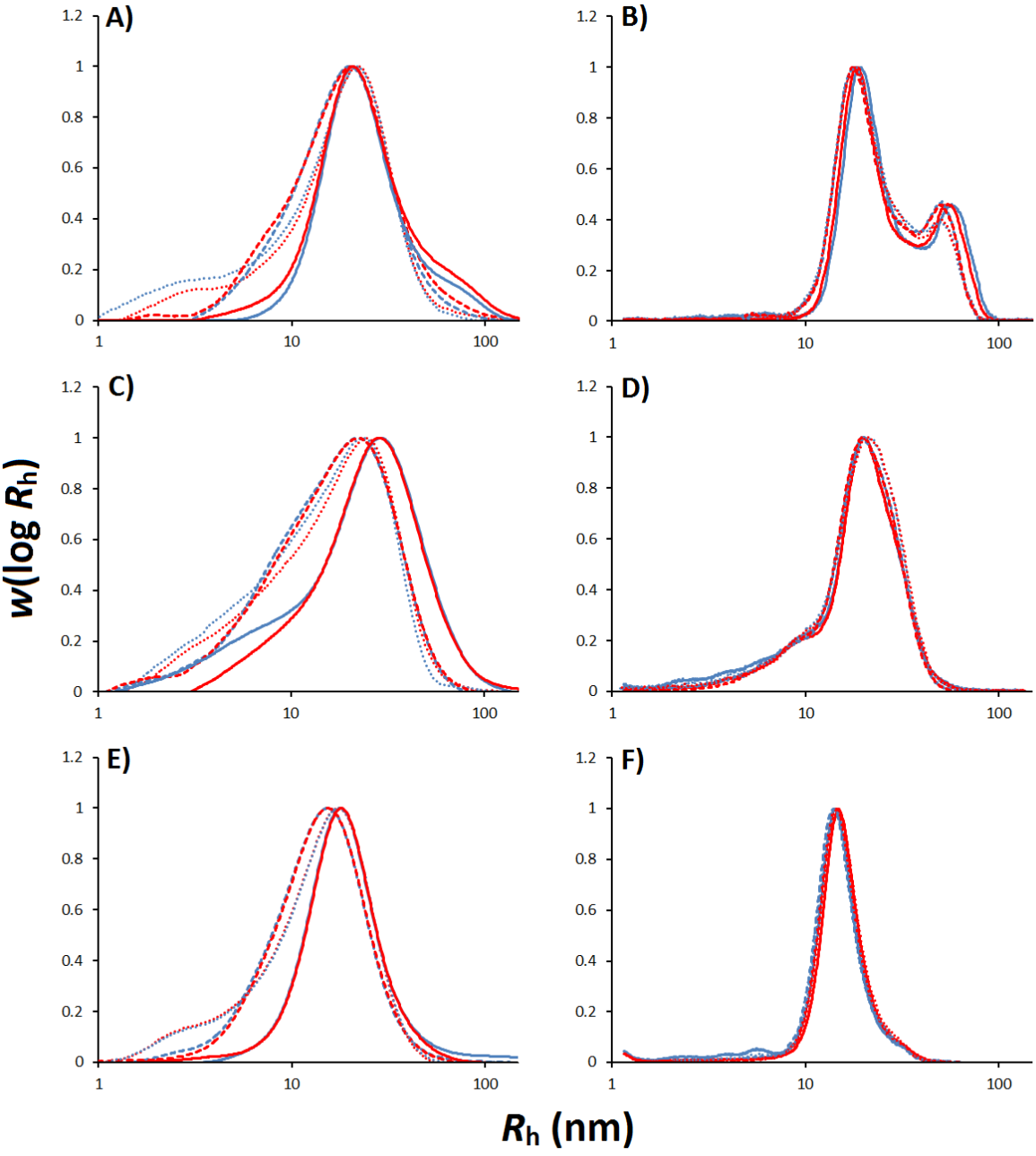

Figure S5. Equivalent to Figure 5 in the main article with the X axis being changed to a logarithmic scale.

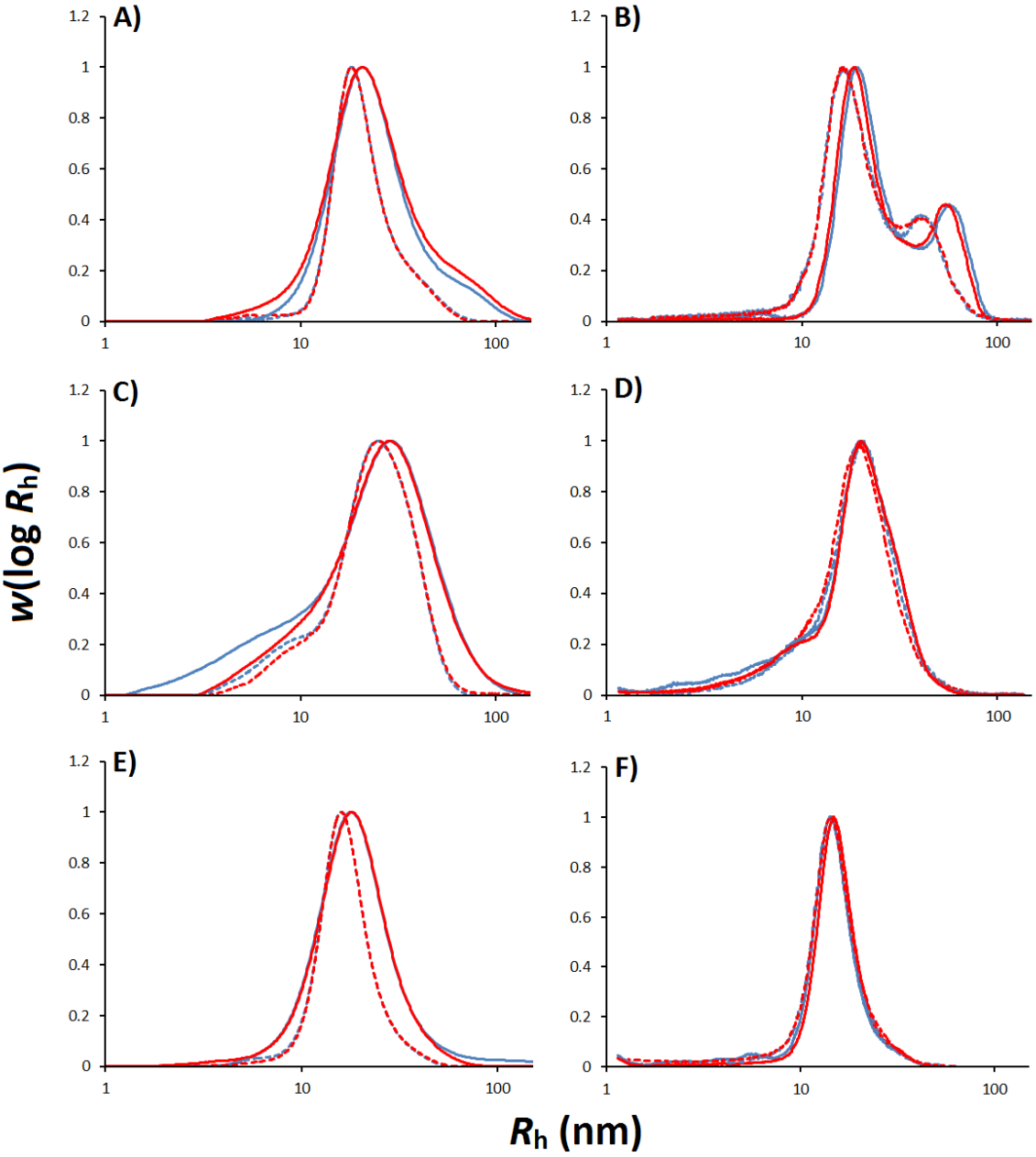

Figure S6. Equivalent to Figure 4 in main article with the X axis being changed to logarithmic.

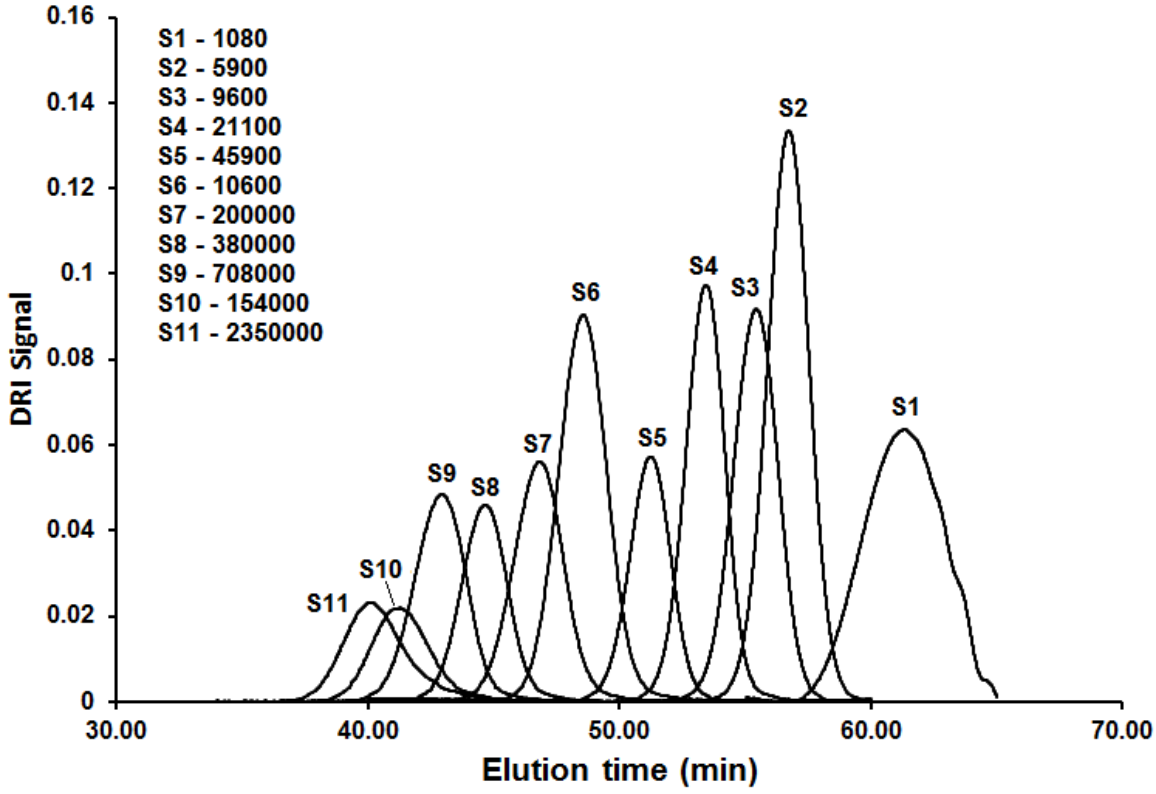

Figure S7. An overlay of the elution plots for pullulan standards in the aqueous 3000 and 30 setup.

8.4 Appendix 4

Supporting Information

A Rapid Extraction Method for Glycogen from Formalin-fixed Liver.

Mitchell A. Sullivan, Shihan Li, Samuel T. N. Aroney, Bin Deng, Cheng Li, Eugeni Roura, Benjamin L. Schulz, Brooke E. Harcourt, Josephine Forbes, Robert G. Gilbert

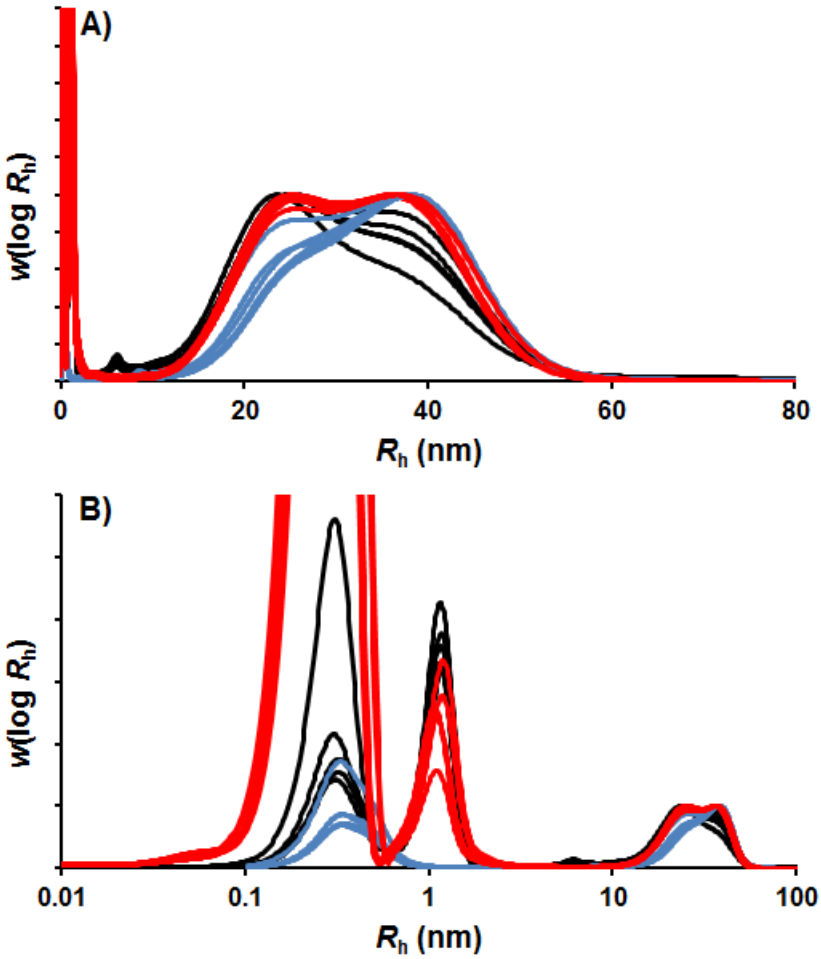

Figure S1. Equivalent to Figure 1 in the main article but with a different pig-liver sample. This repeated experiment shows the same trends as the initial pig sample.

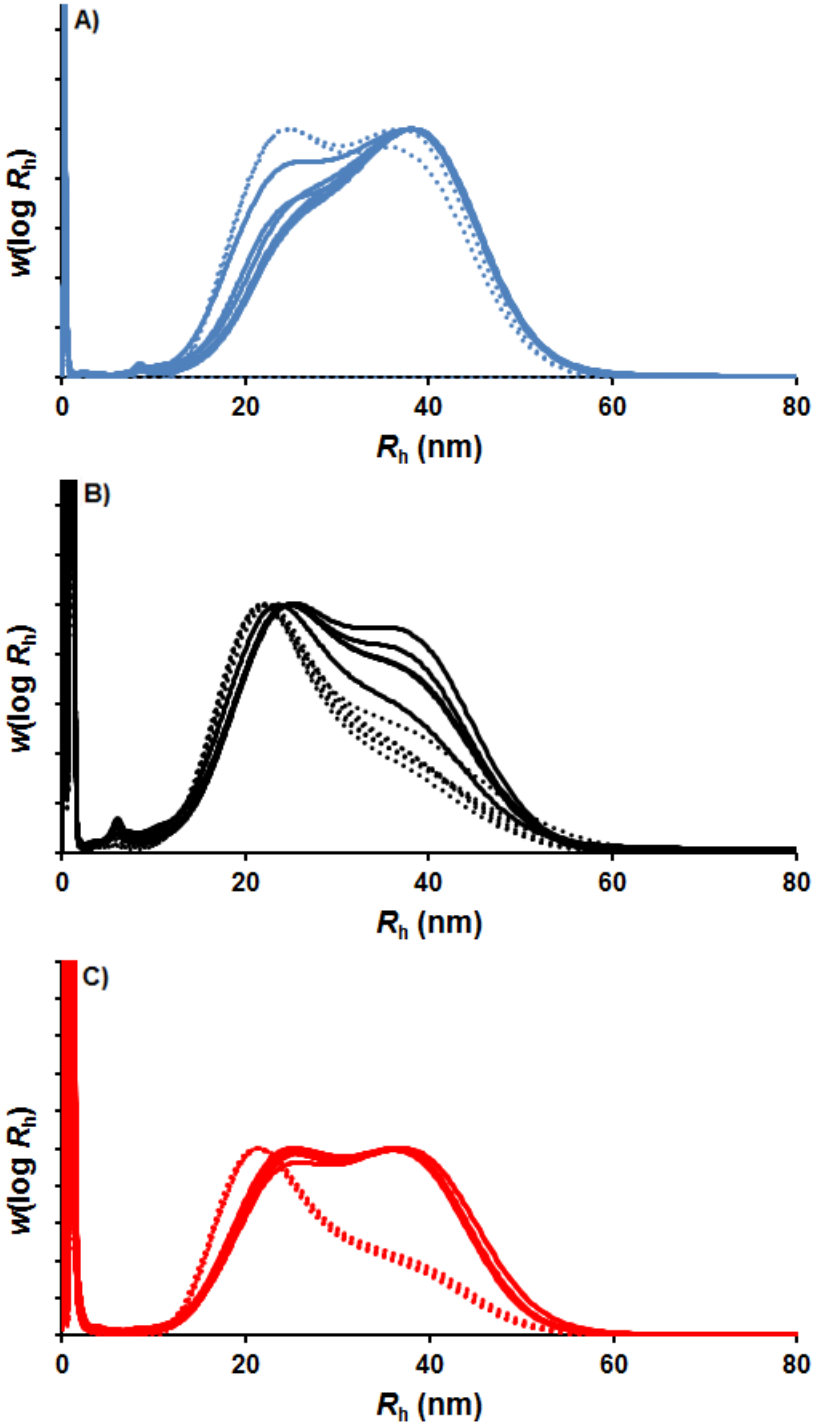

Figure S2. Equivalent to Figure 2 in the main article but with a different pig-liver sample. This repeated experiment shows the same trends as the initial pig sample.

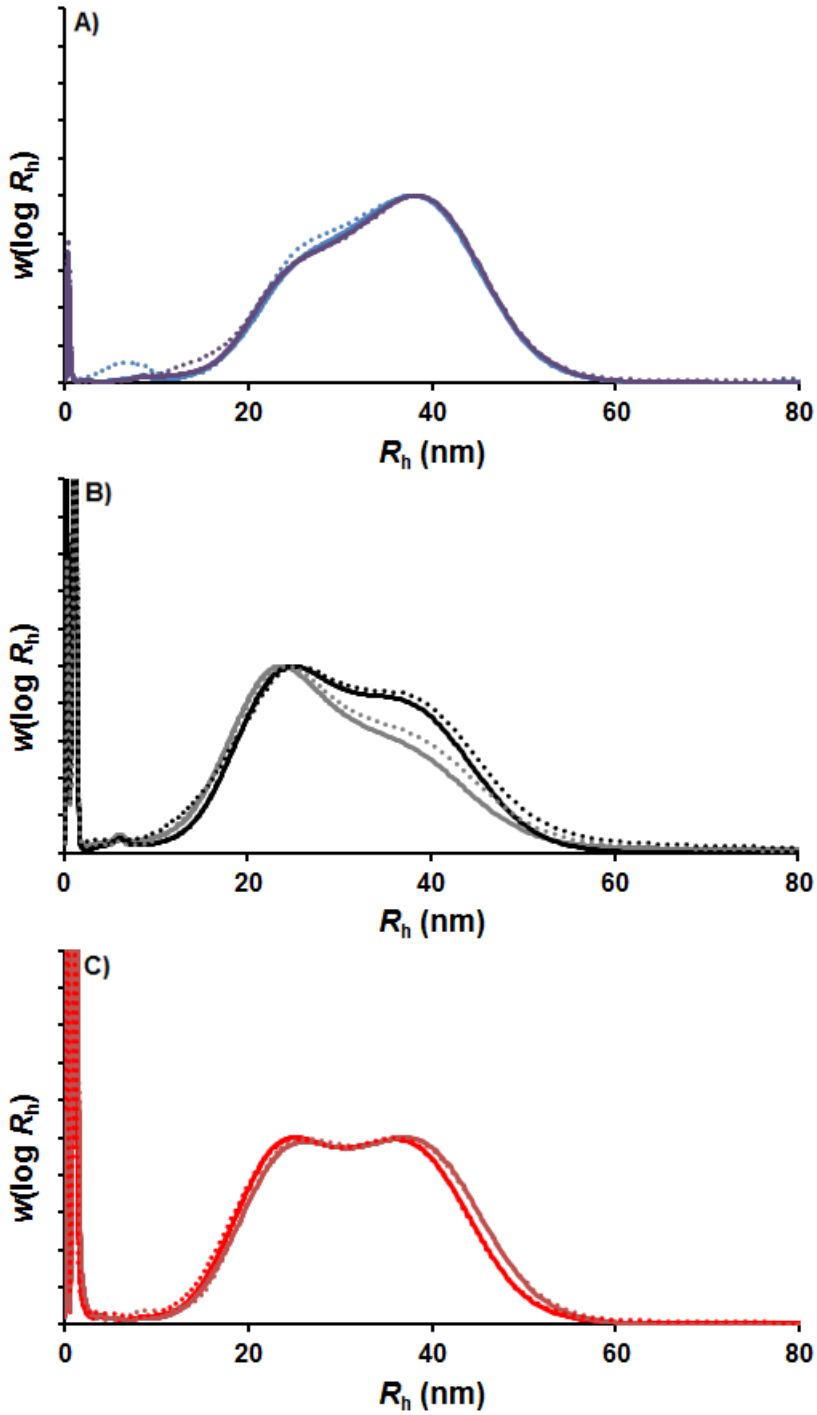

Figure S3. SEC weight distributions, $w(\log R_h)$; normalized to have equal heights for the maximum glycogen peak) as a function of molecular size (the hydrodynamic radius R_h) for 2 pig-liver glycogen samples at 2 mg mL^{-1} (full line) and 0.4 mg mL^{-1} (broken line) extracted via the sucrose method (A), formalin method (B) and formalin/protease method (C).

Table S1. Proteins identified by LC-ESI-MS/MS after glycogen enrichment from formalin fixed tissue.

Accession	Protein	Score	% Cov (95%)	Peptides (95%)
P07724	ALBU_MOUSE	175.39	74.18	136
Q63836	SBP2_MOUSE	83.96	78.39	61
P02762	MUP6_MOUSE	82.07	76.11	67
P04938	MUP8_MOUSE	82.07	90.73	67
B5X0G2	MUP17_MOUSE	79.89	70.56	65
Q00897	A1AT4_MOUSE	79.21	64.41	47
Q61838	A2M_MOUSE	68.89	28.56	35
Q9QXD6	F16P1_MOUSE	56.12	78.11	31
P12710	FABPL_MOUSE	54.82	92.13	66
Q921I1	TRFE_MOUSE	51.42	39.17	29
Q64374	RGN_MOUSE	46.36	66.22	28
P07759	SPA3K_MOUSE	40.25	51.44	25
Q8C196	CPSM_MOUSE	39.63	17.87	21
P16015	CAH3_MOUSE	38.39	61.92	27
Q8R0Y6	AL1L1_MOUSE	36.96	25.61	18
P16460	ASSY_MOUSE	36.36	43.69	21
Q8QZR3	EST2A_MOUSE	36.23	30.29	18
Q9D0F9	PGM1_MOUSE	35.84	43.24	18
P60710	ACTB_MOUSE	33.45	54.67	20
P63260	ACTG_MOUSE	31.01	50.13	19
P19157	GSTP1_MOUSE	32.88	65.24	22
O35215	DOPD_MOUSE	32.22	83.05	20
Q63880	EST3A_MOUSE	32.02	29.42	18
P35505	FAAA_MOUSE	32	51.55	16
P16858	G3P_MOUSE	31.19	51.05	16
Q00623	APOA1_MOUSE	29.76	49.24	16
O08709	PRDX6_MOUSE	29.06	69.64	14
P28665	MUG1_MOUSE	31.16	11.79	15
Q91X72	HEMO_MOUSE	27.06	30.22	14

P30115	GSTA3_MOUSE	27.02	49.32	15
P11352	GPX1_MOUSE	27.02	65.17	14
P23953	EST1C_MOUSE	26.48	27.08	14
P17182	ENOA_MOUSE	24.94	39.63	13
P20029	GRP78_MOUSE	24.85	20.61	12
P24549	AL1A1_MOUSE	26.26	36.33	16
P00329	ADH1_MOUSE	24.04	46.13	14
P10649	GSTM1_MOUSE	23.88	48.62	14
O35490	BHMT1_MOUSE	23.55	37.10	16
Q8VCT4	CES1D_MOUSE	25.35	25.84	13
Q91Y97	ALDOB_MOUSE	22.66	42.58	12
P52760	UK114_MOUSE	22	82.22	12
P08228	SODC_MOUSE	22	67.53	16
Q61176	ARGI1_MOUSE	20.08	47.99	11
Q9JII6	AK1A1_MOUSE	20.06	37.23	10
Q9WVL0	MAAI_MOUSE	19.99	57.87	11
P14152	MDHC_MOUSE	19.8	44.01	13
Q91YI0	ARLY_MOUSE	19.54	26.08	10
P50247	SAHH_MOUSE	19.47	28.47	10
P09103	PDIA1_MOUSE	18.58	24.95	9
Q00898	A1AT5_MOUSE	69.25	50.61	44
O88844	IDHC_MOUSE	18.44	34.30	11
P05201	AATC_MOUSE	16.58	29.78	8
P11499	HS90B_MOUSE	16.39	14.09	8
P06151	LDHA_MOUSE	16.23	26.20	8
Q8VC30	DHAK_MOUSE	16.01	21.80	8
P07309	TTHY_MOUSE	14.89	57.82	8
P02535	K1C10_MOUSE	14.83	18.77	10
P02088	HBB1_MOUSE	14.33	47.62	10
P63017	HSP7C_MOUSE	15.38	14.86	9
P27773	PDIA3_MOUSE	13.47	20.99	8
P09411	PGK1_MOUSE	13.47	28.78	8

P70694	DHB5_MOUSE	13.08	29.72	7
Q78JT3	3HAO_MOUSE	12.77	30.77	8
P08113	ENPL_MOUSE	14.72	12.72	8
P17751	TPIS_MOUSE	12.28	26.42	6
P35700	PRDX1_MOUSE	12.08	27.14	6
Q64442	DHSO_MOUSE	12.04	23.25	6
P49429	HPPD_MOUSE	11.79	18.07	6
Q91WG0	EST2C_MOUSE	16.61	16.76	8
Q9DBE0	CSAD_MOUSE	11.59	14.00	6
P48036	ANXA5_MOUSE	11.41	21.63	6
P10126	EF1A1_MOUSE	11.26	19.26	7
Q9CXN7	PBLD2_MOUSE	10.96	23.61	6
Q9DBJ1	PGAM1_MOUSE	10.86	37.40	6
Q91X83	METK1_MOUSE	10.62	18.94	6
P34914	HYES_MOUSE	10.15	12.64	5
P68372	TBB4B_MOUSE	10	14.38	5
Q9D6F9	TBB4A_MOUSE	8	10.36	4
P99024	TBB5_MOUSE	8	11.04	4
P29391	FRIL1_MOUSE	10	39.89	7
P09813	APOA2_MOUSE	10	33.33	6
P01027	CO3_MOUSE	9.9	4.09	5
Q91X91	NADC_MOUSE	9.84	19.06	5
P14211	CALR_MOUSE	9.79	14.18	5
P01942	HBA_MOUSE	9.73	31.69	7
Q8BVI4	DHPR_MOUSE	9.38	34.02	5
P63101	1433Z_MOUSE	9.26	25.71	5
Q9QXF8	GNMT_MOUSE	9	26.28	5
P28271	ACOC_MOUSE	8.95	9.45	5
Q8VCU1	EST3B_MOUSE	22.93	17.34	13
P56480	ATPB_MOUSE	8.54	13.61	5
O08677	KNG1_MOUSE	8.21	9.53	6
Q5FW60	MUP20_MOUSE	14.91	44.75	9

P07758	A1AT1_MOUSE	75.31	57.63	49
P04104	K2C1_MOUSE	8.06	7.06	4
Q8VCM7	FIBG_MOUSE	8.03	12.84	4
P29699	FETUA_MOUSE	8.02	17.97	4
P62962	PROF1_MOUSE	8	40.00	4
Q9D819	IPYR_MOUSE	8	16.26	4
P97328	KHK_MOUSE	7.7	17.45	4
Q8BH00	AL8A1_MOUSE	7.73	13.14	4
G3X982	AOXC_MOUSE	7.45	4.72	4
Q9ET01	PYGL_MOUSE	7.06	5.06	4
Q8VCN5	CGL_MOUSE	7.04	13.57	4
P21614	VTDB_MOUSE	6.86	11.55	4
P55264	ADK_MOUSE	6.52	12.19	3
Q9CPY7	AMPL_MOUSE	6.35	6.17	3
P06801	MAOX_MOUSE	6.29	8.22	3
P61458	PHS_MOUSE	6.16	25.00	3
Q9CPU0	LGUL_MOUSE	6.11	21.20	3
P32261	ANT3_MOUSE	6.09	8.39	3
O09131	GSTO1_MOUSE	6.03	18.75	3
P70296	PEBP1_MOUSE	6.02	28.34	3
Q8BK48	EST2E_MOUSE	14.73	14.67	8
P01872	IGHM_MOUSE	6	8.59	3
Q923D2	BLVRB_MOUSE	6	30.58	3
P68373	TBA1C_MOUSE	6	10.02	4
P68368	TBA4A_MOUSE	6	10.04	3
P05213	TBA1B_MOUSE	6	9.98	4
P68369	TBA1A_MOUSE	4	6.87	3
Q01853	TERA_MOUSE	5.82	4.72	3
Q8VCR7	ABHEB_MOUSE	5.77	15.71	3
Q9QYG0	NDRG2_MOUSE	5.72	10.78	4
P06728	APOA4_MOUSE	5.68	8.61	3
P53657	KPYR_MOUSE	5.62	8.36	3

P17742	PPIA_MOUSE	5.51	23.17	3
Q8QZR5	ALAT1_MOUSE	5.27	7.06	3
P40936	INMT_MOUSE	5.1	13.64	3
P24472	GSTA4_MOUSE	4.94	20.27	3
Q91ZJ5	UGPA_MOUSE	4.8	8.07	3
Q8BWT1	THIM_MOUSE	4.34	10.08	3
Q91V76	CK054_MOUSE	4.32	9.21	2
P99029	PRDX5_MOUSE	4.11	11.90	2
P31786	ACBP_MOUSE	4.08	34.48	2
Q03265	ATPA_MOUSE	4.05	4.70	2
P54869	HMCS2_MOUSE	4.05	4.13	2
Q9D0J8	PTMS_MOUSE	4.03	16.83	3
Q8K0E8	FIBB_MOUSE	4.01	6.45	3
P11589	MUP2_MOUSE	72.47	76.11	61
Q920E5	FPPS_MOUSE	4	8.21	2
Q9DBF1	AL7A1_MOUSE	4	6.12	2
Q64105	SPRE_MOUSE	4	10.73	2
P15105	GLNA_MOUSE	4	9.92	2
P08226	APOE_MOUSE	4	7.07	2
P01898	HA10_MOUSE	4	7.08	2

Table S2. Proteins identified by LC-ESI-MS/MS after glycogen enrichment from formalin fixed tissue with SDS.

Accession	Protein	Score	% Cov (95%)	Peptides (95%)
P07724	ALBU_MOUSE	61.98	50.0	40
Q63836	SBP2_MOUSE	45.49	51.3	26
P12710	FABPL_MOUSE	26.10	71.6	26
P60710	ACTB_MOUSE	24.25	40.0	15
P63260	ACTG_MOUSE	22.24	35.5	13
P04938	MUP8_MOUSE	20.60	69.5	13
P02762	MUP6_MOUSE	20.60	58.3	13
B5X0G2	MUP17_MOUSE	20.60	58.3	13
P11588	MUP1_MOUSE	19.17	51.7	12
P11352	GPX1_MOUSE	16.18	53.2	9
Q00896	A1AT3_MOUSE	15.82	17.2	9
P22599	A1AT2_MOUSE	13.61	14.8	8
P19157	GSTP1_MOUSE	15.78	26.7	11
Q64374	RGN_MOUSE	14.14	29.4	7
Q91X72	HEMO_MOUSE	13.86	19.1	8
Q8VCU1	EST3B_MOUSE	12.71	14.7	8
Q8C196	CPSM_MOUSE	12.18	4.3	6
P35505	FAAA_MOUSE	12.13	17.7	6
P07759	SPA3K_MOUSE	12.00	18.9	6
Q91WG0	EST2C_MOUSE	10.00	12.5	6
Q8VCT4	CES1D_MOUSE	10.00	11.2	5
P56480	ATPB_MOUSE	10.00	11.7	5
P52760	UK114_MOUSE	10.00	25.9	5
P10649	GSTM1_MOUSE	10.00	27.5	5
P08228	SODC_MOUSE	10.00	29.9	5
P02088	HBB1_MOUSE	10.00	47.6	5
Q91Y97	ALDOB_MOUSE	8.00	15.7	4
O35490	BHMT1_MOUSE	7.59	12.0	4
Q8QZR3	EST2A_MOUSE	9.10	12.4	5

Q61176	ARGI1_MOUSE	6.59	11.8	3
Q00623	APOA1_MOUSE	6.02	12.5	3
P16858	G3P_MOUSE	6.00	15.6	3
Q03265	ATPA_MOUSE	6.00	6.5	3
P14152	MDHC_MOUSE	6.00	8.4	3
P05201	AATC_MOUSE	6.00	9.2	3
P01942	HBA_MOUSE	6.00	25.4	4
O35215	DOPD_MOUSE	6.00	30.5	4
P16015	CAH3_MOUSE	4.57	10.0	2
Q61838	A2M_MOUSE	4.04	1.7	2
P04939	MUP3_MOUSE	4.02	10.9	2
P11725	OTC_MOUSE	4.00	6.2	2
Q921I1	TRFE_MOUSE	4.00	3.3	2
P31786	ACBP_MOUSE	4.00	33.3	2
P07309	TTHY_MOUSE	4.00	17.0	2
P05202	AATM_MOUSE	4.00	7.0	2
P14211	CALR_MOUSE	2.19	4.6	2

Table S3. Proteins identified by LC-ESI-MS/MS after glycogen enrichment from formalin fixed tissue with guanidine-HCl.

Accession	Protein	Score	% Cov (95%)	Peptides (95%)
P07724	ALBU_MOUSE	143.85	62.66	129
P22599	A1AT2_MOUSE	77.27	61.99	57
Q63836	SBP2_MOUSE	76.38	68.64	62
Q61838	A2M_MOUSE	75.2	28.09	41
P02762	MUP6_MOUSE	57.54	69.44	56
P04938	MUP8_MOUSE	57.54	82.78	56
P11588	MUP1_MOUSE	57.4	69.44	56
B5X0G2	MUP17_MOUSE	56.99	63.89	54
P07759	SPA3K_MOUSE	55.16	51.44	37
Q8R0Y6	AL1L1_MOUSE	47.15	33.70	24
Q921I1	TRFE_MOUSE	41.78	32.86	25
Q64374	RGN_MOUSE	40.66	51.51	29
P28665	MUG1_MOUSE	41.52	18.09	20
Q9QXD6	F16P1_MOUSE	39.28	60.36	26
P12710	FABPL_MOUSE	36.46	85.83	62
Q8QZR3	EST2A_MOUSE	35.94	35.48	18
P16015	CAH3_MOUSE	35.81	60.77	23
P16460	ASSY_MOUSE	35.48	39.81	21
Q63880	EST3A_MOUSE	35.22	36.08	23
P20029	GRP78_MOUSE	34.93	29.47	18
P63260	ACTG_MOUSE	33.46	52.80	23
P60710	ACTB_MOUSE	33.46	52.80	23
P35505	FAAA_MOUSE	32.91	53.46	19
Q9D0F9	PGM1_MOUSE	31.43	38.26	16
P23953	EST1C_MOUSE	26.56	27.98	15
P16858	G3P_MOUSE	26.15	45.65	14
P11352	GPX1_MOUSE	26.07	60.70	16
O08709	PRDX6_MOUSE	24.73	52.23	14
Q61176	ARGI1_MOUSE	24.48	48.30	15

P52760	UK114_MOUSE	24.02	76.30	13
O35215	DOPD_MOUSE	23.93	65.25	14
P19157	GSTP1_MOUSE	23.66	53.33	16
P05201	AATC_MOUSE	23.16	46.73	13
P09103	PDIA1_MOUSE	22.71	29.08	12
P10649	GSTM1_MOUSE	22.64	48.62	13
Q8VCT4	CES1D_MOUSE	27.51	29.38	16
P24549	AL1A1_MOUSE	23.02	24.95	13
Q91WG0	EST2C_MOUSE	24.75	36.19	14
Q00898	A1AT5_MOUSE	74.21	59.56	57
Q00623	APOA1_MOUSE	20.84	41.67	12
P11499	HS90B_MOUSE	20.77	20.86	11
P14152	MDHC_MOUSE	20.35	35.33	16
O88844	IDHC_MOUSE	20.6	36.23	12
P17182	ENOA_MOUSE	20.03	39.86	13
Q91X72	HEMO_MOUSE	19.69	19.35	11
P08228	SODC_MOUSE	19.66	61.04	14
P00329	ADH1_MOUSE	19.27	31.73	13
P50247	SAHH_MOUSE	18.55	29.17	10
Q91YI0	ARLY_MOUSE	17.93	24.78	10
Q9JII6	AK1A1_MOUSE	17.91	37.23	11
Q91Y97	ALDOB_MOUSE	17.37	37.64	12
P30115	GSTA3_MOUSE	17.03	35.75	9
P08113	ENPL_MOUSE	19.12	19.20	11
P06151	LDHA_MOUSE	16.63	25.60	8
Q8VC30	DHAK_MOUSE	16.63	25.78	9
Q78JT3	3HAO_MOUSE	16.55	45.45	11
P63017	HSP7C_MOUSE	18.6	19.50	12
P53657	KPYR_MOUSE	16.22	21.08	8
O35490	BHMT1_MOUSE	15.97	31.94	12
P49429	HPPD_MOUSE	15.88	26.72	9
P27773	PDIA3_MOUSE	15.71	21.78	8

Q9ET01	PYGL_MOUSE	15.33	13.06	9
Q8C196	CPSM_MOUSE	15.02	5.80	7
P01027	CO3_MOUSE	14.44	6.13	8
P09411	PGK1_MOUSE	14.01	27.10	8
P10126	EF1A1_MOUSE	13.73	26.41	10
G3X982	AOXC_MOUSE	13.7	9.51	8
P02088	HBB1_MOUSE	13.49	47.62	8
Q9CXN7	PBLD2_MOUSE	13.34	27.43	6
P07309	TTHY_MOUSE	13.29	57.82	7
Q01853	TERA_MOUSE	12.92	13.03	7
Q9WVL0	MAAI_MOUSE	12.69	39.35	6
Q9DBE0	CSAD_MOUSE	12.63	15.21	6
Q64442	DHSO_MOUSE	12.11	23.53	7
Q00897	A1AT4_MOUSE	69.98	64.16	53
P06801	MAOX_MOUSE	11.66	14.16	6
P35700	PRDX1_MOUSE	11.51	29.65	7
P68372	TBB4B_MOUSE	11.47	19.78	7
Q9D6F9	TBB4A_MOUSE	9.35	15.77	6
P55264	ADK_MOUSE	11.22	20.22	7
P14211	CALR_MOUSE	11	23.08	8
P17751	TPIS_MOUSE	10.96	32.78	7
P34914	HYES_MOUSE	10.84	16.25	6
P28271	ACOC_MOUSE	10.8	12.15	6
P70694	DHB5_MOUSE	10.22	24.46	6
P02535	K1C10_MOUSE	10.15	12.28	5
P01942	HBA_MOUSE	10.1	30.28	5
Q8BK48	EST2E_MOUSE	17.21	20.04	11
P09813	APOA2_MOUSE	9.42	33.33	6
Q9DBJ1	PGAM1_MOUSE	9.3	36.22	5
Q8VCM7	FIBG_MOUSE	9	18.81	6
Q91X83	METK1_MOUSE	8.85	16.92	5
P48036	ANXA5_MOUSE	8.72	19.12	5

P17742	PPIA_MOUSE	8.44	23.17	4
Q8VCU1	EST3B_MOUSE	24.14	24.17	14
Q8BVI4	DHPR_MOUSE	8.1	30.29	4
P62962	PROF1_MOUSE	8	40.00	4
P68373	TBA1C_MOUSE	8	12.03	4
P05213	TBA1B_MOUSE	8	11.97	4
P68369	TBA1A_MOUSE	6	8.87	3
Q9CPY7	AMPL_MOUSE	7.92	12.52	6
P32261	ANT3_MOUSE	7.69	12.26	4
P62259	1433E_MOUSE	7.53	22.75	4
Q8VCN5	CGL_MOUSE	7.43	13.82	4
Q9QXF8	GNMT_MOUSE	7.29	21.16	4
Q91ZJ5	UGPA_MOUSE	7.22	12.20	4
Q91X91	NADC_MOUSE	7.13	24.41	6
Q8VCC2	EST1_MOUSE	7.7	9.20	5
P24369	PPIB_MOUSE	6.99	21.76	4
P04104	K2C1_MOUSE	6.89	7.06	4
Q8BH00	AL8A1_MOUSE	6.93	13.35	4
Q923D2	BLVRB_MOUSE	6.79	34.47	4
O08677	KNG1_MOUSE	6.64	9.53	5
P07758	A1AT1_MOUSE	67.94	60.05	57
Q00896	A1AT3_MOUSE	71.67	62.86	59
Q8K0E8	FIBB_MOUSE	6.52	10.81	4
Q9D819	IPYR_MOUSE	6.29	17.99	5
Q9CPU0	LGUL_MOUSE	6.12	21.20	3
P16331	PH4H_MOUSE	6.06	6.84	3
P28474	ADHX_MOUSE	8.16	15.78	4
Q91XD4	FTCD_MOUSE	6	11.65	3
P70296	PEBP1_MOUSE	5.92	28.34	3
P01872	IGHM_MOUSE	5.85	10.79	3
P40142	TKT_MOUSE	5.85	6.90	3
P21614	VTDB_MOUSE	5.82	9.45	3

Q9QYG0	NDRG2_MOUSE	5.42	10.78	3
P06728	APOA4_MOUSE	5.37	8.61	3
Q91V76	CK054_MOUSE	5.02	13.33	3
Q922D8	C1TC_MOUSE	4.93	3.96	3
Q8K157	GALM_MOUSE	4.8	13.45	3
Q06890	CLUS_MOUSE	4.71	10.04	3
Q8VCR7	ABHEB_MOUSE	4.7	14.76	3
Q9DBB8	DHDH_MOUSE	4.63	13.81	3
O09131	GSTO1_MOUSE	4.57	18.75	3
Q9DCQ2	ASPD_MOUSE	4.49	16.38	3
P01898	HA10_MOUSE	4.29	8.31	2
P14430	HA18_MOUSE	2.23	4.29	1
P58252	EF2_MOUSE	4.19	3.38	2
Q9DCG6	PBLD1_MOUSE	12.81	27.43	6
P04939	MUP3_MOUSE	4.15	22.83	4
Q8QZR5	ALAT1_MOUSE	4.1	4.64	2
P35492	HUTH_MOUSE	4.08	4.57	2
P19096	FAS_MOUSE	4.04	1.68	2
Q9JMD3	PCTL_MOUSE	4.03	8.59	2
P40936	INMT_MOUSE	4.02	13.26	2
P29699	FETUA_MOUSE	4.02	11.01	2
Q99J08	S14L2_MOUSE	4.01	7.94	2
P17563	SBP1_MOUSE	64.96	59.96	54
P11589	MUP2_MOUSE	49.35	76.11	52
P63101	1433Z_MOUSE	6.47	17.55	3
Q9JLJ2	AL9A1_MOUSE	4	4.86	2
Q7TPR4	ACTN1_MOUSE	4	2.47	2
P57780	ACTN4_MOUSE	4	2.41	2
Q99PT1	GDIR1_MOUSE	4	15.20	2
Q64105	SPRE_MOUSE	4	10.73	2
Q922R8	PDIA6_MOUSE	4	7.05	2
Q61598	GDIB_MOUSE	4	6.74	2

Table S4. Proteins identified by LC-ESI-MS/MS after sucrose glycogen enrichment.

Accession	Protein	Score	% Cov (95%)	Peptides (95%)
Q8C196	CPSM_MOUSE	444.1	73.07	257
Q9ET01	PYGL_MOUSE	122.53	57.88	74
P16460	ASSY_MOUSE	117.46	64.56	71
P19096	FAS_MOUSE	114.15	31.91	61
Q922D8	C1TC_MOUSE	91.85	63.21	50
Q8R0Y6	AL1L1_MOUSE	83.69	61.75	45
Q05920	PYC_MOUSE	81.36	47.37	46
P47738	ALDH2_MOUSE	71.52	64.55	39
P56480	ATPB_MOUSE	68.67	62.76	35
P16858	G3P_MOUSE	60.75	53.45	32
Q03265	ATPA_MOUSE	52.95	51.18	30
P68372	TBB4B_MOUSE	50.55	65.39	32
P20029	GRP78_MOUSE	50.01	43.36	25
P26443	DHE3_MOUSE	49.16	39.78	29
Q8BWT1	THIM_MOUSE	48.67	63.48	27
Q8BMS1	ECHA_MOUSE	47.44	34.47	23
P24549	AL1A1_MOUSE	46.91	59.68	28
P68373	TBA1C_MOUSE	38.87	48.11	22
P15105	GLNA_MOUSE	36.41	40.75	20
Q91VS7	MGST1_MOUSE	36.11	61.94	20
P53395	ODB2_MOUSE	35.75	45.85	19
P41216	ACSL1_MOUSE	35.46	30.04	18
P10126	EF1A1_MOUSE	34.86	52.81	28
P14148	RL7_MOUSE	34.31	50.00	22
P12970	RL7A_MOUSE	34.29	42.86	18
P25444	RS2_MOUSE	33.47	40.96	22
O35490	BHMT1_MOUSE	33.05	53.81	22
Q63880	EST3A_MOUSE	32.88	38.18	19

P60710	ACTB_MOUSE	32.27	57.33	19
Q8CGC7	SYEP_MOUSE	31.88	15.74	16
Q9D8E6	RL4_MOUSE	30.58	35.32	19
Q91XD4	FTCD_MOUSE	29.34	45.29	16
P09103	PDIA1_MOUSE	28.34	32.81	15
P63038	CH60_MOUSE	28	35.43	15
P07724	ALBU_MOUSE	27.77	26.64	13
P24270	CATA_MOUSE	27.42	37.38	14
P80315	TCPD_MOUSE	27.09	34.32	13
P97351	RS3A_MOUSE	26.12	42.42	13
P14869	RLA0_MOUSE	25.37	44.48	14
P11352	GPX1_MOUSE	25.33	78.61	14
P17717	UDB17_MOUSE	24.97	30.00	14
P62908	RS3_MOUSE	24.91	52.26	13
P47911	RL6_MOUSE	24.43	31.08	14
P63017	HSP7C_MOUSE	32.19	33.13	17
P80318	TCPG_MOUSE	24.15	30.83	12
P53657	KPYR_MOUSE	24.04	31.36	12
P00329	ADH1_MOUSE	23.8	37.87	14
P33267	CP2F2_MOUSE	23.21	31.36	12
P38647	GRP75_MOUSE	23.57	26.36	15
P08113	ENPL_MOUSE	22.96	19.20	12
Q9QXD6	F16P1_MOUSE	22.8	49.70	13
P50247	SAHH_MOUSE	22.44	30.79	13
P62082	RS7_MOUSE	22.43	43.81	13
P11983	TCPA_MOUSE	24.02	28.06	12
Q01853	TERA_MOUSE	22	20.72	11
Q8BH00	AL8A1_MOUSE	22.16	32.24	11
Q99K67	AASS_MOUSE	21.59	14.90	11
P51410	RL9_MOUSE	21.17	64.06	11
P11714	CP2D9_MOUSE	21.04	25.40	11
P62702	RS4X_MOUSE	20.63	40.68	12

P27659	RL3_MOUSE	20.22	27.05	12
Q91Y97	ALDOB_MOUSE	20	40.11	10
O88451	RDH7_MOUSE	19.54	37.34	12
P06151	LDHA_MOUSE	19.5	37.35	10
P11499	HS90B_MOUSE	21.37	19.06	11
P62843	RS15_MOUSE	19.09	55.86	12
P62264	RS14_MOUSE	18.75	62.25	11
Q8QZT1	THIL_MOUSE	18.47	34.91	9
P80316	TCPE_MOUSE	18.36	31.42	9
Q63886	UD11_MOUSE	20.22	20.00	10
P80317	TCPZ_MOUSE	18.17	28.06	9
Q8VCB3	GYS2_MOUSE	18.06	17.76	10
Q9R0H0	ACOX1_MOUSE	18	21.33	9
P80314	TCPB_MOUSE	18	26.54	9
Q9DB20	ATPO_MOUSE	18	53.99	9
P14131	RS16_MOUSE	17.79	46.58	9
P62754	RS6_MOUSE	17.72	23.69	9
Q8VCT4	CES1D_MOUSE	17.68	28.67	12
P80313	TCPH_MOUSE	17.41	27.57	10
P32020	NLTP_MOUSE	17.38	26.14	11
Q9CQ62	DECR_MOUSE	17.22	36.42	9
Q8CIM7	CP2DQ_MOUSE	17.07	26.20	10
P54869	HMCS2_MOUSE	16.73	21.65	10
Q8BMF4	ODP2_MOUSE	16.63	19.63	8
P97872	FMO5_MOUSE	16.59	24.77	10
Q9D379	HYEP_MOUSE	16.56	30.77	11
P47955	RLA1_MOUSE	16.38	74.56	11
Q6ZWN5	RS9_MOUSE	16.21	27.32	10
Q63836	SBP2_MOUSE	16.12	23.73	9
P17563	SBP1_MOUSE	15.4	21.19	8
Q64459	CP3AB_MOUSE	16.01	21.63	8
Q61176	ARGI1_MOUSE	16	34.67	8

P99027	RLA2_MOUSE	16	84.35	8
O08601	MTP_MOUSE	15.92	13.31	9
O09173	HGD_MOUSE	15.92	24.94	8
Q05421	CP2E1_MOUSE	15.79	20.69	9
P02088	HBB1_MOUSE	15.47	62.59	9
O88844	IDHC_MOUSE	15.15	22.95	8
Q9CZM2	RL15_MOUSE	15.09	34.31	8
P51881	ADT2_MOUSE	14.88	30.20	8
P27773	PDIA3_MOUSE	14.83	20.20	7
Q60759	GCDH_MOUSE	14.76	27.40	8
Q68FD5	CLH1_MOUSE	14.58	8.66	10
P97461	RS5_MOUSE	14.3	42.65	9
P29341	PABP1_MOUSE	14.23	13.05	7
P62889	RL30_MOUSE	14.13	51.30	7
Q922B2	SYDC_MOUSE	14.09	17.96	7
P35980	RL18_MOUSE	14.06	29.79	8
P67984	RL22_MOUSE	14	42.97	7
P63276	RS17_MOUSE	13.82	41.48	7
P42932	TCPQ_MOUSE	13.81	16.06	8
P34914	HYES_MOUSE	13.69	20.58	7
O35488	S27A2_MOUSE	13.47	17.74	7
P62301	RS13_MOUSE	13.43	29.80	7
Q99JY0	ECHB_MOUSE	13.34	28.21	10
P19157	GSTP1_MOUSE	13.23	53.81	8
Q61656	DDX5_MOUSE	13.12	11.73	7
Q64458	CP2CT_MOUSE	13.09	13.88	7
Q8VCW8	ACSF2_MOUSE	13.02	15.93	7
P24456	CP2DA_MOUSE	19.35	23.21	10
P62242	RS8_MOUSE	12.85	29.33	8
P57776	EF1D_MOUSE	12.65	33.45	7
P53026	RL10A_MOUSE	12.56	33.18	8
Q9QXF8	GNMT_MOUSE	12.36	28.67	7

Q91ZJ5	UGPA_MOUSE	12.1	18.31	6
P62751	RL23A_MOUSE	12.09	30.13	6
P50136	ODBA_MOUSE	12.04	23.30	7
Q9D2G2	ODO2_MOUSE	12	18.94	7
Q9CPY7	AMPL_MOUSE	12	19.08	6
Q91VR5	DDX1_MOUSE	11.96	14.05	7
O88587	COMT_MOUSE	11.92	33.96	6
P16331	PH4H_MOUSE	11.7	17.88	6
Q91X83	METK1_MOUSE	11.62	19.95	7
P16015	CAH3_MOUSE	11.57	29.62	6
Q9D0I9	SYRC_MOUSE	11.41	11.97	7
Q9WVL0	MAAI_MOUSE	11.41	50.46	7
O09167	RL21_MOUSE	11.33	27.50	8
Q60597	ODO1_MOUSE	11.21	9.38	7
Q6ZWV3	RL10_MOUSE	11.16	22.43	6
P86048	RL10L_MOUSE	8.92	16.36	5
P62245	RS15A_MOUSE	11.12	51.54	8
P58710	GGLO_MOUSE	10.93	20.00	5
Q6ZWX6	IF2A_MOUSE	10.9	23.81	6
P47963	RL13_MOUSE	10.78	20.38	5
P05202	AATM_MOUSE	10.64	18.14	6
P24369	PPIB_MOUSE	10.64	27.31	5
P58252	EF2_MOUSE	10.28	8.04	5
P17182	ENOA_MOUSE	10.24	19.35	5
Q8VEK3	HNRPU_MOUSE	10.15	9.62	5
P62830	RL23_MOUSE	10.14	26.43	5
P62270	RS18_MOUSE	10.1	36.84	6
Q80XN0	BDH_MOUSE	10.1	18.95	5
Q99MN9	PCCB_MOUSE	10.01	14.42	5
O70251	EF1B_MOUSE	11.49	28.44	6
Q07417	ACADS_MOUSE	10	22.09	5
Q922R8	PDIA6_MOUSE	10	17.50	5

P35979	RL12_MOUSE	10	45.45	6
Q91V92	ACLY_MOUSE	9.91	7.15	6
G3X982	AOXC_MOUSE	9.89	5.62	5
Q9CZX8	RS19_MOUSE	9.82	29.66	6
P50544	ACADV_MOUSE	9.81	13.11	5
Q9DB77	QCR2_MOUSE	9.58	18.76	5
Q9CZ13	QCR1_MOUSE	9.43	15.83	5
P62196	PRS8_MOUSE	9.28	17.98	5
P63325	RS10_MOUSE	9.24	23.03	6
P50580	PA2G4_MOUSE	8.99	17.26	5
Q91YI0	ARLY_MOUSE	8.83	13.36	5
Q9QXX4	CMC2_MOUSE	8.8	9.47	4
Q9CPR4	RL17_MOUSE	8.71	31.52	6
Q91VR2	ATPG_MOUSE	8.56	20.81	5
Q8VDM4	PSMD2_MOUSE	8.48	8.92	6
P62918	RL8_MOUSE	8.45	39.30	8
Q8VCR2	DHB13_MOUSE	8.39	25.00	5
P01942	HBA_MOUSE	8.37	38.03	5
P19253	RL13A_MOUSE	8.36	20.20	5
Q9D051	ODPB_MOUSE	8.23	16.99	5
Q9Z0N2	IF2H_MOUSE	8.11	12.92	4
Q9Z0N1	IF2G_MOUSE	8	12.92	4
P62900	RL31_MOUSE	8.05	18.40	4
P62192	PRS4_MOUSE	8.04	15.91	4
P61358	RL27_MOUSE	8.03	36.03	4
P62849	RS24_MOUSE	8.03	29.32	5
Q64442	DHSO_MOUSE	8.03	15.97	4
Q9DBG1	CP27A_MOUSE	8.01	11.44	4
Q4LDG0	S27A5_MOUSE	8.01	9.43	4
Q9DBF1	AL7A1_MOUSE	8	10.58	4
P51660	DHB4_MOUSE	8	7.07	4
P43274	H14_MOUSE	8	21.92	4

Q9CQE8	CN166_MOUSE	8	25.82	4
P56395	CYB5_MOUSE	8	41.04	4
O88685	PRS6A_MOUSE	8	13.57	4
P09405	NUCL_MOUSE	8	7.78	4
P62852	RS25_MOUSE	7.9	24.00	5
Q8VC30	DHAK_MOUSE	7.8	12.28	4
Q9EQ20	MMSA_MOUSE	7.8	9.16	4
P62911	RL32_MOUSE	7.74	28.15	4
P14211	CALR_MOUSE	7.62	17.55	5
Q8BWQ1	UD2A3_MOUSE	7.58	18.35	7
P68368	TBA4A_MOUSE	34.79	40.85	18
Q91ZA3	PCCA_MOUSE	7.48	9.94	5
Q9JJI8	RL38_MOUSE	7.33	47.14	4
Q8CGP2	H2B1P_MOUSE	6.87	26.19	4
Q8CGP1	H2B1K_MOUSE	6.87	26.19	4
Q6ZWY9	H2B1C_MOUSE	6.87	26.19	4
Q64525	H2B2B_MOUSE	6.87	26.19	4
Q64478	H2B1H_MOUSE	6.87	26.19	4
Q64475	H2B1B_MOUSE	6.87	26.19	4
P10854	H2B1M_MOUSE	6.87	26.19	4
P10853	H2B1F_MOUSE	6.87	26.19	4
Q9D2U9	H2B3A_MOUSE	5.35	19.05	3
Q8CGP0	H2B3B_MOUSE	5.35	19.05	3
Q64524	H2B2E_MOUSE	5.35	19.05	3
Q8VDJ3	VIGLN_MOUSE	6.76	5.68	4
Q99PG0	AAAD_MOUSE	6.76	15.33	4
Q99LF4	RTCB_MOUSE	6.72	10.89	4
Q8VEM8	MPCP_MOUSE	6.72	10.92	4
O88569	ROA2_MOUSE	6.7	13.88	4
P62855	RS26_MOUSE	6.66	33.91	4
Q7TMK9	HNRPQ_MOUSE	6.63	9.47	4
Q6NZJ6	IF4G1_MOUSE	6.59	3.94	4

Q9DCN2	NB5R3_MOUSE	6.53	14.62	3
Q9CXW4	RL11_MOUSE	6.45	23.03	4
P35700	PRDX1_MOUSE	6.29	20.10	4
Q9DCX2	ATP5H_MOUSE	6.28	30.43	3
Q9CR57	RL14_MOUSE	6.21	11.52	3
Q61838	A2M_MOUSE	6.17	3.75	4
Q60865	CAPR1_MOUSE	6.15	6.51	4
P50172	DHI1_MOUSE	6.12	15.07	4
P99024	TBB5_MOUSE	43.81	61.04	28
Q9EQK5	MVP_MOUSE	6.09	9.41	5
Q99LC5	ETFA_MOUSE	6.06	12.61	3
Q9CZS1	AL1B1_MOUSE	11.36	14.64	7
Q9WV68	DECR2_MOUSE	6.05	16.44	3
P60867	RS20_MOUSE	6.03	19.33	4
P49722	PSA2_MOUSE	6.02	23.08	3
Q9Z1Q9	SYVC_MOUSE	6.01	3.17	3
P63101	1433Z_MOUSE	6.01	16.73	3
Q62095	DDX3Y_MOUSE	8	7.14	4
Q62167	DDX3X_MOUSE	8	7.10	4
P16381	DDX3L_MOUSE	8	7.12	4
P35505	FAAA_MOUSE	6	7.64	3
P35486	ODPA_MOUSE	6	8.21	3
P62821	RAB1A_MOUSE	6	18.54	3
P55258	RAB8A_MOUSE	4	10.63	2
P61028	RAB8B_MOUSE	4	10.63	2
Q8K386	RAB15_MOUSE	4	10.38	2
Q6PHN9	RAB35_MOUSE	4	10.95	2
P61979	HNRPK_MOUSE	6	10.58	3
P00186	CP1A2_MOUSE	6	8.38	3
A2AS89	SPEB_MOUSE	6	14.25	3
Q9R1P1	PSB3_MOUSE	6	23.90	3
Q8VCH0	THIKB_MOUSE	6	15.09	3

Q921H8	THIKA_MOUSE	4	9.20	2
Q8C0C7	SYFA_MOUSE	6	8.66	3
Q06185	ATP5I_MOUSE	6	50.70	3
P67778	PHB_MOUSE	5.95	14.71	4
P62267	RS23_MOUSE	5.85	22.38	7
Q9Z2U1	PSA5_MOUSE	5.77	18.67	3
Q8BH95	ECHM_MOUSE	5.72	15.86	3
Q9DD20	MET7B_MOUSE	5.72	15.98	3
Q9DBM2	ECHP_MOUSE	5.33	7.52	4
Q99L45	IF2B_MOUSE	5.28	7.55	3
Q8BMJ2	SYLC_MOUSE	5.21	2.89	3
P41105	RL28_MOUSE	5.58	20.44	3
P62717	RL18A_MOUSE	5.05	19.32	3
O55022	PGRC1_MOUSE	4.98	15.38	3
Q8BP67	RL24_MOUSE	4.77	19.11	4
P10649	GSTM1_MOUSE	4.73	11.93	3
P19639	GSTM4_MOUSE	4	7.80	2
Q80W21	GSTM7_MOUSE	4	7.80	2
P15626	GSTM2_MOUSE	4	7.80	2
O35660	GSTM6_MOUSE	4	7.80	2
Q9Z2I9	SUCB1_MOUSE	4.71	10.37	3
Q8QZR3	EST2A_MOUSE	4.69	8.60	4
P62281	RS11_MOUSE	4.69	17.72	2
Q9QZE5	COPG1_MOUSE	4.63	4.69	3
P56135	ATPK_MOUSE	4.46	26.14	3
Q99PL5	RRBP1_MOUSE	4.39	1.93	2
P61255	RL26_MOUSE	4.36	26.90	4
P12710	FABPL_MOUSE	4.3	32.28	3
Q00623	APOA1_MOUSE	4.27	12.50	3
Q9Z2X1	HNRPF_MOUSE	4.26	8.19	2
Q8R1M2	H2AJ_MOUSE	4.25	28.68	2
Q8CGP7	H2A1K_MOUSE	4.25	28.46	2

Q8CGP6	H2A1H_MOUSE	4.25	28.91	2
Q8CGP5	H2A1F_MOUSE	4.25	28.46	2
Q8BFU2	H2A3_MOUSE	4.25	28.46	2
Q6GSS7	H2A2A_MOUSE	4.25	28.46	2
Q64523	H2A2C_MOUSE	4.25	28.68	2
Q64522	H2A2B_MOUSE	4.25	28.46	2
P27661	H2AX_MOUSE	4.25	25.87	2
P22752	H2A1_MOUSE	4.25	28.46	2
P54071	IDHP_MOUSE	5.48	10.62	4
Q3ULD5	MCCB_MOUSE	4.12	6.04	2
P56593	CP2AC_MOUSE	4.11	8.13	3
P47740	AL3A2_MOUSE	4.99	9.50	4
P14115	RL27A_MOUSE	4.04	14.19	3
Q9CQQ7	AT5F1_MOUSE	4.02	8.59	3
Q8BG05	ROA3_MOUSE	4.02	5.54	2
P83882	RL36A_MOUSE	4.02	20.75	3
Q99MR8	MCCA_MOUSE	4.01	3.91	2
Q9R062	GLYG_MOUSE	4.01	7.21	2
Q7TMM9	TBB2A_MOUSE	41.04	54.61	27
Q9CWF2	TBB2B_MOUSE	39.04	51.91	26
P43277	H13_MOUSE	8	21.72	4
Q91X77	CY250_MOUSE	6	8.37	3
P54775	PRS6B_MOUSE	4	6.70	2
P38060	HMGCL_MOUSE	4	11.08	2
Q9D8W5	PSD12_MOUSE	4	5.92	2
Q8K370	ACD10_MOUSE	4	4.30	3
Q01405	SC23A_MOUSE	4	3.53	2
Q9D662	SC23B_MOUSE	2	1.82	1
P14206	RSSA_MOUSE	4	13.56	3
P00405	COX2_MOUSE	4	13.22	2
Q9Z2W0	DNPEP_MOUSE	4	5.71	2
Q8BK72	RT27_MOUSE	4	5.54	2

P62334	PRS10_MOUSE	4	7.46	2
P50285	FMO1_MOUSE	4	5.45	2
P19783	COX41_MOUSE	4	17.75	2
P14685	PSMD3_MOUSE	4	5.09	2
O88986	KBL_MOUSE	4	9.38	2
Q9EQ06	DHB11_MOUSE	4	12.75	2
Q8BG32	PSD11_MOUSE	4	5.92	2
P84099	RL19_MOUSE	4	13.27	2
P46471	PRS7_MOUSE	4	6.00	2

8.5 Appendix 5

Research Proposal

Project Quality and Innovation

(i) Significance: The incidence of type 2 diabetes has reached epidemic proportions, with approximately 1 million Australians currently suffering from this disease and another 2 million Australians having pre-diabetes. The poor control of blood-glucose levels associated with type 2 diabetes poses a serious threat to human health, often leading to complications such as stroke, coronary artery and peripheral vascular disease, amputations, renal failure, blindness and even death[1]. In addition to decreases in life quality, this disease places a major financial burden on Australia's health system, costing over $1 billion per year. The overall economy loses an estimated additional cost of ~ $9 billion in career costs and productivity losses. The scale of this public health issue has resulted in diabetes becoming one of the Australian Government's National Health Priority Areas.

While a determined global effort has resulted in promising advances in the prevention and treatment of type 2 diabetes, the magnitude of this problem is increasing apace and requires urgent attention.

(ii) Background: Liver glycogen, a highly branched glucose polymer, has a critical role in the maintenance of blood glucose homeostasis. After a meal, blood glucose concentrations can be rapidly controlled by trapping glucose in glycogen. Liver glycogen has three levels of structure: 1) glucose units are attached to form linear chains via α-(1→4) linkages; 2) these chains are joined together via α-(1→6)-linked branch points to form highly branched glycogen "β" particles (~20 nm in diameter); and 3) these β particles are able to be joined together to form much larger "α" particles (~100-200 nm).

Given the characteristically poor blood-glucose control associated with type 2 diabetes, a link between the structure/function relationships of liver-glycogen and type 2 diabetes is probable. However such an association has been unexplored until recently, due to the technological difficulties in obtaining even semi-quantitative structural information on a macromolecule as complex as glycogen. My undergraduate research[2], as part of the Advanced Study Program in Science, developed breakthrough technologies capable of obtaining size distributions of native glycogen, extracted and analysed with minimal degradation. For the first time we are able to explore the role of glycogen structure in diabetes. These size distributions are achieved using size exclusion chromatography (SEC), a technique routinely used for synthetic polymers but now, as my research revealed, capable of analysing highly complex structures such as glycogen. Utilising this technology, my Honours year research demonstrated that *db/db* mice, a model for type 2 diabetes with a point mutation in the leptin receptor, have an impaired ability to form the large glycogen α particles synthesized in the healthy controls, and instead contained predominantly the smaller β particles. Given the building evidence (including data presented in one of my recent publications[3] that smaller glycogen particles 1) have a higher association with glycogen phosphorylase[4], a key enzyme involved in glycogen degradation and 2) are degraded more rapidly *in vitro*[3,5], the inability to form larger glycogen α particles is predicted to result in a faster, less controlled degradation into glucose.

While the mechanism for the formation of larger glycogen α particles from β particles is currently unknown, my finding that diabetic (*db/db*) mice lack these macromolecules has sparked a number of studies aimed at resolving this question. Acid hydrolysis experiments on pig-liver glycogen, performed during my PhD, have revealed that the linkage connecting β particles to form α particles is most likely proteinaceous in nature, making the search for such a protein "glue" a promising research area[6]. If indeed there is a protein involved in holding these particles together, any regulator that decreases the expression of this protein may become a promising inhibitory drug target for diabetes management.

In order to understand why *db/db* mice are unable to form many α particles, it is essential to first understand the mechanism by which they form in non-diabetic hepatocytes. Another study during my PhD involved observing the size distribution of liver-glycogen particles from wild-type mice at various time points across a dirunal cycle[3]. This revealed two key insights: 1) glycogen initially forms as separate β particles, only to be subsequently joined together to form larger α particles after the glycogen content has reached its maximum concentration; and 2) during glycogen degradation the larger particles were much more resistant to glycogenolysis, persisting significantly longer than the smaller β particles. Not only does this data support the theory that glycogen structural features such as particle size influence the rate of glycogenolysis, but it strongly suggests that there is a mechanism in which separate β particles are able to conglomerate to form an α particle.
The question still remains, however, as to why *db/db* mice appear to be lacking this mechanism. One potential answer is centred on the observation that while non-diabetic mice go through a diurnal cycle of synthesising glycogen during the dark hours (due to their nocturnal nature) and having this glycogen slowly degraded during the daylight hours, *db/db* mice are continually eating and maintaining a high liver-glycogen content[7]. It is therefore possible that these mice are unable to switch from the glycogen synthesis phase, in which glycogen is being formed as separate β particles, into the next phase where they come together to form the more resistant α particles.
iii) Objectives: The initial primary aim of this research proposal is to determine the mechanism causing *db/db* mice to have an impaired ability to form α particles. By utilising the methods developed during my research to analyse the structure of glycogen, and coupling these with an in-depth analysis of the varying expression levels of a number of key proteins involved in glycogen metabolism, we will build a much richer understanding of not only glycogen metabolism in general, which will include the often neglected (due to hitherto incapable technology) glycogen structure, but more importantly the role glycogen metabolism has in type 2 diabetes. The second primary aim of this research is to provide a better understanding of human glycogen metabolism by comparing human diabetic, prediabetic and non-diabetic samples, moving my research even closer to its ultimate goal of developing better treatments for sufferers' of type 2 diabetes.
(iv) Approach and Methodology: *The effect of leptin administration on the glycogen metabolism of ob/ob mice:* Given the possibility that the impaired α-particle formation observed in *db/db* mice is a direct result of their immediate eating behaviour, being able to separate this aspect of *db/db* mice behaviour from the effects of their obesity and insulin resistance, is of great importance. To do this would involve utilising a mouse model with a similar phenotype to *db/db* mice, but with the ability to control their feeding behaviour, without the stress induced by simply using a calorie restricted diet. Fortunately there is such a model, with *ob/ob* mice exhibiting a very similar phenotype to that of *db/db* mice. The similarities in phenotypes arise as both models are unable to properly use the leptin satiety pathway, making them continuously hungry. The difference between these diabetic models is how this pathway is disrupted. While *db/db* mice are able to produce the peptide leptin in excessive amounts, a point mutation in the leptin receptor makes these mice leptin resistant. *Ob/ob* mice on the other hand, while synthesising a perfectly functioning leptin receptor, have a point mutation on the gene encoding the leptin peptide, destroying its functionality.
It has been shown (in the research group of the overseas host proposed here) that the administration of leptin to *ob/ob* mice leads to a decrease in their food intake and body weight[8]. This research will investigate whether by allowing *ob/ob* mice to become obese and insulin resistant (feeding them *ab libitum* without administration of leptin), *ob/ob* mice also have an impaired mechanism for α particle formation. While expected to also exhibit this phenotype, if *ob/ob* mice do not have a similar impairment to *db/db* mice, this would indicate that the reason why *db/db* mice are unable to form large particles lies within the limited differences between the physiology of *db/db* and *ob/ob* mice. However, if indeed *ob/ob* mice are also unable to form α particles, the administration of leptin can be used to alter the immediate eating behaviour of the mice. By analysing the glycogen size distribution of *ob/ob* mice (compared to controls) before and after leptin administration, where

ob/ob mice are still obese and insulin resistant but have decreased their amount of eating, it could be tested whether the effect observed for diabetic mice is indeed due to continuous eating. If the glycogen α particle formation is still impaired after the administration of leptin to *ob/ob* mice, it will provide strong evidence that the phenomenon initially observed in *db/db* mice is not simply due to continuous eating. If this is the case the leptin treatment would be extended until the *ob/ob* mice have lost a significant amount of body weight, with the size distributions being tested again. Whether or not this extended treatment results in the *ob/ob* mice being able to form α particles will provide very useful insights into the nature of this impairment.

An important aspect of this investigation will be to analyse glycogen content and structure at various time points during a diurnal cycle, allowing a much greater depth of understanding of this diurnal process than simply choosing one time point. The expression levels of key enzymes such as glycogenin, glycogen synthase, glycogen phosphorylase and phosphoylase kinase will be tested using real-time PCR and their total abundance determined using Western blotting. Wild-type (WT) mice with the same genetic background as the *ob/ob* mice will be used as controls. For both *ob/ob* mice and WT mice, half will be administered leptin and half a saline solution, acting as another control (as was performed in Prof. Zierath's recent study[8]). My previous experience indicates that there should be 6 time points evenly distributed across the dirunal cycle. There will be 4 different groups per time point: *ob/ob*-leptin, *ob/ob*-saline, WT-leptin and WT-saline. To allow for strong statistical comparisons there will be 6 mice per group. Therefore this project will require 72 WT and 72 *ob/ob* mice. After this analysis is completed at the Karolinska Institute (within the first 2 years of the project), key glycogen samples that show any interesting differences from each group will be saved for a full proteomics analysis using mass spectroscopy, similar to the methods used previously for mice and rats[9]. This is to be completed at UQ in years 3 and 4 of this project.

The analysis of diabetic and non-diabetic human liver-glycogen: While the use of mouse models is an extremely useful way of studying the metabolism of glycogen in terms of structure, the translation of this research into human liver-tissues will automatically enhance the physiological relevance of any further discoveries. Here I propose to obtain the first size distributions of non-diabetic, prediabetic and type 2 diabetic human-liver, with the expression levels of key enzymes again being compared using rt-PCR and Western blots. This initial analysis will be performed in the first 2 years of the project. Research performed in years 3 and 4 of the project will expand on the initial investigation by doing an in-depth proteomics analysis in order to compare the proteome of extracted liver from these tissue types.

My experience in this analytical approach and the experience of my intended supervisors indicate that the research proposed to be undertaken can be achieved in the 4 years of this fellowship.

(v) Innovation: This project will for the first time use the newly developed structural characterisation techniques to analyse the glycogen structure of diabetic mice that have been administered leptin and therefore have an eating behaviour similar to non-diabetic mice. Combining this with the analysis of the expression levels of key enyzmes involved in glycogen metabolism will greatly improve our understanding of glycogen metabolism in both healthy and diabetic liver. This project will also result in the first structural analysis of human liver glycogen as well as a detailed analysis of protein expression levels, again focusing on the difference between healthy and diabetic tissues. For the first time this project will provide a detailed mass-spectroscopy proteomics analysis of extracted glycogen from human liver. A schematic overview of the project is given in Figure 1.

Research Environment and Feasibility

The research environments overseas and in Australia both allow ready access to the two main requisites for this project: 1) being able to obtain appropriate samples, in this case *ob/ob* mice and human liver tissue; and 2) having access to equipment important for the glycogen structural characterisation and the determination of protein expression levels. This project builds on from my previous research by linking for the first time the glycogen structural analytical approach I pioneered, with the ground breaking research on other biochemical and clinical aspects of glycogen

metabolism, being undertaken at two of the world's leading research teams in this area. This promises to be a fertile ground to help enhance our understanding of glycogen behaviour especially in relation to diabetes, and to determine the potential for new approaches to treatment of this disease based on the moderation of glycogen behaviour.

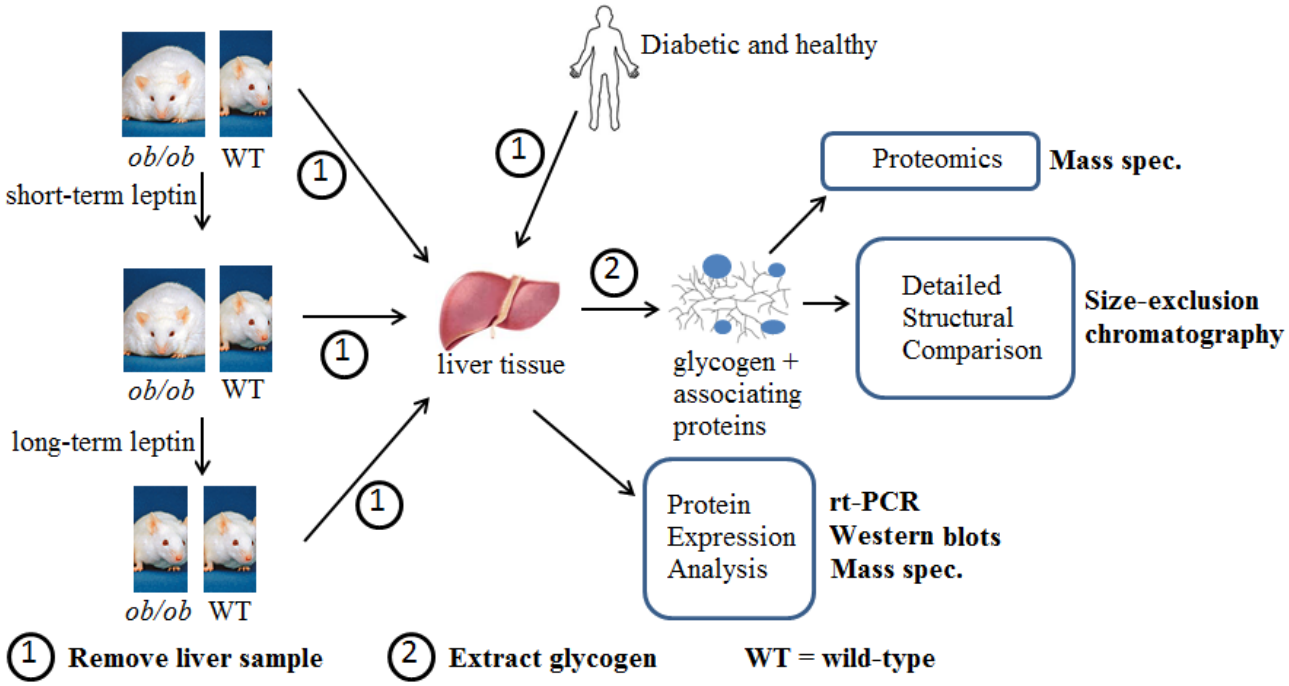

Figure 1. Schematic overview of project.

Years 1 and 2 will be performed in the Karolinska Institute in Stockholm, a prestigious and world leading facility for biomedical research. This work will be performed under the supervision of Prof. Juleen Zierath (H-index of 47), Chair of the Nobel Committee for Physiology or Medicine, who has developed a world-leading team of diabetes researchers. Having recently published a study that has analysed the effects of leptin administration on the mitochondrial function of *ob/ob* mice[8], as well as routinely analysing the protein expression levels of targeted enzymes[10], Prof. Zierath's research team is ideal for this research project. The training I will obtain at the Karolinska Institute will equip me with capacities necessary for a future career in biomedical research. Close collaboration between Prof. Zierath and surgeon Erik Näslind, who specializes in obesity and is enthusiastic to collaborate on this project, allows for the perfect research environment capable of expanding the research into human tissues. The structural characterisation of this liver glycogen will be performed using state-of the-art size separation equipment located in Dr. Fransisco Vilaplana's research group at nearby KTH Royal Institute of Technology in Stockholm. I have already established close collaborative research links with Dr. Vilaplana, as evidenced by him being a co-author on three of my recent publications that involve the structural characterisation of glycogen. The combination of expertise available in Stockholm, between the Karolinska Institute and KTH Royal Institute of Technology provides an ideal research environment for the first stage of the research project outlined here.

Year 3 and 4 of this fellowship will be based at the Mater Research Institute in Brisbane under the supervision of Prof. Josephine Forbes (H-index of 33). The existing close collaboration between Prof. Forbes' diabetes research team and expert clinician Prof. David McIntyre (Head of the Mater Clinical School and Director of Endocrinology and Obstetric Medicine at the Mater hospital) will allow further analysis on human glycogen. The size exclusion chromatography equipment at the University of Queensland has been proven to be excellent at analysing glycogen structure, with all

of our publications looking at glycogen structure using these facilities. Prof. Robert Gilbert (my current PhD supervisor), a world-leading physical chemist (H-index of 58), will be an enthusiastic and active collaborator for the project outlined here. Proteomics of human samples will be determined via collaboration with Dr. Ben Schulz using the world-class mass spectrometry facilities available in the School of Chemistry and Molecular Bioscience at The University of Queensland, and with whom I have already started collaborative proteomic analysis of mouse-liver glycogen.

Benefit and Expected Outcomes

Given the rapidly increasing incidence of type 2 diabetes and the tragic effects this disease is having on human health, the benefits of enhancing our understanding of this disease and in developing improved methods to prevent and treat this poor control of blood glucose are considerable. My unexpected discovery that diabetic (*db/db*) mice have an impaired ability to form large glycogen α particles and the evidence that this may leave them vulnerable to rapid glycogen degradation has made this research a very promising new area for finding new drug targets. This research project aims to explain why diabetic mice have an impaired ability to form α particles, moving us closer to determining whether it is possible to reverse this effect by medication. By expanding our research to human samples this project will move this research closer to the ultimate goal of enhanced diabetes treatment. Given the highly innovative yet entirely feasible project outline proposed here, we expect there to be high impact journal publications resulting from this work. These outputs will derive from the behaviour associated with the administration of *ob/ob* mice with leptin. One will focus on the immediate effects of leptin in which case the *ob/ob* mice have an altered eating behaviour but are still obese and insulin resistant. Another will examine the extended treatment of *ob/ob* mice with leptin, where the mice have a similar body weight to the non-diabetic controls. The potential for benefits and novel outcomes arising from the studies using human glycogen samples are substantial. We expect the first outcomes to focus on comparisons between the liver-glycogen structure between healthy and diabetic humans. Other significant research outcomes will result from doing a detailed proteomics analysis on those same samples using mass spectroscopy techniques that have been already established for mouse- and rat-liver glycogen[9].

References

(1) Amos, A. F.; McCarty, D. J.; Zimmet, P. *Diabetic Medicine* **1997**, *14*, S7.

(2) Sullivan, M. A.; Vilaplana, F.; Cave, R. A.; Stapleton, D. I.; Gray-Weale, A. A.; Gilbert, R. G. *Biomacromolecules* **2010**, *11*, 1094.

(3) Sullivan, M. A.; Aroney, S. T. N.; Li, S.; Warren, F. J.; Joo, L.; Mak, K. S.; Stapleton, D. I.; Bell-Anderson, K. S.; Gilbert, R. G. *Biomacromolecules* **2014**, *15*, 660.

(4) Barber, A. A.; Orrell, S. A.; Bueding, E. *Journal of Biological Chemistry* **1967**, *242*, 4040.

(5) Orrell, S. A.; Bueding, E. *J. Biol. Chem.* **1964**, *239*, 4021.

(6) Sullivan, M. A.; O'Connor, M. J.; Umana, F.; Roura, E.; Jack, K.; Stapleton, D. I.; Gilbert, R. G. *Biomacromolecules* **2012**, *13*, 3805.

(7) Roesler, W. J.; Helgason, C.; Gulka, M.; Knandelwal, R. L. *Hormone and Metabolic Research* **1985**, *17*, 572.

(8) Holmstrom, M. H.; Tom, R. Z.; Bjornholm, M.; Garcia-Roves, P. M.; Zierath, J. R. *Metabolism-Clinical and Experimental* **2013**, *62*, 1258.

(9) Stapleton, D.; Nelson, C.; Parsawar, K.; McClain, D.; Gilbert-Wilson, R.; Barker, E.; Rudd, B.; Brown, K.; Hendrix, W.; O'Donnell, P.; Parker, G. *Proteomics* **2010**, *10*, 2320.

(10) Nascimento, E. B. M.; Osler, M. E.; Zierath, J. R. *Am. J. Physiol.-Endocrinol. Metab.* **2013**, *305*, E1408.